SISSA
Scuola
Internazionale
Superiore di
Studi Avanzati

Physics Area - PhD course in
Statistical Physics

Novel phases in long-range many-body systems

Candidate:
Guido Giachetti

Advisors:
Prof. Stefano Ruffo
Prof. Andrea Trombettoni

Academic Year 2021-22

A mia madre

Non torba m'ha assediato, ma gli eventi
di una realtà incredibile e mai creduta.

I hereby declare that, except where specific reference is made to the work of others, the contents of this dissertation are original and have not been submitted in whole or in part for consideration for any other degree or qualification in this, or any other University. This dissertation is the result of my own work and includes nothing which is the outcome of work done in collaboration, except where specifically indicated in the text.

Guido Giachetti
August 2022

Contents

Acknowledgments

Sarò presto in utroque dottore,
'che di studio ancor poco mi manca.

F.M. Piave, *La forza del destino*

I would like to express my gratitude to my advisors, S. Ruffo and A. Trombettoni, and to my collaborators N. Defenu, A. Solfanelli, L. Correale whose contribution was fundamental for the development of the ideas present in this work.

My deepest thanks go to Patrizia, who always remembers everyone's name, and to the rest of the canteen staff, the true backbone of SISSA.

As man shall not live by bread alone (especially me) I cannot forget about all who made this troubled, plague-stricken, years a pretty pleasant times. It is impossible to thank one by one the dear persons I have shared my life with in this gruff, graceful city (both the sane ones and my fellow PhD students). Sticking to a strict (and unjust) spatial-proximity policy, I will mention Chiara, who does not drink enough and shared a haunted flat with me for a while, and my barely bearable office mate, Alessandro, whose opinion are always worth listening to, in spite of being invariably wrong.

Last but not least, challenging an annoying name degeneracy, and knowing that this is not nearly enough, I have to thank Alessandro, my more patient collaborator, best drinking buddy, life companion.

List of Publications

Invano accumula progetti e calcoli
non sa che fabbrica castelli in aria

G.D. Ruffini, *Don Pasquale*

Chapter 2 of the present work is based on the following publications

- **G. Giachetti**, N. Defenu, S. Ruffo and A. Trombettoni, *Self-consistent harmonic approximation in presence of non-local couplings*, EPL 133(5) (Apr 2021), p. 57004
- **G. Giachetti**, N. Defenu, S. Ruffo and A. Trombettoni, *Berezinskii-Kosterlitz-Thouless phase transitions with long-range couplings*, Phys. Rev. Lett. 127 (Oct 2021), p. 156801
- **G. Giachetti**, A. Trombettoni, S. Ruffo and N. Defenu, *Berezinskii-Kosterlitz-Thouless transitions in classical and quantum long-range systems*, Phys. Rev. B 106 (July 2022), p. 014106

Chapter 3 of the present work is based on the following publications

- **G. Giachetti**, N. Defenu, S. Ruffo and A. Trombettoni, *Villain model with long-range couplings*, arXiv preprint at arXiv:2209.11810 (Sep 2022)

Chapter 4 of the present work is based on the following publication

- **G. Giachetti** and N. Defenu, *Entanglement propagation and dynamics in non-additive quantum systems*, arXiv preprint at arXiv:2112.11488 (Dec 2021)

Chapter 5 is based on the following publication

- **G. Giachetti**, A. Solfanelli, L. Correale and N. Defenu, *High-order time crystal phases and their fractal nature*, arXiv preprint at arXiv:2203.16562 (Apr 2022)

Other publications during this PhD course:

- **G. Giachetti** and L. Casetti, *Violent relaxation in the Hamiltonian mean field model: I. Cold collapse and effective dissaption*, J. Stat. Mech. 4 (Apr 2019), p. 043201
- A. Santini, **G. Giachetti** and L. Casetti, *Violent relaxation in the Hamiltonian mean field model: II. Non-equilibrium phase diagrams*, J. Stat. Mech., 1 (Jan 2022), p. 013210

- L. Barbieri, P. Di Cintio, **G. Giachetti**, A. Simon-Petit and L. Casetti, *Symplectic coarse graining approach to the dynamics of spherical self-gravitating systems*, MNRAS 2 (Feb 2022), p. 3015
- **G. Giachetti**, S. Gherardini, A. Trombettoni and S. Ruffo, *Quantum-heat fluctuation relations in three-level systems under projective measurements*, Cond. Matt. 5(1), (Mar 2020), p. 17
- S. Gherardini, **G. Giachetti**, S. Ruffo and A. Trombettoni, *Thermalization processes induced by quantum monitoring in multilevel systems*, Phys. Rev. E 104 (Sep 2021), p. 034114
- S. Gherardini, L. Buffoni, **G. Giachetti**, A. Trombettoni and S. Ruffo, *Energy fluctuation relations and repeated quantum measurements*, Chaos, Solitons and Fractals 156 (Mar 2022), p. 111890
- L. Capizzi, **G. Giachetti**, A. Santini and M. Collura, *Spreading of a local excitation in a Quantum Hierarchical Model*, arXiv preprint at arXiv:2207.06790 (Jul 2022)
- A. Solfanelli, **G. Giachetti**, M. Campisi, S. Ruffo, N. Defenu, *Quantum heat engine with long-range advantages*, arXiv preprint at arXiv:2208.09492 (Aug 2022)

Preface

Many-body systems with long-range power-law decaying potentials among their microscopic components are known to fall outside the traditional framework of complex systems. While some peculiarities in their behavior had emerged since the very early days of statistical mechanics, the possibility of engineering such systems in experimental setups based on molecular and optical systems has stimulated an impressive theoretical activity in the last decades, unveiling a plethora of new physical phenomena. In particular, depending on the exact form of the couplings, long-range-interacting systems may avoid thermalization, remaining trapped in long-lived metastable phases, or exhibit new equilibrium phases at thermal equilibrium. The study of such novel phases, emerging both in the equilibrium behavior and in the dynamics, has been the core of my Ph.D. work in the last three years.

The aim of the present thesis is twofold. First, to present my results, which have been partially published, more concisely, in peer review journals, embedding my work in the conceptual framework of long-range interacting systems. Second, to (hopefully) provide the reader with a path to explore such a rich and stunning landscape, well knowing that other choices of presentations are equally valid.

Chapter 1 is intended to summarize some known features of long-range interacting systems. Sec. 1.1 introduces the main distinction between weak and strong long-range interaction and gives a brief overview of the experimental techniques used to engineer long-range systems. Sec. 1.2 briefly revisits the critical properties of weak long-range models, while 1.3 is devoted to the dynamics of closed quantum strong long-range systems and their spectral proprieties.

The original results of this thesis are discussed in Chapters 2 to 5. Part I (Chapters 2, 3) is devoted to the emergence of new equilibrium phases in systems with $O(2)$ symmetry, which may exhibit a non-trivial interplay between long-range couplings and topological excitations. As we are mainly interested in finite-temperature behavior, we will make use almost exclusively of classical spin models. Part II (Chaps. 4, 5) is instead devoted to the study of the dynamical phases emerging in strong long-range quantum systems.

In particular, Chapter 2 explores the fate of the Berezinskii-Kosterlitz-Thouless (BKT) universality class in presence of non-local interactions are added, which had been so-far a long-standing problem, using as a paradigmatic example the generalization to long-range couplings of the two-dimensional XY model (introduced in Sec. 2.1). The study of the crossover between long-range and short-range regimes is addressed using different tools, such as the low-temperature expansion (Sec 2.2) and the so-called self-consistent-harmonic approximation (Sec. (2.3)). The introduction of a suitable field theory (Sec. 2.5), which describes the long-distance behavior of the model leads to a set of perturbative renormalization-group (RG) equations de-

scribing the infrared behavior of the model. The resulting phase-diagram (Sec. 2.6) features the emergence of a new ordered phase which takes over the usual quasi-long-range-ordered phase as the range of the interaction is increased. The interplay between the two phases, as well as the non-trivial scaling of the order parameter with the temperature, are both unprecedented. Finally, in Sec. 2.7, it is shown how our results can be extended to describe the $T = 0$ behavior of the one-dimensional quantum XXZ chain.

In Chapter 3 the fate of the long-range counterpart of the two-dimensional Villain model is discussed. For nearest-neighbors couplings, the model is known to fall within the same universality class of the two-dimensional XY model. As motivated in Sec. 3.2, for sufficiently non-local couplings such equivalence is expected to break down, so that the understanding of the critical properties of the model becomes important in order to discuss the Berezinskii-Kosterlitz-Thouless universality in presence of long-range interactions. The best way to extend the Villain model to non-local couplings is discussed in Sec. 3.1. In Sec. 3.3 and Sec. 3.4 the vortex-gas description of the model and the corresponding real-space renormalization-group equations, respectively, are derived. Quite unexpectedly, the phase diagram derived in Sec. 3.5 partially coincides with the one of the one-dimensional Ising model with $1/r^2$ interactions. Finally, in Sec. 3.6 a field-theoretical description of the model is proposed.

Chapter 4 addresses dynamical phases emerging on mesoscopic timescales in the strong long-range interacting systems, using as a prototypical example the quench dynamics of the quantum $O(n)$ model, introduced in Sec. 4.1. While similar phenomena have been observed in other systems, in the limit $n \to \infty$ it is possible to interpret it in terms of parametric resonances of the spin-waves, as discussed in Sec. 4.2 and Sec. 4.3. Finally, in Sec. 4.4 it is shown how such resonances affect the production of entanglement.

Finally, Chapter (5) is devoted to periodically driven strong long-range interacting systems, which are known to exhibit robust dynamical phases in which the discrete time-translation symmetry induced by the driving is spontaneously broken (the so-called Floquet time-crystalline phases, introduced in 5.1). In particular, the physics of the recently-introduced higher-order time crystalline phases is investigated: in Sec. 5.2 a new order parameter is introduced in the context of the paradigmatic kicked Lipkin-Meshkov-Glieb model, which is able to unambiguously characterize such a phase. In Sec. 5.3 the properties of the corresponding phase diagram are investigated and, in Sec. 5.4, it is shown how, for high-frequency driving, these can be captured analytically. Sec. 5.5 introduces a semiclassical approximation, valid for large (but finite) sizes, and discusses the robustness of our picture against finite size effects.

1 | Long-range-interacting systems

In this chapter we will briefly review the main features of long-range interacting systems, i.e. many-body systems whose microscopic components interact via slow-decaying, power-law potentials. Such non-local interactions are known to be able to alter both the equilibrium and the out-of-equilibrium behavior of classical and quantum systems [1–3]. Long-range interacting systems do occur, e.g. in the context of astrophysics [4], or can be engineered in experimental setups such as trapped ions [5, 6], Rydberg gases [7] and optical cavities [8, 9], showing promising features for the development of quantum technologies.

The Chapter is structured as follows: in Sec. 1.1 we introduce the basic nomenclature regarding the subject and examine the possibility of experimental realization of quantum many-body systems. In the remaining part of the Chapter we will address closely the two main topics which correspond to Part I and II, respectively, of the present work, namely the equilibrium critical behavior in the non-mean field regime in Sec. 1.2 and the dynamics of long-range quantum systems which avoid thermalization 1.3.

1.1 | Weak and strong long-range regimes

We want now to introduce a first, important, classification of non-local interaction, in order to distinguish between different regimes. We will use here the conventions and the nomenclature of Ref. [1], although different conventions can be found in the literature as well.

Let us consider then a d-dimensional physical system whose elementary components interact through a power-law coupling of the form

$$J(r) = \frac{J}{r^{\alpha}}. \tag{1.1}$$

If we now consider, for sake of simplicity, a uniform configuration as the typical one, we have that the corresponding energy can be estimated as

$$E \sim \int d^d\mathbf{r} \int d^d\mathbf{r}' \, |\mathbf{r} - \mathbf{r}'|^{-\alpha} \sim N \int_a^L dr \, r^{d-\alpha-1}, \tag{1.2}$$

L being the linear size of the system, $N \sim L^d$ the number of microscopic components, a the typical distances among the nearest ones.

We see now that a first, important, distinction arises depending whether $\alpha > d$ or $\alpha < d$. In particular, if $\alpha > d$ the above integral is infrared convergent and we have

$$E \sim N, \tag{1.3}$$

while, for $\alpha < d$,

$$E \sim NL^{d-\alpha} = N^{2-\alpha/d}. \tag{1.4}$$

In the latter case, thus, we lose the additivity of the energy [2]. Physically speaking this means that, as one two copies of the system are positioned next to each other, the interface energy is no longer negligible, so that the energy does not scale linearly with N.

This situation corresponds to the so-called *strong long-range regime*. Because of the fact that the energy grows over-extensively, the energetic contribution is going to dominate over the entropic one, resulting in a trivial thermodynamics. On the other hand, let us notice that it is possible to recover the extensive nature of the energy by performing an appropriate rescaling of the coupling constant J, namely

$$J \to \frac{J}{N^{1-\alpha/d}}, \tag{1.5}$$

which is known as *Kac scaling* [2, 10]. Let us remark that, even if (after the scaling) $E \sim N$, the system is still non-additive.

Although the choice of a N dependent coupling may appear unphysical, it is worth noticing that we always deal with finite systems, so the definition of the coupling J is somewhat arbitrary. Kac's prescription can be thus read as a way of tuning the interaction strength in such a way that its contribution is of the same order as the entropic one. On the other hand, one can understand the scaling by thinking that the usual thermodynamic limit ($N, L \to \infty$, NL^{-d} constant) is no longer meaningful when we are dealing with non-additive systems, in which the importance of surface effects is growing with the size of the system.

While it is clear that in the strong long-range regime long-range interactions do actually influence the physics of the system, they may change the physics of the system for $\alpha > d$ as well (albeit less dramatically). It turns out that the long-range nature of the couplings indeed affects the universal critical behavior of the system, provided that

$$\alpha < \alpha^*, \tag{1.6}$$

where $\alpha^* > d$ is a critical value of the exponent which, in general, depends on the model considered [11, 12]. This is the so-called *weak long-range regime*. It is customary in this case to parametrize the exponent through the quantity

$$\sigma = \alpha - d, \tag{1.7}$$

with the weak-long range regime corresponding to $0 < \sigma < \sigma^*$ for some σ^*.

Another fundamental difference between the strong-long range regime and the weak-long range one arises when we look at the dynamical properties. Indeed, it is known that, for $\alpha < d$, the timescale on which the system thermalizes diverge with N [2, 13–15]. Systems interacting through gravitational [15] or (unscreened) electromagnetic [14] forces, e.g., are known to remain trapped in non thermal quasi-stationary states whose lifetime grows with the number of particles [2, 4]. We can understand intuitively why this happens by looking at the $\alpha = 0$ case, i.e. the so-called *fully-connected* limit: here, in the limit $N \to \infty$, we recover a mean-field dynamics, in which the fluctuations are suppressed, so that the system is prevented from thermalizing. Let us notice how, in this case, the Kac prescription can be thought of as a time rescaling: without it, the frequency of the short-time oscillations would diverge with N. On the other hand, while the thermalization process in the weak-long-range regime is known to be analogous to its short-range counterpart [16, 17], the non-local nature of the interaction affects the propagation of information [18–20], dynamical critical exponents [12] and defect scaling [21, 22].

In summarizing, we can distinguish three fundamental regimes

- For $\alpha < d$ ($\sigma < 0$) the strong-long range regime, in which the thermodynamic quantities are no longer additive, and the Kac's rescaling (1.5) is needed in order to find a meaningful thermodynamic limit, with extensive thermodynamic potentials. The timescale under which the system thermalizes diverges with N.

- For $d < \alpha < \alpha^*$ ($0 < \sigma < \sigma^*$) the weak long-range regime in which long-range couplings can still influence the critical behavior and the propagation of excitations.

- For $\alpha > \alpha^*$ ($\sigma > \sigma^*$) the interaction is still non-local; still, the universal properties of the system are the same of the $\sigma \to \infty$ limit, i.e. of the short-range case.

This classification of course holds even in the case of generic $J(r)$ which behaves as Eq. (1.1) only asymptotically for large r [3]. On the other hand, this classification has the advantage to provide a simple conceptual scheme and ease our discussion, but it does not pretend to be comprehensive or rigorous. New phenomena may arise, e.g., if there is a competition between different short-range and long-range interactions, or if the system spontaneously forms non-homogeneous patterns [23]. Similarly, screening processes can take place, as in the case of the Coulomb interaction [24].

Finally let us notice that, also for arbitrarily large σ, the power law nature of the coupling can have an effect on the physics of the system. Most notably, as shown in Ref. [25], the two-point correlation functions do not decay as an exponential for high temperatures but, rather, they decay with the same power law of the coupling.

1.1.1 | Experimental realizations

Before going on with the analysis of long-range physics it is important to take a closer look at the possibility of engineering such interactions in experimental setups, and in particular in the quantum realm, on atomic, molecular and optical (AMO) systems [1]. As mentioned above, the advancement in the control and manipulation techniques of AMO systems has resulted in rising interest in long-range systems. As the focus of the present work is on the theoretical analysis, however, we will limit ourselves to briefly introducing the main classes of AMO setups that are relevant to long-range physics.

Trapped ions allows for the almost unique possibility of tuning the exponent of the effective interaction within the range $\alpha \in (0, 3)$, and thus to reach, in one-dimensional arrays of ion, both the weak and the strong long-range regime [5, 6]. Such systems are formed by Coulomb-interacting ions, confined by an external, harmonic potential. When laser-cooled, they arrange themselves as a Wigner crystal. By exerting an optical force on the spin degrees of freedom through coherent radiation, an effective spin-spin, phonon-mediated, interaction arises. The range of such interaction can be modified by tuning the parameters of the setup.

Quantum gases in cavities can be used to engineer all-to-all interacting, fully-connected models [8, 9], such as the Lipkin-Meshov-Glick model [26] examined in Sec. 1.3.3 or the Hamiltonian Mean Field model [27, 28]. Such systems are formed by neutral Bose-Einstein condensates inside an optical cavity and illuminated by a transverse standing-wave laser field, far-detuned from the atomic resonance so that the condensate behaves as a dielectric medium. By tuning the frequency of the cavity frequency, the atoms of the condensate effectively interact by scattering photons in the cavity mode and back. As such photons are delocalized over the cavity mode, this interaction is flat.

Finally, *dipolar systems* [7], and in particular Rydberg atoms, are an ideal framework for the study of the emergence of modulated structures which break translational invariance [23].

1.2 | Critical behavior of weak long-range models

In the weak-long range regime, the presence of non-local interaction does not prevent thermalization. At the same time, it influences the critical behavior of the model. We will now discuss briefly the main features of the critical behavior in weak-long range systems. Let us notice that, as long as we are interested in the finite temperature behavior, we may neglect the quantum nature of elementary components of the system, and restrict ourselves to their classical counterpart.

As a prototypical example, we introduce the long-range version of the classical

$O(n)$ model. Let us consider thus a d-dimensional square lattice, with N lattice sites; let us associate with each site $\mathbf{j} \in \mathbb{Z}^d$ a n-component classical spin variable $\mathbf{s_j}$. such that $s_{\mathbf{j}}^2 = 1$. The interaction among those variables is given by the

$$\beta H = \frac{1}{2} \sum_{\mathbf{i} \neq \mathbf{j}} J(r) \left(1 - \mathbf{s_i} \cdot \mathbf{s_j}\right) \tag{1.8}$$

with $\mathbf{r} = \mathbf{i} - \mathbf{j}$, $r = |\mathbf{r}|$, and $J(r)$ which decays asymptotically as

$$J(r) \sim J r^{-d-\sigma}. \tag{1.9}$$

As we are interested in the weak long-range regime, we consider here $\sigma > 0$. As the name of the model suggests, Hamiltonian (1.8) is invariant under a global $O(n)$ symmetry.

For $n = 1$ we recover the $\mathbb{Z}_2$-symmetric Ising model, for $n = 2$ the XY model, for $n = 3$ the Heisenberg model. In the nearest-neighbours regime ($\sigma \to \infty$) the Ising model is known to undergo an order-disorder phase transition of the second order for $d \geq 2$ while the same happens in the $n \geq 2$ case for $d > 2$ [29]. This is in agreement with the celebrated Hohenberg-Mermin-Wagner theorem [30] which forbids the spontaneous breaking of a continuous symmetry at finite temperatures in $d \leq 2$, provided that the couplings decay fast enough. The two-dimensional nearest-neighbors XY model is known to exhibit the so-called Berezinskii-Kosterlitz-Thouless (BKT) transition [31, 32] which is not of the order-disorder kind.

The presence of non-local interactions may alter this picture not only quantitatively (e.g. by modifying the critical exponents of the system) but also qualitatively, as the model will in general exhibit a low-temperature phase transition as the couplings decay slowly enough. Physically speaking, this is due to the fact that a long-range ferromagnetic interaction inevitably favors ordered phases.

Generally speaking, by looking at the critical behavior of the system, we may distinguish two cases [1]:

- For $0 < \sigma < \sigma_{\text{mf}}$ the critical behavior is well described by a Gaussian fixed point, in which the usual short-range dispersion relation is replaced by its long-range (σ-dependent) counterpart. The critical exponents thus can be obtained by a saddle-point approximation (even though their value is σ-dependent and thus different from the usual short-range critical exponent).

- For $\sigma_{\text{mf}} < \sigma < \sigma^*$ the universal quantities are still σ dependent, but they are not given by the mean-field ones, as the critical behavior of the system interpolates between the Gaussian and the short-range one.

- For $\sigma > \sigma^*$ the critical behavior corresponds to the nearest-neighbors ($\sigma \to \infty$) one, and the phase transition may actually disappear in lower dimensions.

In the rest of the Section, we will discuss the value of $\sigma_{\rm mf}$ and σ^* for the $O(n)$ model. Let us anticipate some key results. First, regardless of the value of n,

$$\sigma_{\rm mf} = d/2, \tag{1.10}$$

for any $d < 4$. The determination of σ^* is instead more delicate. For $d \geq 4$, as the short-range critical point is Gaussian, we have $\sigma^* = 2$ (let us notice how $\sigma^* = \sigma_{\rm mf}$ at $d = 4$, signaling that the phase transition is described everywhere by a mean-field analysis). For $d < 4$ we have $\sigma^* < 2$; in particular, according to the criterion firstly introduced by Sak [33]

$$\sigma^* = 2 - \eta_{\rm sr}, \tag{1.11}$$

$\eta_{\rm sr}$ being the anomalous dimension of the system in the short-range regime.

Before going on let us notice how the above analysis cannot be straightforwardly applied to the $d = 2$ $n = 2$ case, because of its peculiar short-range behavior. Indeed its generalization to the long-range case is more delicate and will constitute the main topic of Chapter 2.

1.2.1 | Field-theoretical analysis

In order to motivate the results exposed above, it is convenient to provide a field-theory description of the Hamiltonian (1.8). The simplest way to do so is to replace $\mathbf{s}_j$ with a continuous n-component bosonic field $\boldsymbol{\phi}(\mathbf{x})$, enforcing a loose version of the constraint $\mathbf{s}_j^2 = 1$ by adding a potential $V_0(|\boldsymbol{\phi}|) = u(\boldsymbol{\phi}^2 - 1)^2$. We find thus a euclidean action of the form

$$S = -\int d^d\mathbf{x} \int d^d\mathbf{x}' \frac{\phi_j(\mathbf{x})\phi_j(\mathbf{x}')}{|\mathbf{x}-\mathbf{x}'|^{d+\sigma}} + \int d^d\mathbf{x}\, V_0\left(|\boldsymbol{\phi}(\mathbf{x})|\right). \tag{1.12}$$

By reabsorbing a quadratic term into the definition of $V(|\boldsymbol{\phi}|)$, we can write the kinetic term in the momentum space so that S takes the form

$$S = \int \frac{d^d\mathbf{q}}{(2\pi)^d}\omega(q)|\boldsymbol{\phi}(\mathbf{q})|^2 + \int d^d\mathbf{x}\, \left(r|\boldsymbol{\phi}(\mathbf{x})|^2 + u|\boldsymbol{\phi}(\mathbf{x})|^4\right), \tag{1.13}$$

where we introduce the long-range dispersion relation

$$\omega(q) = \int_{r>a} d^d\mathbf{r} J(r)\left(1 - e^{i\mathbf{q}\cdot\mathbf{r}}\right) \tag{1.14}$$

a being the ultraviolet cutoff of the theory. By dimensional analysis, it can be shown that the large wavelengths behavior of the above quantity is given by

$$\omega(q) \sim J(q^\sigma + a^{2-\sigma}q^2) \tag{1.15}$$

(see Appendix B for a detailed discussion in the $d = 2$ case), so that the large-distances continuous description of the model can be written as

$$S = \int \frac{d^d\mathbf{q}}{(2\pi)^d}(q^\sigma + g\, q^2)|\boldsymbol{\phi}(\mathbf{q})|^2 + \int d^d\mathbf{x}\, \left(r|\boldsymbol{\phi}(\mathbf{x})|^2 + u|\boldsymbol{\phi}(\mathbf{x})|^4\right). \tag{1.16}$$

At a Gaussian level ($u = 0$), long-range interactions become relevant for $\sigma < 2$, so that, $\sigma^* = 2$. The corresponding length dimension of the field $|\phi(\mathbf{q})|$ is given by

$$[\phi(\mathbf{x})] \sim L^{-(d-\sigma)/2} \tag{1.17}$$

for $\sigma < 2$, while

$$[\phi(\mathbf{x})] \sim L^{-(d-2)/2} \tag{1.18}$$

for $\sigma > 2$. If follows that, at criticality, for $\sigma < 2$, we have

$$\langle\phi(\mathbf{x})\phi(0)\rangle \sim \frac{1}{x^{d-\sigma}} = \frac{1}{x^{d-2+\eta(\sigma)}}, \tag{1.19}$$

with $\eta(\sigma) = 2 - \sigma$. Let us notice that $\eta(\sigma)$ it is an anomalous dimension only with respect to the usual definition, but it is already present on the Gaussian level. Thus, it can be thought of as a measure of how the correlations decay is different from the short-range mean-field case. As $[r] = L^{-\sigma}$ for $\sigma < 2$ we have that the correlation length ξ in proximity of the transition temperature T_c behaves as $|T - T_c| \sim \xi^{-\sigma}$ and

$$\nu(\sigma) = \frac{1}{\sigma}. \tag{1.20}$$

The exponent $\gamma(\sigma)$ of the magnetic susceptibility can be extracted by the scaling relation [29, 34, 35]

$$\gamma(\sigma) = \nu(\sigma)(2 - \eta(\sigma)) = 1, \tag{1.21}$$

i.e., independently on σ (and d), the value predicted by Landau's theory [36].

Let us now introduce interactions in our picture. By considering the term $\propto u$ in Eq. (1.16) as a perturbation of the Gaussian theory we have that, for $\sigma < 2$

$$\left[\phi^4\right] \sim L^{-2(d-\sigma)}, \tag{1.22}$$

so that the perturbation is irrelevant as long as $\sigma < d/2$. In this regime thus our results (1.19) and (1.20) becomes exact. Let us also notice that for $d \geq 4$ the Gaussian regime extends up to $\sigma = 2$.

Finally, for $d < 4$, the presence of a relevant interaction is expected to modify the value of σ^*. The problem has been addressed by Sak in his seminal paper Ref. [33] by means of the perturbative renormalization group (RG) around the $d = 4$, $\sigma = 2$ Gaussian fixed point, in terms of $\epsilon = d - 2\sigma$. For $\epsilon = 0$, the long-range term in

Eq. (1.16) is a marginal perturbation. One of the main findings is the observation that the $\propto q^\sigma |\boldsymbol{\phi}(\mathbf{q})|^2$ term in the action (1.16) does not acquire an anomalous scaling. Intuitively, this may be traced back to the fact that such a perturbative expansion can only generate integer powers of q^2, not affecting the non-analytic $\propto q^\sigma$ behavior. As a consequence, even in presence of interaction, the scaling dimension Δ_σ of the long-range kinetic term in the Hamiltonian is given by:

$$\Delta_\sigma = 2\Delta_\phi + \sigma. \tag{1.23}$$

By definition, however, in the short-range limit $\Delta_\phi = (d - 2 + \eta_{\rm sr})/2$, so that we have

$$\Delta_\sigma = d + \eta_{\rm sr} - 2 + \sigma. \tag{1.24}$$

We find then that the long-range perturbation is relevant for

$$\sigma < \sigma^* = 2 - \eta_{\rm sr}. \tag{1.25}$$

Let us notice how the above analysis predict that the scaling found in Eq. (1.19) is actually valid even outside of the mean-field region, up to σ^*, when $\eta(\sigma^*) = \eta_{\rm sr}$. The same does not happen for the exponent $\nu(\sigma)$ which may acquire an anomalous scaling. However, according to Sak's argument, $\nu(\sigma)$ is still a continuous function of σ, which interpolate between the mean field value for $\sigma = d/2$ and the short-range one for $\sigma = 2 - \eta_{\rm sr}$.

The validity of Sak's criterion for the classical $O(n)$ models has been the subject of considerable scrutiny. Indeed, numerical evidence supporting (or rejecting) Sak's result is notoriously hard to obtain [37–39]. Intense theoretical investigations both via Monte-Carlo simulations [37, 40, 41], renormalization group (RG) theory [42] and conformal bootstrap [43] appeared all to confirm the validity of Sak's conjecture for the long-range/short-range crossover [12, 44–46]. Let us notice, however how it is not clear whether Sak's criterion is useful in absence of a spontaneous-symmetry breaking in the short-range regime. While some examples of such low-dimensional model are worked out in the following, the status of the $d = 2$ XY model is particularly delicate, also due to the notorious difficulty of numerically detecting the BKT transition, and will be addressed in Chapter 2.

1.2.2 | The $d = 1$ long-range Ising model

The one-dimensional Ising model ($n = 1$, $d = 1$) is a good example of a model exhibiting a non-trivial short-range/long-range crossover, which can be nevertheless addressed easily [47–49]. In this case the lattice variables s_j can only take the values $s_j = \pm 1$, and the Hamiltonian (1.8) takes the form

$$\beta H = \frac{1}{2}\sum_{j\neq j'} J(r)\left(1 - s_j s_{j'}\right) = \frac{1}{4}\sum_{j\neq j'} J(r)\left(s_j - s_{j'}\right)^2, \tag{1.26}$$

where $r = |i - j|$ and, for $r >> 1$,

$$J(r) \sim J\, r^{-1-\sigma}. \tag{1.27}$$

Following Ref. [49], we notice that we can equivalently describe the model in terms of the domain walls or kinks, each one associated with a point of the dual lattice, defined as

$$m_j = \frac{1}{2}(s_{j+1} - s_j). \tag{1.28}$$

We notice that $m_j = -1, 0, 1$ and $m_j \neq 0$ only if there is a domain wall between the site j and the site $j+1$. Moreover, the m_j are actually constrained, since between any pair of sites with $m = 1$ there is necessarily a site with $m = -1$, and vice versa. In terms of the m_j the Hamiltonian (1.26) becomes

$$\beta H = \sum_{j \neq j'} U(r) m_j m_{j'} + \varepsilon_c \sum_j m_j^2, \tag{1.29}$$

where

$$\varepsilon_c = \sum_{r=1}^{\infty} J(r) > 0 \tag{1.30}$$

and $U(r)$ is such that

$$J(r) = U(r+1) + U(r-1) - 2U(r). \tag{1.31}$$

As in Hamiltonian (1.29) only the lattice sites corresponding to a pair of domain walls actually contribute, we can think of such sites as the position of a set of particles. Performing the continuum limit thus, it is thus possible to interpret the model as a gas of point-like charges, with alternating signs, moving on a line. While ε_c plays now the role of a chemical potential, $U(r)$ is an interacting potential such that

$$J(r) = \frac{d^2}{dr^2} U(r), \tag{1.32}$$

and then behaves asymptotically as

$$U(r) \sim -J \frac{r^{1-\sigma} - 1}{\sigma(1-\sigma)}. \tag{1.33}$$

The partition function can be written as a sum of sectors with different numbers of charges

$$Z = \sum_p y^p \int_{x_p > x_{p-1} > \cdots > x_1} dx_1 \cdots dx_p e^{-\sum_{k,k'} m_k m_{k'} U(x_k - x_{k'})} \tag{1.34}$$

where $y = e^{-\epsilon_c}$ is the fugacity of the gas, x_k is the position of the k-th kink and $m_k = (-1)^k$ its charge.

If $\sigma > 1$ the interaction vanishes at large distances, so that in the infrared the system behaves as a collection of free particles, so that the number of domain walls proliferates leading to a disordered phase at every temperature. If $\sigma < 1$, on the other hand, the interaction potential is confining, so that, at low temperatures, the charges arrange themselves as a collection of far-away pairs of opposite-charged particles interacting through residual dipole interactions. As the temperature is raised, the dipoles will eventually unbound, as the average size of a dipole becomes comparable with their average distance. This qualitative picture may be made rigorous by a real-space RG analysis in which the closest pairs of charges are perturbatively integrated out (see e.g. [48, 49]). It follows

$$\sigma^* = 1, \tag{1.35}$$

which is different from the mean-field value of $\sigma^* = 2$. Close to $\sigma = 1^-$ the critical exponents take the form

$$\eta(\sigma) = 2 - \sigma \qquad \nu(\sigma) = \frac{1}{\sqrt{2(1-\sigma)}}. \tag{1.36}$$

As expected, $\eta(\sigma)$, contrary to $\nu(\sigma)$, coincides with its mean-field value.

In spite of the fact that the short-range one-dimensional Ising model does not exhibit a phase transition, so that Sak's criterion is not straightforwardly useful, let us notice how the two-point critical correlation function

$$\langle s_i s_j \rangle \sim \frac{1}{|i-j|^{d-2+\eta(\sigma)}} = \frac{1}{|i-j|^{1-\sigma}}, \tag{1.37}$$

as $\sigma \to 1$, goes to $\langle s_i s_j \rangle \sim$ const, i.e. the same behavior of the short-range correlation function for $T = 0$. As for any one-dimensional $O(n)$ model the correlations are expected to decay as Eq. (1.37) as well, this suggests $\sigma^* = 1$ for such models as well.

1.2.3 | The long-range spherical model

In the nearest-neighbors case, the $n \to \infty$ limit of the $O(n)$ model is exactly solvable. In this limit, indeed, it can be shown [50] the unit vector variable $\mathbf{s}_\mathbf{j}$ can be replaced by a continuous variable s_j with a single global constraint of the form

$$\sum_{\mathbf{j}} s_{\mathbf{j}}^2 = N, \tag{1.38}$$

so that the $O(n)$ Hamiltonian can be replaced by the so-called spherical model [51, 52]. As the other $O(n)$ models with $n > 2$, it undergoes a second-order phase transition for $d > 2$, while its critical behavior becomes mean field for $d \geq 4$. For $2 < d < 4$ the critical exponents are given by

$$\eta_{\text{sr}} = 0 \qquad \nu_{\text{sr}} = \frac{1}{d-2} \tag{1.39}$$

The long-range counterpart of the model, described by the Hamiltonian

$$\beta H = -\frac{1}{2} \sum_{\mathbf{i} \neq \mathbf{j}} J(r) s_{\mathbf{i}} s_{\mathbf{j}} \tag{1.40}$$

with $r = |\mathbf{i} - \mathbf{j}|$, $J(r) \sim J r^{-d-\sigma}$ for $r >> 1$, has been addressed in [53].

As in the nearest-neighbors case, the constraint (1.38) can be enforced by introducing a Lagrange multiplier in the Hamiltonian (1.40), obtaining

$$\beta H = -\frac{1}{2} \sum_{\mathbf{i} \neq \mathbf{j}} s_{\mathbf{i}} s_{\mathbf{j}} + \mu \sum_{\mathbf{j}} s_{\mathbf{j}}^2, \tag{1.41}$$

and imposing that

$$\frac{1}{N} \sum_{\mathbf{j}} \left\langle s_{\mathbf{j}}^2 \right\rangle = 1. \tag{1.42}$$

In the momentum space, we have

$$\beta H = \sum_{\mathbf{q} \in IBZ} (\mu + \omega(\mathbf{q})) \, |s(\mathbf{q})|^2 \tag{1.43}$$

where, similarly to Eq. (1.14), $\omega(\mathbf{q})$ is the long-range dispersion relation

$$\omega(\mathbf{q}) = \sum_{\mathbf{r}} J(r)(1 - e^{i\mathbf{q}\cdot\mathbf{r}}); \tag{1.44}$$

and IBZ denotes the first Brillouin zone of the lattice. Eq. (1.42) becomes similarly

$$\frac{1}{N} \sum_{\mathbf{q} \in IBZ} \frac{1}{\mu + \omega(q)} = 1. \tag{1.45}$$

As the critical behavior is determined by the long-wavelength behavior, let us consider $q << 1$. In this regime, as in Sec. 1.2.1, we have that

$$\omega(q) \sim J(q^\sigma + g q^2), \tag{1.46}$$

so that for $\sigma > 2$ we recover the same dispersion relation of the short-range regime. Let us restrict ourselves to the region $\sigma < 2$, in this case, the constraint (1.44) can be approximated by

$$I(\mu, J) = \int_{q<\Lambda} \frac{d^d\mathbf{q}}{(2\pi)^d} \frac{1}{\mu + Jq^\sigma} = 1 \tag{1.47}$$

(Λ being an ultraviolet cutoff), without altering the critical behavior.

The phase transition corresponds to the value of J such that $\mu = 0$ and the theory is effectively massless. If $I(\mu, J)$ diverges for $\mu = 0$, μ will remain finite for every temperature, otherwise there will exist a critical temperature T_c such that, for $T < T_c$ we have a macroscopic occupation of the mode $q = 0$, signaling a finite magnetization. It follows that, in order to have spontaneous symmetry breaking we must have $d > \sigma$, so that the phase transition occurs for $\sigma < 1$ in $d = 1$, $\sigma < 2$ in $d = 2$. This implies $\sigma^* = 1$ in $d = 1$, $\sigma^* = 2$ in $d \geq 2$. This is in agreement with Sak's picture, as $\eta_{\text{sr}} = 0$ in $d > 2$, and with the general understanding of one-dimensional, long-range spin systems.

Close to the transition temperatures T_c we have that

$$I(\mu, J) \sim 1 + a_0(T - T_c) - a_1\mu^{d/\sigma-1} - a_2\mu. \tag{1.48}$$

For $\sigma < d/2$ we have that, close to the critical point

$$\mu \sim T - T_c \tag{1.49}$$

and, by noticing that $\mu \sim \xi^{-\sigma}$, we find that, as expected,

$$\nu(\sigma) = \frac{1}{\sigma}. \tag{1.50}$$

For $\sigma > d/2$, similarly we have

$$\mu \sim (T - T_c)^{d/\sigma-1} \tag{1.51}$$

which implies

$$\nu(\sigma) = \frac{1}{d - \sigma}, \tag{1.52}$$

which, for $d > 2$, correctly interpolates between the mean field value and the short-range one as σ varies from $\sigma_{\text{mf}} = d/2$ to $\sigma^* = 2$.

1.2.4 | Effective dimension

The key result of this Section may be tough of as if long-range interactions were able to effectively increase the dimensionality of the system. Intuitively, this makes sense,

as a long-range coupling increases the number of neighbors with which a given lattice site actually interacts.

Indeed, within Sak's picture, the qualitative critical behavior of the long-range $O(n)$ in the $\sigma < 2 - \eta_{\rm sr}$ regime can be related to the one of its nearest-neighbours counterpart in an effective fractional dimension d_{eff} such that [11]

$$d_{eff} = \frac{2 - \eta_{\rm sr}(d_{eff})}{\sigma} d. \tag{1.53}$$

As expected $d_{eff} > d$, and $d_{eff} = 4$ at $\sigma = d/2$, while $d_{eff} \to d$ as $\sigma \to \sigma^* = 2 - \eta_{sr}(d)$

Besides giving a qualitative understanding of what is going on, this picture provides quantitative insights into the critical behavior of the model. Indeed, as shown in Ref. [40], Eq. (1.53) can be obtained by assuming that, together with Sak's picture, a sort of super-universality holds, so that the exponent $\gamma(\sigma)$ (which is independent on σ in the Gaussian region) is a function of σ/d alone. By means of the scaling relations among critical exponents, we also find the following estimate for $\nu(\sigma)$

$$\nu(\sigma) = \frac{2 - \eta_{\rm sr}(d_{eff})}{\sigma} \nu_{\rm sr}(d_{eff}). \tag{1.54}$$

Let us notice that, both in the mean-filed regime ($d_{eff} \geq 4$) and in the $n \to \infty$ spherical limit, these relation become exact, as in both cases $\eta_{\rm sr}(d_{eff}) = 0$.

Even outside of the mean-field region, the super-universality hypotheses is valid at the first perturbative order in $\epsilon = \sigma - d/2$ [54]

$$\gamma(\sigma) \approx 1 + \frac{n+2}{n+8} \left(2 - \frac{d}{\sigma}\right), \tag{1.55}$$

while the second order of this expansion breaks the correspondence [44]. Eq. (1.54) can be derived from a functional renormalization group analysis, within a modified local potential ansatz [1, 11].

Here we will not address in detail the topic of quantum phase transitions in presence of long-range couplings. Even in this case, however, it is possible to extend the effective dimension picture [1]. In the nearest-neighbours case, it is known that the critical behavior of quantum rotor models [55] in dimension d is the same of those of a classical $O(n)$ model in dimension $D = d + 1$. Similarly, in the weak long-range regime, we can introduce an effective dimension D_{eff}

$$D_{eff} = \frac{2 - \eta_{\rm sr}(D_{eff})}{\sigma} d + 1, \tag{1.56}$$

valid for $\sigma < 2 - \eta_{\rm sr}(D_{eff})$. The correspondence becomes exact in the mean-field regime.

1.3 | Dynamical behavior

We now analyze the dynamic properties of long-range quantum systems, which will be the subject of Part II of the present work. The dynamics of closed quantum many-body-system have been the subject of thorough scrutiny in the last decades [56–58]. Generic non-integrable quantum systems are generally expected to reach the stationary microcanonical equilibrium. This behavior can be traced back to the spectral properties of the system, and in particular to the so-called eigenstate thermalization hypotheses[59, 60].

As remembered in Sec. 1.1, while this picture is not seriously hindered in the presence of weak long-range interaction [16, 17], systems interacting through strong long-range couplings are known to avoid thermalization in the thermodynamic limit [2]. Recently, such a behavior has been linked to their peculiar spectral structure [61], and in particular to the fact that the single-particle dispersion relation does not converge to a continuous function of the spectrum as in Eq. (1.14).

1.3.1 | Single-particle spectrum

In order to understand the spectral properties of strong long-range interacting systems, let us consider the simple case of a set of particles hopping in a one-dimensional chain with N sites

$$H = -\sum_{j\neq j'} J(r)\left(a_j a_{j'}^\dagger + a_j^\dagger a_{j'}\right) + \mu \sum_j a_j a_j^\dagger, \tag{1.57}$$

with $r = |j - j'|$, μ is the chemical potential. We are of course interested in the case of a strong long-range hopping so that we can choose

$$J(r) = \frac{1}{N_\alpha} r^{-\alpha}, \tag{1.58}$$

with $0 < \alpha < 1$ and

$$N_\alpha = \sum_{r\neq 0} J(r) \sim N^{1-\alpha} \tag{1.59}$$

enforces the Kac scaling. Neither the nature (bosonic or fermionic) of the particles nor the dimensionality of the system is crucial for what follows.

Hamiltonian (1.57) can be diagonalized by means of a Fourier transform. Assuming periodic boundary conditions ($a_j = a_{j+N}$) we have

$$H = -\sum_q \epsilon(q) a_q a_q^\dagger, \tag{1.60}$$

where the allowed momenta are $q = \frac{2\pi m}{N}$ with $m = -N/2 + 1, \dots N/2$ and

$$\epsilon(q) = \mu - \sum_{r \neq 0} J(r) \cos(qr). \tag{1.61}$$

Since

$$\sum_{r \neq 0} J(r) \cos(qr) = \frac{1}{N_\alpha} \sum_{r \neq 0} \cos(qr) r^{-\alpha}, \tag{1.62}$$

we can write the spectrum as

$$\epsilon(q) = \mu - \frac{t_q}{t_0}, \tag{1.63}$$

where

$$t_q = \sum_{r=1}^{N/2} \cos(qr) r^{-\alpha}. \tag{1.64}$$

It is now crucial to notice that the behavior of this Fourier sum is dramatically different from those of its weak long-range counterpart of Eq. (1.14). Indeed, by recalling that $k = \frac{2\pi}{N} q$, as $N \to \infty$, we have

$$\begin{aligned} t_q &= N^{1-\alpha} \sum_{r=1}^{N/2} N^{-1} \left(\frac{r}{N}\right)^{-\alpha} \cos \frac{2\pi m r}{N} \\ &= \left(\frac{N}{2\pi}\right)^{1-\alpha} \int_0^\pi ds \, \frac{\cos(ms)}{s^{-\alpha}} + O(1). \end{aligned} \tag{1.65}$$

In particular, as

$$t_0 = \left(\frac{N}{2\pi}\right)^{1-\alpha} \int_0^\pi ds \, s^{-\alpha} + O(1) = \left(\frac{N}{2\pi}\right)^{1-\alpha} \frac{\pi^{1-\alpha}}{1-\alpha} + O(1) \tag{1.66}$$

we have

$$\epsilon(q) = \mu - \frac{1}{u_\alpha} \int_0^\pi ds \, \frac{\cos(ms)}{s^{-\alpha}} \tag{1.67}$$

up to $O(N^{\alpha-1})$ corrections, with

$$u_\alpha = \frac{\pi^{1-\alpha}}{1-\alpha} \tag{1.68}$$

Let us notice how ϵ depends on q only through m, so that the spectrum does not converge to a continuous function of q. Rather, we have a finite gap between the ground state $\epsilon(0) = \mu - 1$ and the first excited states (corresponding to $|m| = 1$). For $|m| >> 1$ the eigenvalues accumulate around $\epsilon_\infty = \mu$ as the integral in Eq. (1.67)

in vanishes. This means that an extensive number of single-particle states is almost degenerate. In the limit $\alpha \to 0$ this degeneracy becomes exact $\forall\, m \neq 0$.

Let us now consider the spectral average of a regular function $G(x)$, namely

$$\langle G(\epsilon)\rangle = \frac{1}{N}\sum_q G(\epsilon(q)). \tag{1.69}$$

As $\epsilon(q)$ accumulates around μ, we expect that in the thermodynamic limit

$$\langle G(\epsilon)\rangle \to G(\mu). \tag{1.70}$$

This suggests that, as long as we are dealing with observables of this form, the case $0 < \alpha < 1$ behaves effectively as a fully-connected $\alpha = 0$ system in the thermodynamic limit. On the other hand, we expect this convergence to be faster for smaller values of α, so that the finite size scaling of this quantity is expected to give us information about how fast the spectrum converges to its limiting value (this quantity will moreover play an important role in Chapter 4, where it is shown that, for finite N, α may play a dramatic role).

Let us notice, however, how Eq. (1.67), being accurate only up to $O(N^{\alpha-1})$, is not reliable, so that we have to use the exact expressions of Eq. (1.63) and Eq. (1.64). By exploiting the latter ones, it follows that

$$\begin{aligned} \sum_q t(q) &= 0, \\ \sum_q t^2(q) &= \frac{N}{2}\sum_{r\neq 0} r^{-2\alpha}. \end{aligned} \tag{1.71}$$

Then, at the lowest non-trivial order

$$\langle G(\epsilon)\rangle \approx G(\mu) + \frac{G''(\mu)}{4t(0)^2}\sum_{r=1}^{N/2} r^{-2\alpha}. \tag{1.72}$$

In order to estimate this correction let us notice that $t(0) \sim N^{1-\alpha}$ and

$$\sum_{r=1}^{N/2} r^{-2\alpha} \sim N^{1-2\alpha} \tag{1.73}$$

for $\alpha < 1/2$, while

$$\sum_{r=1}^{N/2} r^{-2\alpha} \to \text{const} \tag{1.74}$$

for $1/2 < \alpha < 1$. It follows that the correction is of order N^{-1} if $\alpha < 1/2$ and of order $N^{2(1-\alpha)}$ for $1/2 < \alpha < 1$.

1.3.2 | Long-lived states

The key spectral properties found above for the case of a free system are expected to be robust against the presence of interactions. Indeed if we perturb Hamiltonian (1.57) with an interaction term H_{int}, we have [62]

$$E_n = E_n^0 + \left\langle \Psi_n^0 \right| H_{\text{int}} \left| \Psi_n^0 \right\rangle + \sum_{n' \neq n} \frac{|\left\langle \Psi_n^0 \right| H_{\text{int}} \left| \Psi_{n'}^0 \right\rangle|^2}{E_n^0 - E_{n'}^0} + O(H_{\text{int}}^3) \tag{1.75}$$

where E_n^0, $\left|\Psi_n^0\right\rangle$ are respectively the unperturbed eigenvalues and eigenvectors of the unperturbed Hamiltonian (1.57) (which are, in turn, given by the sum of the single-particle energies $\epsilon(q)$). The unperturbed energies can be labeled by the collection of single particles occupation numbers $n = \langle \nu(q) \rangle$, each relative to a given Fourier mode, so that

$$E_n = \sum_q \nu(q)\epsilon(q). \tag{1.76}$$

(in the fermionic case $\nu(q) = 0, 1$ while in the bosonic case $\nu(q) \in \mathbb{N}$). For a generic many-body system, the presence of a continuum of states in the single particle spectrum hinders the applicability of the usual perturbative result (1.75) for any finite perturbation, as the denominator in the sum becomes arbitrarily small in the thermodynamic limit. On the other hand, the peculiar form of our one particle spectrum (1.67) in the strong-long range regime leads to a different picture. Indeed: as in the thermodynamic limit the energy gap between adjacent states remains finite, weak enough perturbation will not alter the main features of the spectrum. In other words, the presence of a discrete spectrum is expected to be a generic feature of quantum many-body systems in presence of strong-long range interactions, so that the usual picture describing the thermalization in generic many-body systems breaks down. The fact that the single-particle energies accumulate around a finite value as $m \to \infty$ is crucial in stabilizing collective motion, avoiding the loss of coherence and allowing for the presence of long-lived quasi-stationary states [61]. Intuitively speaking, this can be understood by thinking that the effective number of non-commensurable frequencies in the system is small.

Similar results have been obtained for the dynamics of a quantum spin-1/2 Ising model in a parallel field, in presence of strong long-range interactions [63]. The model is described by the Hamiltonian

$$H = -\frac{1}{2N_\alpha} \sum_{j \neq j'} r^{-\alpha} \hat{\sigma}_x^j \hat{\sigma}_x^{j'} + h \sum_j \hat{\sigma}_x^j \,, \tag{1.77}$$

where $\hat{\sigma}_x^j$, $\hat{\sigma}_y^j$, $\hat{\sigma}_z^j$ are the Pauli operators relative to the site j, h is the magnetic field, $r = |j - j'|$, and $N_\alpha = \sum_{r \neq 0} r^{-\alpha}$ is the Kac rescaling. Exact results can be obtained for

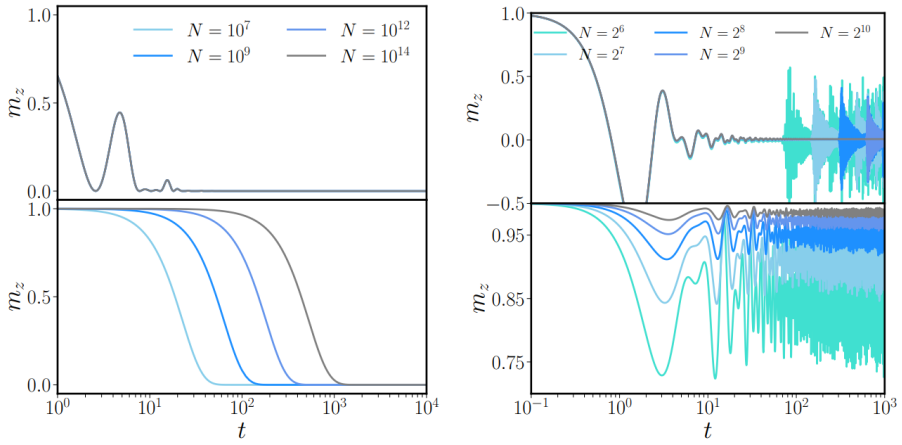

(a) Ising model (b) Kitaev chain

FIGURE 1.1: Evolution of the magnetization for the Ising Hamiltonian (1.77) and the Kitaev Hamiltonian (1.80) respectively after a quench $h = \infty$ to $h = 0$ for different values of the system size N. In the bottom panels we have $\alpha < 1$ ($\alpha = 0.5$ and $\alpha = 0.4$ respectively for the left and right panel) while in the top panel $\alpha > 1$ ($\alpha = 2$ and $\alpha = 12$ respectively for the left and right panel). The emergence of long-lived states in the strong long-range regime is apparent. From Ref. [1].

the dynamics of the transverse magnetization

$$\hat{m}_z = \frac{1}{N}\sum_j \hat{\sigma}_z, \tag{1.78}$$

provided that the initial state corresponds to $|\Psi(0)\rangle = |\rightarrow, \cdots \rightarrow\rangle$ (i.e. to the ground state of the $h = \infty$ Hamiltonian). We have

$$\langle \hat{m}_z \rangle (t) = \langle \hat{m}_z \rangle (0) \cos(2ht) \prod_{j=1}^{N} \cos^2 \left(N_\alpha^{-1} j^{-\alpha} \right). \tag{1.79}$$

For $h = 0$, the above expression describes a relaxation from the initial value to $\langle m_z \rangle (t) = 0$; however, because of the diverging factor N_α, coming from the Kac rescaling, the timescale on which such relaxation happens diverges with N, so that in the thermodynamic limit the system is trapped in a quasi-stationary state. Similar results can be obtained studying the corresponding dynamics of a the strong long-range Kitaiev chain [1]

$$H = -\frac{1}{2N_\alpha}\sum_{j\neq j'} r^{-\alpha}(c_j + c_j^\dagger)(c_{j'} + c_{j'}^\dagger) - h\sum_j (1 - 2c_j^\dagger c_j) \tag{1.80}$$

where c_j are fermionic operators ($[c_j, c'_j]_- = \delta_{j,j'}$).

Besides this very general consideration, long-lived oscillations may also arise, in the thermodynamic limit, as it is the case of Eq. (1.79) for $h \neq 0$, in which they may be interpreted as a global Larmor precession. This is also the case of the fully-connected Ising model in a transverse field (i.e. the so-called LMG model), addressed in Sec. 1.3.3. In any case, the peculiar spectral properties of strong long-range prevent thermalization, which seems to be a distinctive feature of such systems.

1.3.3 | Dynamical phases in the LMG model

As a paradigmatic example of the dynamics of an interacting strong long-range system, let us consider the fully-connected ($\alpha = 0$) version of the quantum spin-1/2 Ising model in a transverse magnetic field. The model was first introduced by Lipkin, Meskhov and Glick in Ref. [26] in the context of nuclear physics (and thus sometimes referred to as the LMG model) and it has become an important tool for the study of strong-long range quantum systems [64–67]. It is described by the Hamiltonian

$$H = -\frac{1}{4N}\sum_{j\neq j'}\hat{\sigma}_x^j\hat{\sigma}_x^{j'} + h\sum_j \hat{\sigma}_z^j \,, \tag{1.81}$$

where h is the magnetic field and $\hat{\sigma}_x^j$, $\hat{\sigma}_y^j$, $\hat{\sigma}_z^j$ are the Pauli operators relative to the site j

$$[\sigma_a^j, \sigma_b^k] = 2i\delta_{j,k}\,\epsilon_{abc}\sigma_c^k \tag{1.82}$$

In order to understand the main features of such system, here we want to analyse the quench dynamic of a the model which at $t = 0^-$ is in the ground state with $h = 0$, namely $|\Psi(0)\rangle = |\rightarrow, \ldots, \rightarrow\rangle$, after a finite magnetic field is switched on at $t = 0$. By introducing the global spin

$$\hat{S}_a = \frac{1}{2}\sum_j \hat{\sigma}_a^j \,, \tag{1.83}$$

we may write the Hamiltonian (1.81) as

$$H = -\frac{1}{N}\hat{S}_x^2 + 2h\hat{S}_z. \tag{1.84}$$

In the thermodynamic limit the $\hat{S}_a$ become classical spins [66]. In particular, if we introduce the magnetization

$$\hat{m_a} = \frac{2}{N}\hat{S}_a \tag{1.85}$$

we have that $[\hat{m}_a, \hat{m}_b] = O(1/N)$. In the thermodynamic limit, we may replace them with classical variables m_a which, because of our choice of the initial conditions, are

constrained on a sphere ($m_x^2 + m_y^2 + m_z^2 = 1$). The equation of motion for the m_a become

$$\dot{\mathbf{m}} = -(m_z \hat{\mathbf{x}} + 2h\hat{\mathbf{z}}) \times \mathbf{m}, \tag{1.86}$$

with initial conditions $m_x(0) = 1$, $m_y(0) = m_z(0) = 0$. The spherical constraint can be solved by introducing $I \in [0, 1]$ and $\phi \in [-\pi, \pi]$ such that

$$(m_x, m_y, m_z) = (\sqrt{1 - I^2}\cos\phi, \sqrt{1 - I^2}\sin\phi, I). \tag{1.87}$$

In term of the new variables, Eqs. (1.86) become the Hamilton equation associated with the classical Hamiltonian

$$\mathcal{H} = -\frac{1}{2}(1 - I^2)\cos^2\phi + 2hI, \tag{1.88}$$

where I and ϕ play the role of a canonical conjugate pair

$$\{\phi, I\} = 1. \tag{1.89}$$

In terms of the new variables the initial conditions read $I(0) = 0$, $\phi(0) = 0$, so that the dynamics in the (I, ϕ) phase space is described by

$$(1 - I^2)\cos^2\phi - 4hI = 1. \tag{1.90}$$

Depending on the value of h Eq. (1.90) describes a different kind of dynamics: for $h < h_c = 1/4$ we have a libration, as ϕ oscillates around two limiting values $\pm\phi_{\max}$; for $h > h_c = 1/4$ we have a rotation, in which the angle ϕ is allowed to go from $-\pi$ to π; for $h = h_c = 1/4$ we have a separatrix. Anyway, for $\forall\, h \neq h_c$ the motion is periodic, while the period diverges for $h \to 1$. By introducing, as an order parameter,

$$\bar{m}_x = \frac{1}{T}\int_0^T dt\; m_x(t), \tag{1.91}$$

(T being the period of the oscillation). As this is non-zero for $h < h_c$, while vanishes for $h > h_c$, the phenomenon can be seen as a dynamical phase transition between a ferromagnetic and a paramagnetic phase.

While the above analysis is exact for $\alpha = 0$, $N \to \infty$, its robustness against finite-size effect and competing short-range interactions has been recently addressed in Refs. [67, 68]. For large, but finite, values of N, the semiclassical analysis shows that such oscillatory behavior is damped on a timescale t_Q which grows as a N for $h \neq h_c$, while at criticality

$$t_Q \sim \ln N, \tag{1.92}$$

which can be interpreted as a signature of chaotic behavior. Similarly, the presence of competing short-range coupling leads to the formation of an intermediate chaotic region. In Chapter 4 it is shown how these phenomena can be explained in terms of parametric resonances and linked to the peculiar spectral properties of such systems (Sec. 1.3.1).

References

[1] N. Defenu *et al.* "Long-range interacting quantum systems". *arXiv preprint arXiv:2109.01063* (2021).

[2] A. Campa, T. Dauxois, D. Fanelli, and S. Ruffo. *Physics of Long-Range Interacting Systems*. Oxford Univ. Press, 2014.

[3] D. Mukamel. "Statistical mechanics of systems with long range interactions". *AIP Conference Proceedings*. Vol. 970. 1. American Institute of Physics. 2008, pp. 22–38.

[4] D. Lynden-Bell. "Statistical Mechanics of Violent Relaxation in Stellar Systems". *Mon. Not. R. Astron. Soc.* 136 (1 1967). doi: 10.1093/mnras/136.1.101.

[5] C. Monroe *et al.* "Programmable quantum simulations of spin systems with trapped ions". *Rev. Mod. Phys.* 93 (2 Apr. 2021), p. 025001. doi: 10.1103/RevModPhys.93.025001.

[6] J. W. Britton *et al.* "Engineered two-dimensional Ising interactions in a trapped-ion quantum simulator with hundreds of spins". *Nature* 484(7395) (2012), pp. 489–492.

[7] M. A. Baranov, M. Dalmonte, G. Pupillo, and P. Zoller. "Condensed matter theory of dipolar quantum gases". *Chemical Reviews* 112(9) (2012), pp. 5012–5061.

[8] R. Landig *et al.* "Quantum phases from competing short-and long-range interactions in an optical lattice". *Nature* 532(7600) (2016), pp. 476–479.

[9] F. Mivehvar, F. Piazza, T. Donner, and H. Ritsch. "Cavity QED with quantum gases: new paradigms in many-body physics". *Adv. Phys.* 70(1) (Jan. 2021), 1â153. issn: 1460-6976. doi: 10.1080/00018732.2021.1969727.

[10] M. Kac, G. E. Uhlenbeck, and P. C. Hemmer. "On the van der Waals Theory of the Vapor-Liquid Equilibrium. I. Discussion of a One-Dimensional Model". *Journal of Mathematical Physics* 4(2) (Feb. 1963), pp. 216–228. doi: 10.1063/1.1703946.

[11] N. Defenu, A. Trombettoni, and A. Codello. "Fixed-point structure and effective fractional dimensionality for $O(N)$ models with long-range interactions". *Phys. Rev. E* 92(5) (Nov. 2015), p. 052113.

[12] N. Defenu, A. Trombettoni, and S. Ruffo. "Criticality and phase diagram of quantum long-range $O(N)$ models". *Phys. Rev. B* 96(10) (Sept. 2017), p. 104432. doi: 10.1103/PhysRevB.96.104432.

[13] S. Chandrasekhar. *Principles of stellar dynamics*. Courier Corporation, 2005.

[14] S. GUPTA and S. RUFFO. "The world of long-range interactions: A birdâs eye view". *International Journal of Modern Physics A* 32(09) (2017), p. 1741018.

[15] M. JOYCE and T. WORRAKITPOONPON. "Relaxation to thermal equilibrium in the self-gravitating sheet model". *Journal of Statistical Mechanics: Theory and Experiment* 2010(10) (2010), P10012.

[16] M. VAN REGEMORTEL, D. SELS, and M. WOUTERS. "Information propagation and equilibration in long-range Kitaev chains". *Physical Review A* 93(3) (2016), p. 032311.

[17] A. CHANDRAN, A. NANDURI, S. GUBSER, and S. SONDHI. "Equilibration and coarsening in the quantum O (N) model at infinite N". *Physical Review B* 88 (Apr. 2013). DOI: 10.1103/PhysRevB.88.024306.

[18] P. HAUKE and L. TAGLIACOZZO. "Spread of correlations in long-range interacting quantum systems". *Physical review letters* 111(20) (2013), p. 207202.

[19] M. G. NEZHADHAGHIGHI and M. RAJABPOUR. "Entanglement dynamics in short-and long-range harmonic oscillators". *Physical Review B* 90(20) (2014), p. 205438.

[20] J. SCHACHENMAYER, B. LANYON, C. ROOS, and A. DALEY. "Entanglement growth in quench dynamics with variable range interactions". *Physical Review X* 3(3) (2013), p. 031015.

[21] N. DEFENU, T. ENSS, M. KASTNER, and G. MORIGI. "Dynamical critical scaling of long-range interacting quantum magnets". *Physical review letters* 121(24) (2018), p. 240403.

[22] N. DEFENU, G. MORIGI, L. DELL'ANNA, and T. ENSS. "Universal dynamical scaling of long-range topological superconductors". *Physical Review B* 100(18) (2019), p. 184306.

[23] M. SEUL and D. ANDELMAN. "Domain shapes and patterns: the phenomenology of modulated phases". *Science* 267(5197) (1995), pp. 476–483.

[24] D. C. BRYDGES and P. A. MARTIN. "Coulomb systems at low density: A review". *Journal of Statistical Physics* 96(5) (1999), pp. 1163–1330.

[25] H. SPOHN and W. ZWERGER. "Decay of the Two-Point Function in One-Dimensional $O(N)$ Spin Models with Long-Range Interactions". *J. Stat. Phys.* 94(5-6) (Mar. 1999), pp. 1037–1043. DOI: 10.1023/A:1004595419419.

[26] H. J. LIPKIN, N. MESHKOV, and A. GLICK. "Validity of many-body approximation methods for a solvable model:(I). Exact solutions and perturbation theory". *Nuclear Physics* 62(2) (1965), pp. 188–198.

[27] S. Schütz and G. Morigi. "Prethermalization of Atoms Due to Photon-Mediated Long-Range Interactions". *Phys. Rev. Lett.* 113 (20 Nov. 2014), p. 203002. DOI: 10.1103/PhysRevLett.113.203002.

[28] M. Antoni and S. Ruffo. "Clustering and relaxation in Hamiltonian long-range dynamics". *Physical Review E* 52(3) (1995), p. 2361.

[29] J. Cardy. *Scaling and Renormalization in Statistical Physics*. Cambridge University Press, 1996.

[30] N. D. Mermin and H. Wagner. "Absence of ferromagnetism or antiferromagnetism in one-or two-dimensional isotropic Heisenberg models". *Physical Review Letters* 17(22) (1966), p. 1133.

[31] J. M. Kosterlitz and D. J. Thouless. "Ordering, metastability and phase transitions in two-dimensional systems". *J. Phys. C* 6(7) (Apr. 1973), pp. 1181–1203. DOI: 10.1088/0022-3719/6/7/010.

[32] V. L. Berezinskii. "Destruction of Long-range Order in One-dimensional and Two-dimensional Systems Possessing a Continuous Symmetry Group. II. Quantum Systems". *Sov. Phys. JETP* 34 (1972), p. 610.

[33] J. Sak. "Recursion Relations and Fixed Points for Ferromagnets with Long-Range Interactions". *Phys. Rev. B* 8(1) (July 1973), pp. 281–285. ISSN: 0556-2805. DOI: 10.1103/PhysRevB.8.281.

[34] A. Z. Patashinskii. "Fluctuation theory of phase transitions" (1979).

[35] N. Goldenfeld. *Lectures on phase transitions and the renormalization group*. CRC Press, 2018.

[36] L. D. Landau and E. M. Lifshitz. *Statistical Physics: Volume 5*. Vol. 5. Elsevier, 2013.

[37] E. Luijten and H. W. Blöte. "Boundary between long-range and short-range critical behavior in systems with algebraic interactions". *Physical review letters* 89(2) (2002), p. 025703.

[38] T. Blanchard, M. Picco, and M. Rajabpour. "Influence of long-range interactions on the critical behavior of the Ising model". *EPL (Europhysics Letters)* 101(5) (2013), p. 56003.

[39] P. Grassberger. "Two-dimensional SIR epidemics with long range infection". *Journal of statistical physics* 153(2) (2013), pp. 289–311.

[40] M. C. Angelini, G. Parisi, and F. Ricci-Tersenghi. "Relations between short-range and long-range Ising models". *Physical Review E* 89(6) (2014), p. 062120.

[41] T. HORITA, H. SUWA, and S. TODO. "Upper and lower critical decay exponents of Ising ferromagnets with long-range interaction". *Physical Review E* 95(1) (2017), p. 012143.

[42] E. BREZIN, G. PARISI, and F. RICCI-TERSENGHI. "The crossover region between long-range and short-range interactions for the critical exponents". *Journal of Statistical Physics* 157(4) (2014), pp. 855–868.

[43] C. BEHAN, L. RASTELLI, S. RYCHKOV, and B. ZAN. "A scaling theory for the long-range to short-range crossover and an infrared duality". *Journal of Physics A: Mathematical and Theoretical* 50(35) (2017), p. 354002.

[44] E. LUIJTEN. PhD thesis. Technische Universiteit Delft, 1997.

[45] N. DEFENU, A. CODELLO, S. RUFFO, and A. TROMBETTONI. "Criticality of spin systems with weak long-range interactions". *Journal of Physics A Mathematical General* 53(14), 143001 (Apr. 2020), p. 143001. DOI: 10.1088/1751-8121/ab6a6c.

[46] A. DUTTA and J. BHATTACHARJEE. "Phase transitions in the quantum Ising and rotor models with a long-range interaction". *Physical Review B* 64(18) (2001), p. 184106.

[47] P. W. ANDERSON and G. YUVAL. "Exact Results in the Kondo Problem: Equivalence to a Classical One-Dimensional Coulomb Gas". *Phys. Rev. Lett.* 23 (2 July 1969), pp. 89–92. DOI: 10.1103/PhysRevLett.23.89.

[48] J. M. KOSTERLITZ. "Phase Transitions in Long-Range Ferromagnetic Chains". *Phys. Rev. Lett.* 37 (23 Dec. 1976), pp. 1577–1580. DOI: 10.1103/PhysRevLett.37.1577.

[49] J. L. CARDY. "One-dimensional models with $1/r^2$ interactions". *Journal of Physics A: Mathematical and General* 14(6) (June 1981), pp. 1407–1415. DOI: 10.1088/0305-4470/14/6/017.

[50] M. KAC and C. J. THOMPSON. "Spherical model and the infinite spin dimensionality limit". *Physica Norvegica* 5(3-4) (1971), pp. 163–168.

[51] T. H. BERLIN and M. KAC. "The spherical model of a ferromagnet". *Physical Review* 86(6) (1952), p. 821.

[52] R. J. BAXTER. *Exactly solved models in statistical mechanics*. Elsevier, 2016.

[53] G. JOYCE. "Spherical model with long-range ferromagnetic interactions". *Physical Review* 146(1) (1966), p. 349.

[54] M. FISHER, S. MA, and B. NICKEL. "Critical exponents for long-range interactions". *Physical Review Letters* 29(14) (1972), p. 917.

[55] S. SACHDEV. "Quantum phase transitions". *Physics world* 12(4) (1999), p. 33.

[56] A. Polkovnikov, K. Sengupta, A. Silva, and M. Vengalattore. "Colloquium: Nonequilibrium dynamics of closed interacting quantum systems". *Reviews of Modern Physics* 83(3) (2011), p. 863.

[57] L. D'Alessio, Y. Kafri, A. Polkovnikov, and M. Rigol. "From quantum chaos and eigenstate thermalization to statistical mechanics and thermodynamics". *Advances in Physics* 65(3) (2016), pp. 239–362.

[58] J. v. Neumann. "Beweis des Ergodensatzes und desH-Theorems in der neuen Mechanik". *Zeitschrift für Physik* 57(1) (1929), pp. 30–70.

[59] J. M. Deutsch. "Quantum statistical mechanics in a closed system". *Physical review a* 43(4) (1991), p. 2046.

[60] M. Srednicki. "Chaos and quantum thermalization". *Physical review e* 50(2) (1994), p. 888.

[61] N. Defenu. "Metastability and discrete spectrum of long-range systems". *Proceedings of the National Academy of Sciences* 118(30) (2021). issn: 0027-8424. doi: 10.1073/pnas.2101785118.

[62] J. J. Sakurai and E. D. Commins. *Modern quantum mechanics, revised edition*. 1995.

[63] M. Kastner. "Diverging equilibration times in long-range quantum spin models". *Physical Review Letters* 106(13) (2011), p. 130601.

[64] P. Ribeiro, J. Vidal, and R. Mosseri. "Thermodynamical limit of the Lipkin-Meshkov-Glick model". *Physical review letters* 99(5) (2007), p. 050402.

[65] J. I. Latorre, R. Orús, E. Rico, and J. Vidal. "Entanglement entropy in the Lipkin-Meshkov-Glick model". *Physical Review A* 71(6) (2005), p. 064101.

[66] A. Das, K. Sengupta, D. Sen, and B. K. Chakrabarti. "Infinite-range Ising ferromagnet in a time-dependent transverse magnetic field: Quench and ac dynamics near the quantum critical point". *Physical Review B* 74(14) (2006), p. 144423.

[67] A. Lerose *et al.* "Impact of nonequilibrium fluctuations on prethermal dynamical phase transitions in long-range interacting spin chains". *Physical Review B* 99(4) (2019), p. 045128.

[68] A. Lerose *et al.* "Chaotic dynamical ferromagnetic phase induced by nonequilibrium quantum fluctuations". *Physical review letters* 120(13) (2018), p. 130603.

Part I

2 | The long-range XY model in two dimensions

In this chapter we analyze the critical behavior of the XY model (i.e. the $O(2)$ model) in two dimensions when long-range couplings are added. The description of such a behavior has been a long-standing problem within the field of the long-range $O(n)$ models.

The Chapter is based on the Refs. [69–71] and it is structured as follows: in Sec. 2.1 we introduce the model and briefly recap the main results known in the nearest-neighbors regime. In Secs. 2.2 to 2.5, we examine the peculiar nature of the crossover between long-range and short-range regimes, with various methods. The main result of these sections is a set of perturbative renormalization-group (RG) equations describing the infrared behavior of the model. In Sec. 2.6 these results are used to derive the phase diagram of the model, which features a non-trivial interplay between a novel ordered phase and the usual quasi-long-range ordered BKT phase. The transition line is characterized by a non-trivial, unprecedented, scaling of the order parameter. Finally, in Sec. 2.7 we examine the relationship between the $d = 2$ classical XY model and the $d = 1$ quantum XXZ chain, showing how our results can be used to make predictions about the $T = 0$ phase diagram of the latter.

2.1 | The XY model

The model consists of a set of N planar spins $\mathbf{s}_j$, such that $\mathbf{s}_j^2 = 1$, arranged in a two-dimensional square lattice, interacting through an $O(2)$-invariant quadratic Hamiltonian, which can be obtained by putting $n = 2$, $d = 2$ in Eq. (1.8). By exploiting the constraint on the single spin variable, it is convenient to parameterize its state by introducing the phase θ_j as $\mathbf{s}_j \equiv (\cos\theta_j, \sin\theta_j)$, obtaining,

$$\beta H = \frac{1}{2} \sum_{i \neq j} J(r) \left[1 - \cos(\theta_i - \theta_j) \right] \tag{2.1}$$

with $\mathbf{i}, \mathbf{j} \in \mathbb{Z}^2$, $\mathbf{r} = \mathbf{i} - \mathbf{j}$, $r = |\mathbf{r}|$ and

$$J(r) \sim J r^{-2-\sigma} \tag{2.2}$$

for $r \gg 1$. We will moreover assume $\sigma > 0$ so that the thermodynamic quantities are extensive. In terms of the angular variables $\theta_\mathbf{j}$ the $O(2)$ symmetry becomes a global translational symmetry $\theta_\mathbf{j} \to \theta_\mathbf{j} + \alpha$. Moreover, the model is characterized by the periodicity of the phases $\theta_\mathbf{j}$, which results in the local symmetry

$$\theta_\mathbf{j} = \theta_\mathbf{j} + 2\pi N_\mathbf{j} \tag{2.3}$$

where, for each $\mathbf{j}$, $N_\mathbf{j} \in \mathbb{Z}$.

Let us remind briefly the properties of the $\sigma \to \infty$ limit, i.e. the nearest-neighbors regime. In this case, we may derive the possibility of a spontaneous symmetry-breaking (SSB) is ruled out by the Hohenberg-Mermin-Wagner theorem; however the low-temperature phase is characterized by quasi-long-range-order, i.e. power-law behavior in the connected correlations functions with a temperature-dependent exponent $\eta_{\text{sr}}(T)$. In their seminal paper [31], Kosterlitz and Thouless linked this behavior to a peculiar structure of the renormalization-group (RG) flow of the model, which exhibits a line of non-isolated Gaussian fixed points, which become unstable for certain values of the couplings (the so-called BKT transition). This means that, below a transition temperature T_{BKT}, the model is well described by a corresponding quadratic model, whose excitations are described in terms of spin waves (the so-called low-temperature, or Berezinskii, expansion [32]). The breaking down of such an approximation has been described in terms of the proliferation of topological, vortex-like, configurations of the spins $\mathbf{S}_\mathbf{j}$.

When the decay of the couplings is slow enough, we expect a SSB phase to appear at low temperature. This crossover between the short-range and long-range regime is not straightforwardly described by Sak's criterion [33], whose applicability is hindered by the peculiar structure of the BKT RG flow, which does not feature isolated fixed points. The correlation exponent $\eta_{\text{sr}}(T)$ latter, in turn, does not obey the common definition of anomalous dimension at a symmetry-breaking transition and, except for $T = T_{\text{BKT}}$, is not universal.

In the nearest-neighbors regime the effect of vortices can be understood by a real-space renormalization group, by mapping the Hamiltonian into a Coulomb gas of point-like charges [72, 73]; or within the formalism of the statistical field theory, by mapping it into a Sine-Gordon model [73, 74]. These mappings can be obtained by decomposing the spin-wave and the topological excitation or, more rigorously, through the so-called duality construction [75]. Unfortunately, both these procedures break down for slowly decaying coupling (the latter already in the case of next-to-nearest-neighbors couplings). Another way of obtaining the same mappings is the so-called Villain approximation [76, 77] (i.e. the substitution of Hamiltonian

(2.4) with a quadratic one which takes into account the phase periodicity). However, as shown in Chapter 3 of this work, there is reason to believe that this latter Hamiltonian is no longer in the same universality class for sufficiently slow-decaying couplings.

Finally, let us notice that numerically results are hard to obtain for two order of reasons. First, the large number of non-vanishing couplings makes Monte-Carlo updates computationally expensive. Second, even at the level of long-range interaction, the BKT scaling is notoriously hard to see for small sizes (the so-called *Texas state's argument*, see Refs. [78–80])

2.2 | Low temperature expansion

For $T < T_{BKT}$, the nearest-neighbours XY model flows in the infrared to an effective Gaussian description so that its behavior is captured by the Berezinskii approximation [32] in which the cosine in Eq. (2.1) is expanded to the second order. Analogously, we expect the long-range version of the model to be well described by a similar approximation for low enough temperatures. By expanding H we get then

$$\beta H \sim \frac{1}{4} \sum_{\mathbf{i} \neq \mathbf{j}} J(r) \left(\theta_{\mathbf{i}} - \theta_{\mathbf{j}}\right)^2 . \tag{2.4}$$

This can be diagonalized by means of a Fourier transform

$$\theta_{\mathbf{q}} = \frac{1}{\sqrt{N}} \sum_{\mathbf{j}} e^{-i\mathbf{q}\cdot\mathbf{j}}\, \theta_{\mathbf{j}} \qquad \theta_{\mathbf{j}} = \frac{1}{\sqrt{N}} \sum_{\mathbf{q} \in IBZ} e^{i\mathbf{q}\cdot\mathbf{j}}\, \theta_{\mathbf{q}}. \tag{2.5}$$

We obtain

$$\beta H \sim \frac{1}{2} \sum_{\mathbf{q} \in IBZ} \omega(\mathbf{q}) |\theta_{\mathbf{q}}|^2, \tag{2.6}$$

where we introduced, as before, the long-range dispersion relation

$$\omega(\mathbf{q}) = \sum_{\mathbf{r}} J(\mathbf{r}) \Big(1 - \cos(\mathbf{q} \cdot \mathbf{r})\Big). \tag{2.7}$$

If we are interested in the long-wavelength modes, we can approximate the above sum with an integral, obtaining:

$$\omega(q) = \int_{r>a} d^2\mathbf{r} J(r) \Big(1 - \cos(\mathbf{q} \cdot \mathbf{r})\Big). \tag{2.8}$$

As shown in Appendix A, this quantity grows as $\omega(q) \sim q^2$ if $\sigma > 2$, while it shows a non-analitic behavior $\omega(q) \sim q^\sigma$ for $\sigma < 2$. The difference between the two regimes can be fully appreciated if we consider the two-point correlation function:

$$\langle \mathbf{s}_\mathbf{r} \cdot \mathbf{s}_0 \rangle = \langle \cos(\theta_\mathbf{r} - \theta_0) \rangle \,. \tag{2.9}$$

Being the theory quadratic in this approximation, the above quantity can be evaluated quite easily by exploiting the identity $\langle \cos A \rangle_0 = e^{-\frac{1}{2}\langle A^2 \rangle_0}$. From Eq. (2.6), it follows immediately that $\left\langle \theta_\mathbf{q} \theta_{\mathbf{q}'} \right\rangle_0 = \delta_{\mathbf{q}+\mathbf{q}'} \omega(\mathbf{q})^{-1}$ so that we find $\langle \cos(\theta_\mathbf{r} - \theta_0) \rangle = e^{-G(\mathbf{r})}$ with

$$G(\mathbf{r}) = \frac{1}{2} \left\langle (\theta_0 - \theta_\mathbf{r})^2 \right\rangle_0 = \frac{1}{N} \sum_{\mathbf{q} \in IBZ} \frac{1 - \cos(\mathbf{q} \cdot \mathbf{r})}{\omega(\mathbf{q})}. \tag{2.10}$$

The long-distance behavior can be once again captured by replacing the sum with an integral

$$G(r) = a^2 \int_{q<\Lambda} \frac{d^2\mathbf{q}}{(2\pi)^2} \frac{1 - \cos(\mathbf{q} \cdot \mathbf{r})}{\omega(q)}, \tag{2.11}$$

where we approximated the first Brillouin zone with a sphere of radius $\Lambda = \sqrt{8\pi} a^{-1}$, so that its volume is preserved, i.e. $\int_{q<\Lambda} d^2\mathbf{q} = (2\pi)^2 a^{-2}$. As shown in Appendix A, the asymptotic behavior of $G(r)$ depends on σ. In particular, if $\sigma > 2$ we have

$$G(r) \sim \eta(J) \ln \frac{r}{a} + A J^{-1} \tag{2.12}$$

with $\eta(J) = p/J$, and A, p are non-universal constants (see a study of these constants in [69]). If $\sigma < 2$ instead, we have that

$$G(r) \sim A J^{-1}. \tag{2.13}$$

Then, depending on whether $\sigma < 2$ or $\sigma > 2$ we have that the correlation $\langle \mathbf{s}_\mathbf{r} \cdot \mathbf{s}_0 \rangle \sim$ const or $\langle \mathbf{s}_\mathbf{r} \cdot \mathbf{s}_0 \rangle \sim r^{-\eta(J)}$ respectively. In the latter case then, we recover the short-range low-temperature BKT [32] behavior, in which the correlations decay as a power law with a temperature-dependent exponent. The former case, instead, gives rise to a finite-magnetization ordered phase, with

$$m^2 = \lim_{r \to \infty} \langle \mathbf{s}_\mathbf{r} \cdot \mathbf{s}_0 \rangle = \lim_{r \to \infty} e^{-G(r)}. \tag{2.14}$$

This argument then suggests that $\sigma_* = 2$. If compared with Sak's criterion, this implies an effective anomalous exponent $\eta = 0$. Let us notice, however, how the low-temperature approximation *per se* is unable to describe the topological configurations, since $\theta_\mathbf{i}$ is no longer a phase, and thus no longer defined up to multiples of 2π. As a consequence, even in the short-range case, the approximation is unable to correctly reproduce all the phenomenology of the BKT transition.

2.3 | Self-consistent approach

The simplest way to improve the low-temperature approximation is to replace the quadratic Hamiltonian (2.4), obtained by expanding the cosine in Eq. (2.1), with a temperature-dependent effective one, obtained self-consistently through the request of the minimization of a variational free energy with respect to the true Hamiltonian (2.1). In the nearest-neighbors case, such a self-consistent-harmonic-approximation (SCHA) is able to foresee the breaking down of the Berezinskii approximation above a certain temperature [81, 82] as in this case the variational coupling $\tilde{J}$ jumps discontinuously to zero as the temperature increases. In retrospect, the success of such a crude approximation traces back to the fact that the model behaves effectively as a Gaussian theory for all $T < T_{BKT}$. We want now to extend this analysis to the long-range XY model.

To achieve this scope, we replace the cosine in the original Hamiltonian (2.4) with a quadratic term

$$\beta H_0 = \frac{1}{4} \sum_{\mathbf{i},\mathbf{j}} \tilde{J}(\mathbf{r})(\theta_\mathbf{i} - \theta_\mathbf{j})^2, \tag{2.15}$$

$\tilde{J}(r)$ being a completely arbitrary function of $\mathbf{r} = \mathbf{i} - \mathbf{j}$, to be determined from free energy minimization in a self-consistent way.

The quadratic Hamiltonian H_0 induces the Boltzmann measure

$$\langle \cdot \rangle_0 = \frac{1}{Z_0} \int \prod_\mathbf{j} d\theta_\mathbf{j} \, e^{-\beta H_0}, \tag{2.16}$$

where

$$Z_0 = e^{-\beta F_0} = \int \prod_\mathbf{j} d\theta_\mathbf{j} \, e^{-\beta H_0} \tag{2.17}$$

is the partition function of the model. The variational principle establishes that our best ansatz minimizes the variational free energy

$$\mathcal{F} = \beta F_0 + \beta \langle H \rangle_0 - \beta \langle H_0 \rangle_0 . \tag{2.18}$$

On the other hand, from the equipartition theorem it follows that $\langle H_0 \rangle_0 = \frac{N}{2\beta}$ is independent on the choice of $\tilde{J}(\mathbf{r})$, so that we can safely ignore it. Let us notice moreover that H_0 has the same quadratic structure of the low-temperature Hamiltonian, so that we can diagonalize H_0 as well by means of the Fourier transform

$$\beta H_0 = \frac{1}{2} \sum_{\mathbf{q} \in IBZ} \tilde{\omega}(\mathbf{q}) |\theta_\mathbf{q}|^2, \tag{2.19}$$

where $\tilde{\omega}(\mathbf{q})$ is given by Eq. (2.7) with $J(r)$ replaced by $\tilde{J}(r)$. Since, $\langle \cos A \rangle_0 = e^{-\frac{1}{2}\langle A^2 \rangle_0}$, as valid for every Gaussian measure, we find

$$\begin{aligned} \beta \langle H \rangle_0 &= -\frac{1}{2} \sum_{\mathbf{i},\mathbf{j}} J(r) \left\langle \cos\left(\theta_{\mathbf{i}} - \theta_{\mathbf{j}}\right) \right\rangle_0 \\ &= -\frac{1}{2} \sum_{\mathbf{i},\mathbf{j}} J(r) e^{-\frac{1}{2}\left\langle (\theta_{\mathbf{j}} - \theta_{\mathbf{j}})^2 \right\rangle_0} \\ &= -\frac{N}{2} \sum_{\mathbf{r}} J(r) e^{-\tilde{G}(|\mathbf{j}-\mathbf{i}|)} \\ &= -\frac{N}{2} \sum_{\mathbf{r}} J(r) e^{-\tilde{G}(\mathbf{r})}, \end{aligned} \tag{2.20}$$

where $\tilde{G}(\mathbf{r})$ is given by Eq. (2.10) with $\omega(q)$ replaced by $\tilde{\omega}(q)$. Finally, the first term on the r.h.s can be also computed easily from the diagonal form (2.19) of H_0:

$$\beta F_0 = \frac{1}{2} \sum_{\mathbf{q} \in IBZ} \ln \omega(\mathbf{q}). \tag{2.21}$$

Plugging this result into the expression for $\mathcal{F}$, we find that the variational free energy takes the form

$$\mathcal{F} = \frac{1}{2} \sum_{\mathbf{q} \in IBZ} \ln \tilde{\omega}(\mathbf{q}) - \frac{N}{2} \sum_{\mathbf{r}} J(r) e^{-\tilde{G}(\mathbf{r})}, \tag{2.22}$$

In order to simplify the notation, in the following we will drop the $\sim$ symbol for $\omega(\mathbf{q})$.

Since in Eq. (2.22) $\tilde{J}(\mathbf{r})$ appears only through the $\omega(\mathbf{q})$, in order to find the minimum is sufficient to derive $\mathcal{F}$ with respect to the latter. By exploiting the fact that

$$\frac{\delta \tilde{G}(\mathbf{r})}{\delta \omega(\mathbf{q})} = -\frac{1}{N} \frac{1 - \cos(\mathbf{q} \cdot \mathbf{r})}{\omega(\mathbf{q})^2}, \tag{2.23}$$

we find

$$\frac{\delta \mathcal{F}}{\delta \omega(\mathbf{q})} = \frac{\omega(\mathbf{q}) - \sum_r J(r) \left(1 - \cos(\mathbf{q} \cdot \mathbf{r})\right) . e^{-G(\mathbf{r})}}{2\omega(\mathbf{q})^2}. \tag{2.24}$$

By using the definition (2.7) of $\omega(q)$ and noticing that the above expression has to be valid for each value of $\mathbf{q} \in IBZ$, we find the condition

$$J(r) = \tilde{J}(\mathbf{r}) e^{\tilde{G}(\mathbf{r})}. \tag{2.25}$$

Since we are interested in the large length-scales regime (i.e in the continuum limit), we can assume $\tilde{J}$ to be a function of r only: in this case, indeed, $\tilde{G}(\mathbf{r})$ only depends

on the modulus r as well, so that the above condition can be written in terms of single variable functions

$$J(r) = \tilde{J}(r)e^{\tilde{G}(r)}. \tag{2.26}$$

Let us notice how, in this limit, one has to redefine $\mathbf{r} \to a\mathbf{r}$, $\mathbf{q} \to a^{-1}\mathbf{q}$, $J, \tilde{J} \to a^{-2}J, a^{-2}\tilde{J}$.

Let us now discuss the possible solutions of Eq. (2.26). The possible asymptotic behaviors of $\omega(q)$ and $\tilde{G}(q)$ in terms of σ are examined in Appendix A. We have that:

- If $\tilde{J}(r)$ decays at infinity faster than r^{-4} (e.g. an exponential or a fast-decaying power law), then we have that $\tilde{G}(r) \sim \ln(r)$ as $r \to \infty$. Since in this case $e^{\tilde{G}(r)}$ is a power law, it follows from Eq. (2.26) that $\tilde{J}(r)$ must behave asymptotically as a power-law as well. We can then assume that for large r

  $$\tilde{J}(r) \sim \tilde{J}r^{-2-s} \tag{2.27}$$

  for some $s > 2$ to be determined, so that

  $$\tilde{G}(r) \sim \eta(\tilde{J}) \ln \frac{r}{a} + A\tilde{J}^{-1}, \tag{2.28}$$

  where $\eta(\tilde{J}) = p\tilde{J}^{-1}$ and A, p are non-universal constants. Finally, from Eq. (2.26), we have the conditions

  $$\sigma = s - \eta(\tilde{J}); \qquad J = \tilde{J}e^{A/\tilde{J}}. \tag{2.29}$$

  In this case the correlation functions decay as $e^{-\tilde{G}(r)} \sim r^{-\eta(\tilde{J})}$. Then, as long as $\tilde{J}$ is non-vanishing, we find a quasi-long-range order, characteristic of the BKT phenomenology.

- If the variational coupling behaves as $\tilde{J}(r) \sim \tilde{J}r^{-2-s}$ with $s \in (0, 2)$, then $G(r) = A\tilde{J}^{-1} + O(r^{s-2})$. In this case we then have:

  $$\sigma = s; \qquad J = \tilde{J}e^{A/\tilde{J}}, \tag{2.30}$$

  leading to correlations behaving as $e^{-\tilde{G}(r)} \sim e^{-A\tilde{J}^{-1}}$. Then as long as $\tilde{J}$ is non-vanishing, we find a finite magnetization $\sim e^{-A\tilde{J}^{-1}/2}$.

In both cases, the equation for $\tilde{J}$ has the same form of the nearest-neighbour case. By introducing $\tilde{J} = Ax$, $J = Ay$ it can be written as:

$$y = xe^{1/x}. \tag{2.31}$$

The minimum of the r.h.s. term is in correspondence of $x = 1, y = e$ so that we have two solutions for $J > J_c \equiv eA$, and only the trivial solution for $J < J_c$, signaling a

jump in $\tilde{J}$ from $\tilde{J}_c = A$ to zero. However, only the larger of the two solutions present for $J > J_c$ is physically acceptable. Indeed it is the only one to have the correct asymptotic behavior $\tilde{J}(r) \sim J(r)$ in the large J regime, in which our SCHA becomes the low-temperature approximation studied in Sec. III. The meaning of this low-temperature, finite $\tilde{J}$ phase, however, depends on the whether $s < 2$ (ordered phase) or $s > 2$ (quasi-long-range-ordered BKT phase). Let us notice that, in the latter case, we have that $\eta = p\tilde{J}^{-1}$ of Eq. (2.28) cannot be larger than a given value $\eta_c = p\tilde{J}_c^{-1}$. As a consequence we have that:

- For $\sigma > 2$, the only possibility is that $s = \sigma + \eta_{\text{sr}} > 2$. We are then in the first case, so that we get the usual BKT phenomenology. (see [69] for further details).
- For $\sigma < 2 - \eta_c$, the only possibility is that $s = \sigma$ with $s < 2$. We are then in the second case, i.e. we find a finite magnetization for low temperature.
- For $2 - \eta_c < \sigma < 2$ both solutions are actually viable so that it is unclear whether the system is in the ordered or in the quasi-long-range ordered phase. To establish which solution should we choose we should compute $\mathcal{F}$ on both solutions. The dependence of $\mathcal{F}$ on the non-universal details of the model, and in particular on the short-range behavior of $\tilde{J}(r)$, hinders the possibility to reach a definite conclusion for this regime within the SCHA.

Although non-conclusive, our self-consistent analysis accounts for the possibility of the existence of an intermediate region, in which the ordered phase or the BKT behavior can prevail, depending on the temperature. Keeping in mind the results of the Berezinskii approximation, it appears sensible to think that the magnetized phase will prevail at lower temperatures, while the quasi-long-range ordered phase will, possibly, correspond to an intermediate range of temperature. Let us notice, however, that the predictions of our analysis are non-universal and, thus, their quantitative outcome depends on the peculiar model under study. Moreover, the first-order phase transition foreseen for $\sigma < 2 - \eta_c$ could be an artifact of the approximation, since the critical behavior of the model is known to be captured by the mean-field approximation for $\sigma < 1$, which foresees a second-order phase transition, see e.g. Ref. [12].

2.4 | Field-theoretical approach

In order to go beyond the limits of the SCHA, and capture the universal quantities we are interested in, we resort to a field-theoretical approach, introducing a continuous action, which encodes the same physics of our Hamiltonian (2.4). Indeed, both the low-temperature approximation and the SCHA are incapable to reproduce the local

symmetry (2.3) and, ultimately, to capture the periodic nature of the phase θ. In the nearest neighbors case, the main consequence of this is that the approximation does not take into account the topological configurations in which, following a closed loop on the plane, the phase θ increases by an integer multiple of 2π. In the long-range regime, we expect the same problem to arise also for non-topological configurations, as the Hamiltonian couples pairs of sites which are far away. We want then to derive a field theory that correctly takes into account the periodic nature of the phase θ in the long-range regime.

First, we write the coupling as $J(r) = J^S(r) + J_{LR} r^{-(2+\sigma)}$, $J^S(r)$ being a short-range term which accounts for the small-distances behavior. This decomposition allows us to refine our low-temperature approximation. This, in fact, is fully justified for the short-range coupling, even at intermediate temperatures, since it couples neighboring sites. At the same time, it can become problematic for the long-range part of the Hamiltonian, which couples far-away pairs: there can instead be smooth configurations for which the phase difference $\theta_\mathrm{i} - \theta_\mathrm{j}$ is not necessarily small, and these configurations may give a significant contribution to the Hamiltonian in an intermediate range of temperatures. Let us remember, however, how this approximation *a là* Berezinskii is unable to capture the presence of vortices even in the short-range regime.

To further proceed, we expand the cosine in the short-range part

$$1 - \cos(\theta_\mathrm{i} - \theta_\mathrm{j}) \approx \frac{1}{2}\left(\theta_\mathrm{i} - \theta_\mathrm{j}\right)^2 \approx \frac{1}{2}|\nabla\theta|^2, \tag{2.32}$$

where the last substitution is justified by the fact that in the short-range part of the Hamiltonian only neighbouring lattice sites are important. We then find

$$S[\theta] = \frac{J}{2}\int d^2x |\nabla\theta|^2 + S_{LR}[\theta], \tag{2.33}$$

where we introduced the long-range perturbation

$$S_{LR} = J_{\mathrm{LR}} \int d^2x \int_{r>a} \frac{d^2r}{r^{2+\sigma}} [1 - \cos\left(\theta(\mathbf{x}) - \theta(\mathbf{x}+\mathbf{r})\right)]. \tag{2.34}$$

In turn, this term can be rewritten in terms of the fractional Laplacian, whose definition is given, along with the details of the calculation, in Appendix B. We obtain

$$S_{LR} = \frac{g}{2}\int d^2x\, e^{-i\theta}\, \nabla^\sigma e^{i\theta}, \tag{2.35}$$

with $g = J_{\mathrm{LR}}/\gamma_{2,\sigma}$ and $\gamma_{2,\sigma} = 2^\sigma \Gamma(\frac{1+\sigma}{2})\pi^{-1}|\Gamma(-\frac{\sigma}{2})|^{-1}$. This term is intrinsically interacting. Moreover it is invariant under global translations $\theta(\mathbf{x}) \to \theta(\mathbf{x}) + \alpha$,

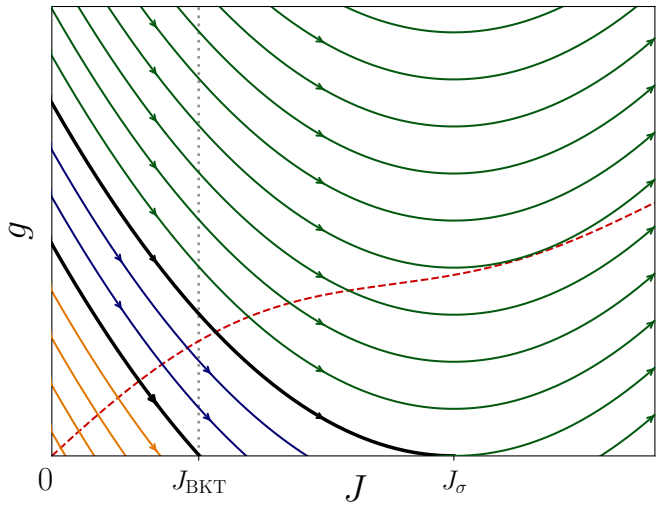

FIGURE 2.1: Sketch of the RG flow lines for $\frac{7}{4} < \sigma < 2$ in the $y = 0$ section. The dashed red line is a possible realization of the physical parameters line, from which the flow starts, as the temperature is varied. On the right/left of the gray dotted line the vortex fugacity y is irrelevant/relevant ($\dot{y}_\ell / y_\ell \gtrless 0$). We see that the two separatrices (bold black lines) divide the flow in three regions: an high-temperature region (orange lines), where the flow ends up in the disordered phase, the intermediate one (blue lines), where the flow reaches one of the stable fixed points and the low-temperature region (green lines), in which the long-range perturbation brings the system away from the critical line.

and it correctly catches the fact that the field θ is periodic. However, because of the kinetic term in $S[\theta]$, the whole action still does not correctly describes topological phenomena.

Let us remind briefly of the $g = 0$ case. Here one can introduce vortices in Eq. (2.33) i.e. evaluating the energy cost of a vortex configuration, and the core energy cost of a single vortex ε_c, which can be absorbed into the definition of the vortex fugacity $y = \exp(-\varepsilon_c)$. Since topological and non-topological configurations decouple in the quadratic part of the action, this leads to the Coulomb gas picture and to the well-known Kosterlitz-Thouless RG equations [31]. In turn, this implies that all the fixed points for $y = 0$ and $J > \frac{2}{\pi}$, which correspond to a Gaussian massless action, are stable. There, the low-temperature approximation becomes correct (with the original $J(T)$ replaced by the one corresponding to the fixed point), so that the power-law scaling observed for the two-point functions is recovered. For $J < \frac{2}{\pi}$, however, vortices become relevant and the theory flows towards the disordered regime.

In order to study the transition between the short-range and the long-range regime,

we can consider the effect of a small g deformation of the Gaussian fixed points. In this case, we expect to be able to parametrize our theory in terms of three parameters: J, g and y. In the next section, we will derive the RG flow perturbatively in y, g. However, we provide here an argument to understand what one can expect on general grounds. First, we notice that the fixed points with $J < \frac{2}{\pi}$ are already unstable under topological perturbations so that we will stick to the stable fixed line with $J > \frac{2}{\pi}$. Here, the long-range perturbation can be relevant or not depending on the scaling dimension Δ_g of the coupling g, $g_\ell \approx \exp(\Delta_g \ell)$ for $\ell \gg 1$, where $\ell = \ln(r/a)$ is the RG time.

Due to the quadratic nature of the measure, one has

$$\left\langle e^{i\left(\theta(\mathbf{x})-\theta(\mathbf{x}')\right)}\right\rangle = e^{-\frac{1}{2}\left\langle(\theta(\mathbf{x})-\theta(\mathbf{x}'))^2\right\rangle} = |\mathbf{x}-\mathbf{x}'|^{-\eta_{\mathrm{sr}}(J)}, \tag{2.36}$$

where $\eta_{\mathrm{sr}}(J) = \frac{1}{2\pi J}$ corresponds to the exponent of the two-point function for $g = 0$ [31, 77, 83]. Then

$$\Delta_g = 2 - \sigma - \eta_{\mathrm{sr}}(J). \tag{2.37}$$

The long-range perturbation is relevant only in the regime $\sigma < 2 - \eta_{\mathrm{sr}}(J)$. This bears some similarly with the SSB case [11], but with the main difference that the anomalous dimension is temperature dependent.

For $\sigma > 2$, the long-range term is always irrelevant. For $\sigma < 2$ Eq. (2.37) predicts that the long-range perturbation is always relevant at low enough temperatures. Since the points which are stable under the proliferation of vortices are those with $J > \frac{2}{\pi}$, we have that $0 < \eta_{\mathrm{sr}} < \frac{1}{4}$, as in the usual BKT theory (which indeed corresponds to the $g = 0$ theory). As a consequence, for $\frac{7}{4} < \sigma < 2$, we have that it exists an intermediate range of values of J for which the Gaussian theory is stable with respect to both the topological and the long-range perturbations, leading to conventional quasi-long-range order in a given temperature window. Instead, for $\sigma < 7/4$ the BKT stable fixed line is completely swallowed by the action of the long-range perturbation, so that our perturbative picture breaks down. However, it is sensible to assume that in this regime the system simply undergoes an order-disorder phase transition.

This picture is essentially in agreement with the results of the SCHA. However, our results no longer depend on the regularization procedure or the exact form of $J_S(r)$ and are genuinely universal.

2.5 | Renormalization procedure

Our observation can be made rigorous by computing the RG flow of the action (2.33) perturbatively around the short-range gaussian point. Let us then consider the action

$S[\theta]$ written as

$$S[\theta] = \int d^2x \left(\frac{J_\ell}{2} |\nabla\theta|^2 + \frac{g_\ell}{2} \int_{r>a} \frac{d^2r}{r^{2+\sigma}} \left[1 - \cos\left(\Delta_{\mathbf{r}}\theta(\mathbf{x})\right)\right] \right) \tag{2.38}$$

with $\Delta_{\mathbf{r}}\theta(\mathbf{x}) = \theta(\mathbf{x}+\mathbf{r}) - \theta(\mathbf{x})$. We are going to compute the RG flow equations perturbatively in g and in the vortex fugacity y. Let us notice, however, how the effect of vortices is not encoded in Eq. (2.38). On the other hand, at the first perturbative order in y and g the two perturbations act independently, so that we can consider the effect of the renormalization of the vortices on the short-range kinetic term only. As usual in this case, one can map this theory into the Sine-Gordon action [73, 74]:

$$S_{\mathrm{SG}} = \int d^2\mathbf{x} \left(\frac{1}{2J_\ell} |\nabla\varphi|^2 - y_\ell \cos 2\pi\varphi \right). \tag{2.39}$$

At the first order of the renormalization group, y varies according to the scaling dimension of the vertex operator $\cos(2\pi\varphi)$

$$\frac{dy_\ell}{d\ell} = (2 - \pi J)y, \tag{2.40}$$

while J_ℓ is left unchanged. This is in agreement with the Kosterlitz-Thouless RG for the short-range, in which $\dot{J} = O(y^2)$.

Let us now consider the first-order effect of the long-range perturbation: in this case we can set $y = 0$. We can then write the field $\theta(\mathbf{x})$ as the sum of a fast-varying and a slow-varying component. In particular, introducing the momentum cutoff $\Lambda = \frac{2\pi}{a}$, we have $\theta = \theta^> + \theta^<$ with

$$\begin{aligned} \theta^<(\mathbf{x}) &= \int_{q<\Lambda e^{-d\ell}} \frac{d^2q}{(2\pi)^2} \theta(\mathbf{q}) e^{i\mathbf{q}\cdot\mathbf{x}} \\ \theta^>(\mathbf{x}) &= \int_{\Lambda>q>\Lambda e^{-d\ell}} \frac{d^2q}{(2\pi)^2} \theta(\mathbf{q}) e^{i\mathbf{q}\cdot\mathbf{x}}, \end{aligned} \tag{2.41}$$

and integrate out $\theta^>$. The non-Gaussian part of the action can be expanded in cumulant: at the first order we have

$$S_{\mathrm{efb}}[\theta^<] = S_0[\theta^<] + \langle S_{\mathrm{LR}} \rangle_> + O(g^2). \tag{2.42}$$

Because of the $\mathbb{Z}_2$ symmetry in θ, we can make the replacement

$$\cos(\Delta_{\mathbf{r}}\theta) \to \cos\left(\Delta_{\mathbf{r}}\theta^>\right) \cos\left(\Delta_{\mathbf{r}}\theta^<\right), \tag{2.43}$$

finding, up to immaterial constants,

$$\langle S_{\mathrm{LR}} \rangle_> = \frac{g_\ell}{2} \int d^2x \int \frac{d^2r}{r^{2+\sigma}} \left\langle \cos\left(\Delta_{\mathbf{r}}\theta^>\right) \right\rangle_> \left[1 - \cos\left(\Delta_{\mathbf{r}}\theta^<\right)\right] \tag{2.44}$$

(from now on we let the integration run from $r = 0$). Exploiting the identity $\langle \cos(\Delta_{\mathbf{r}}\theta^{>})\rangle_{>} = e^{-\frac{1}{2}\left\langle(\theta(\mathbf{r})-\theta(0))^2\right\rangle_{>}}$, valid on the Gaussian measure, one has

$$\begin{aligned}\frac{1}{2}\left\langle(\theta(\mathbf{r})-\theta(0))^2\right\rangle_{>} &= \int_{\Lambda>q>\Lambda e^{-d\ell}} \frac{d^2q}{(2\pi)^2}\frac{1-\cos(\mathbf{q}\cdot\mathbf{r})}{J_\ell q^2} \\ &= \frac{d\ell}{2\pi J_\ell}\Big(1-\mathcal{J}_0(\Lambda r)\Big),\end{aligned} \tag{2.45}$$

where we denoted with $\mathcal{J}_0(x)$ the zeroth-order Bessel function of the first kind. Then, remembering that $\eta_{\rm sr}(J) = \frac{1}{2\pi J_\ell}$, we have

$$\begin{aligned}\left\langle\cos\left(\Delta_{\mathbf{r}}\theta^{>}\right)\right\rangle_{>} &= e^{-\eta_{\rm sr}(J_\ell)d\ell\,(1-\mathcal{J}_0(\Lambda r))} \\ &= 1-\eta_{\rm sr}(J_\ell)d\ell+\eta_{\rm sr}(J_\ell)d\ell\,\mathcal{J}_0(\Lambda r)\end{aligned} \tag{2.46}$$

The first two terms provide, as expected, an anomalous dimension of the coupling g, namely $g_{\ell+d\ell} = g_\ell e^{-\eta_{\rm sr}(J_\ell)d\ell}$. The last term, however, results in a new term in the action of the form

$$\begin{aligned}\left\langle S_g\right\rangle_{>} =& \frac{1}{2}\int d^2x\Bigg\{\int\frac{d^2r}{r^{2+\sigma}} g e^{-\eta_{\rm sr}(J_\ell)d\ell}\left[1-\cos\left(\Delta_{\mathbf{r}}\theta^{<}\right)\right] \\ &+g\eta_{\rm sr}(J_\ell)d\ell\int\frac{d^2r}{r^{2+\sigma}}\mathcal{J}_0(\Lambda r)\left[1-\cos\left(\Delta_{\mathbf{r}}\theta^{<}\right)\right]\Bigg\}.\end{aligned} \tag{2.47}$$

The second term of l.h.s. has the same form of the original XY form. However, for $x \gg 1$ $\mathcal{J}_0(x) \sim x^{-1/2}\cos(x-\pi/4)$ so that this effective interaction has a fast-decaying oscillating behavior. Since this act as a natural cutoff for $r \sim \Lambda^{-1} \sim a$ this can be interpreted as an additional local interaction, and reabsorbed into the short-range part of $S[\theta]$. One natural way to proceed is to expand $1-\cos(\Delta_r\theta) \approx \frac{1}{2}(\mathbf{r}\cdot\nabla_{\mathbf{x}}\theta)^2$ so that

$$\int\frac{d^2r}{r^{2+\sigma}}\mathcal{J}_0(\Lambda r)(\mathbf{r}\cdot\nabla_{\mathbf{x}}\theta^{<})^2 = \pi|\nabla_{\mathbf{x}}\theta^{<}|^2\int_a^{\Lambda^{-1}} dr r^{1-\sigma}\mathcal{J}_0(\Lambda r). \tag{2.48}$$

For $\sigma > \frac{1}{2}$ the integral is infrared convergent so that one can neglect the cutoff (this is safe, since we are interested in the $\sigma > 7/4$ regime). Finally, putting $r = au$, we find the correction of the action as

$$\frac{C_\sigma}{2}(g_\ell a^{2-\sigma})\eta_{\rm sr}(J_\ell)d\ell\int d^2x|\nabla_{\mathbf{x}}\theta^{<}|^2, \tag{2.49}$$

where $C_\sigma = \frac{\pi}{2}\int_1^\infty du u^{1-\sigma}\mathcal{J}_0(2\pi u) > 0$. However, the precise expression of the coefficient is not important for what follows.

Summarizing, we found that the effect of the integration over the fast modes can be reabsorbed, at the first order in g,y, into a redefinition of the couplings $g \to g+dg$, $J \to g + dJ$ with

$$\begin{aligned} dg &= -\eta_{\rm sr}(J_\ell) g_\ell d\ell \\ dJ &= C_\sigma \eta_{\rm sr}(J_\ell)(g_\ell a^{2-\sigma}) d\ell . \end{aligned} \tag{2.50}$$

Finally, we ought to perform the rescaling $\mathbf{x} \to \mathbf{x}e^{-d\ell}$, in order to obtain a theory with the same cutoff as the original one. Then g, J are further modified by their own bare length-dimension (namely $2-\sigma$ and 0)

$$\begin{aligned} dg &= (2 - \sigma - \eta_{\rm sr}(J_\ell)) g_\ell d\ell \\ dJ &= C_\sigma \eta_{\rm sr}(J_\ell)(g_\ell a_0^{2-\sigma}) d\ell . \end{aligned} \tag{2.51}$$

Together with Eq. (2.40), we get to the desired set of equations:

$$\begin{aligned} \frac{dy_\ell}{d\ell} &= (2 - \pi J_\ell) y_\ell , \\ \frac{dg_\ell}{d\ell} &= \left(2 - \sigma - \frac{1}{2\pi J_\ell}\right) g_\ell , \\ \frac{dJ_\ell}{d\ell} &= C_\sigma \eta_{\rm sr}(J_\ell) g_\ell , \end{aligned} \tag{2.52}$$

(we absorbed the dimensional part $a^{2-\sigma}$ into the definition of the constant C_σ). Let us notice how our naive dimensional argument was able to correctly guess the first two equations, but not the third one, i.e. the renormalization of the spin-waves stiffness.

2.6 | Analysis of the RG flow

Let us now analyse the set of Eqs. (2.52) in some detail. In particular, for $7/4 < \sigma < 2$, we find a line of stable quadratic fixed points for $g = y = 0$ and $J_{\rm BKT} \equiv \frac{2}{\pi} < J < J_\sigma \equiv \frac{1}{2\pi(2-\sigma)}$, as expected. The behavior of y_ℓ, at this order, is completely determined by J and, as long as $J > J_{\rm BKT}$, $y_\ell \to 0$.

Then, for $7/4 < \sigma < 2$ we can characterize the transition between the ordered phase and the quasi-long-range ordered one by looking at the $y = 0$ plane. As long as g is small, we can explicitly identify the form of the flow trajectories of Eqs. (2.52):

$$g_\ell(J) = \frac{\pi(2-\sigma)}{C_\sigma} \left[(J_\ell - J_\sigma)^2 + k \right] . \tag{2.53}$$

If $k < 0$ the trajectory arrives at the fixed point line $g = 0$ for some $J < J_\sigma$, while for $k > 0$ the trajectory starts from the $g = 0$ line for $J > J_\sigma$ and it goes to infinity,

signaling the existence of a new, low-temperature, phase. The separatrix is given by the semi-parabola with $k = 0$, $J \leq J_\sigma$. The graphical depiction of the RG flow of Eqs. (2.52), in the $y = 0$ plane, is shown in Fig. 2.1.

Being Eqs. (2.52) a perturbative result we derived for small g_ℓ and y_ℓ, its use in the low temperature region ($T < T_c$) is not justified, as g_ℓ grows indefinitely. However, for $T \to T_c^-$, the amount of time spent by the flow in the region close to $J = J_\sigma$, $g = 0$ becomes larger and larger, so that the scaling behavior of g_ℓ with T in this regime can be reliably obtained from Eqs. (2.52). In order to derive such a scaling, let us notice that we can obtain the formal solution for g_ℓ

$$g_\ell = g e^{(2-\sigma)\ell} e^{-\int \eta_{\rm sr}(J_\ell) d\ell}, \tag{2.54}$$

which is a reliable as long as g_ℓ is small. Now let us consider a RG flow which starts very close to the critical temperature T_c: the corresponding trajectory will follow the separatrix up to the vicinity of the fixed point $g = 0, J = J_\sigma$, which is given by Eq. (2.53) with $k \to 0^+$. We now consider a point in the flow ℓ^* such that $g(\ell^*)$ is small and $J(\ell^*) > J_\sigma$. Then

$$\begin{aligned} \int_0^{\ell^*} \eta_{\rm sr}(J_\ell) d\ell &= \int_{J_0}^{\ell^*} \eta_{\rm sr}(J) \frac{dJ}{\dot{J}} = C_\sigma^{-1} \int_{J_0}^{\ell^*} \frac{dJ}{g(J)} \\ &= \pi(2-\sigma) \int_{J_0}^{J(\ell^*)} \frac{dJ}{(J-J_\sigma)^2 + k} \end{aligned} \tag{2.55}$$

Let us consider now the physical bare parameter J_0 as a function of the temperature. This will cross the separatrix ($k \to 0^+$) for some $J_c < J_\sigma$ (which corresponds to T_c) so that $k \sim T_c - T$. In this case the second order singularity J_σ lies within the integration interval of Eq. (2.55), so that the integral diverges as $k^{-1/2}$ as $k \to 0^+$. Then we have

$$g_{\ell^*} \sim e^{-B(T-T_c)^{-1/2}}, \tag{2.56}$$

where B is a non universal constant.

Although the infrared regime is beyond the reach of our perturbative analysis, it is possible to guess the corresponding form taken by the action on physical grounds. Indeed, the coupling J diverges there, suppressing spatial fluctuations of the phase $\theta(\mathbf{x})$, as confirmed by the rigorous results of Ref. [84], which predict a finite magnetization for low enough temperatures. This suggests that, in the infrared region corresponding to the low-temperature phase, we are allowed to Taylor expand the exponential in Eq. (2.33), so that the action becomes

$$S_{\rm LR} = -\frac{g}{2} \int d^2\mathbf{x}\, \theta \nabla^\sigma \theta, \tag{2.57}$$

where we absorbed in g some immaterial constants. A further evidence in favour of this action comes from the fact that, in the limit $J \to \infty$, we have $\Delta_g = 2 - \sigma -$

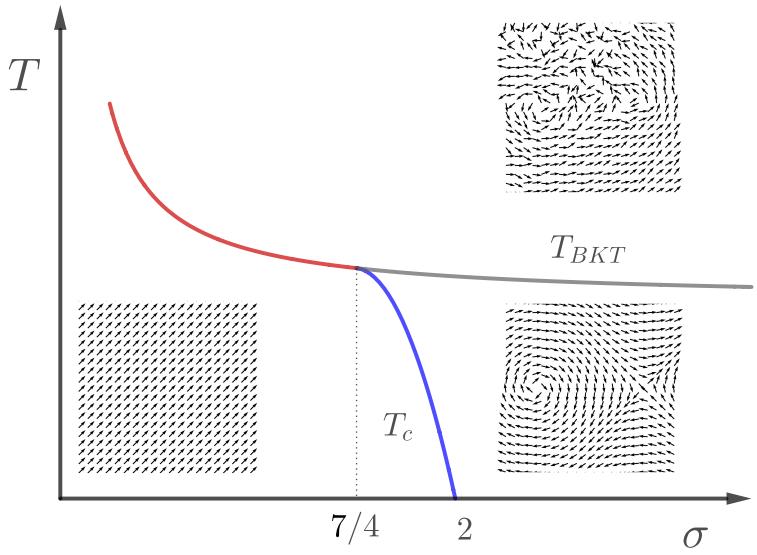

FIGURE 2.2: Qualitative phase diagram for the long-range XY model in $d = 2$, in which the three phases of the model (ordered, quasi-long-range-ordered, disordered) are shown. For $\sigma > 2$ the system undergoes the usual BKT transition (gray line). The value σ^* at which the long-range term becomes relevant is here a function of the temperature and varies from $\sigma = 2$ (at $T = 0$) to $7/4$ (when it met the BKT transition temperature). In this range of σ then, as the temperature varies, beyond the BKT transition, we find an infinite order symmetry-breaking transition (blue line). For $\sigma < 7/4$ the quasi-long-range ordered phase disappears so that we only have an order-disorder transition.

$\eta_{\rm sr}(J) \to 2 - \sigma$, which is exactly the scaling dimension of g in Eq. (2.57). This also suggests that in this regime topological excitations are suppressed.

Physically speaking, this is due to the fact that, as $J \to \infty$, the energy cost of highly non-local excitations like the topological one becomes higher and higher, and the presence of relevant long-range perturbation further contributes to this. Let us notice that the action of Eq. (2.57) is nothing but the continuous version of the approximation *a lá* Berezinskii. This tells us that, for small enough temperature, the approximation is indeed reliable. In particular, we can use Eq. (2.14) to derive the magnetization

$$\ln m \sim g^{-1} \int q^{-\sigma} d^2\mathbf{q} \tag{2.58}$$

Finally, from Eq. (2.56) we find the scaling of the magnetization

$$\ln m \sim -e^{B(T_c - T)^{-1/2}} \tag{2.59}$$

Here, the phase transition is of infinite order as all the derivatives of the order parameter with respect to the temperature vanish at $T = T_c$. The same can be said for

the free energy which would as well exhibit an essential singularity. A similar behavior in T is found approaching T_{BKT} from above, so that this seems to be a general property of the BKT phase. The presence of a SSB phase is, however, proper of the long-range regime. A similar, albeit not identical, coexistence of finite order parameter and infinite order scaling signatures has been also observed in other long-range statistical mechanics models [47, 49, 85–87], see also Ref.[88] for more examples in this direction.

As $\sigma \to 7/4^+$, T_c reaches $T_{\rm BKT}$ from below, leaving only a SSB phase transition. Unfortunately however, our set of equations (2.52) is not reliable in this regime: the RG flow spends a considerable amount of RG time close to the $g = 0$, $J = J_\sigma$ fixed point, which, in this regime, corresponds to $\dot{y}_\ell > 0$. As a consequence, y_ℓ will not remain small.

Summarizing, while for $\sigma > 2$ we find the same universality of the nearest-neighbours model, we cannot derive any prediction from our analysis of the $2d$ XY model in the region $\sigma < 7/4$. When $7/4 < \sigma < 2$, we find a rich and non-trivial beahvior *i)* for $T < T_c$, finite magnetization (ordered phase); *ii)* for $T_c < T < T_{\rm BKT}$ quasi-long-range-order with zero magnetization and temperature-dependent power-law decay in the two-point correlation function (BKT phase); *iii)* for $T > T_{\rm BKT}$ zero magnetization (disordered phase). The system, due to the power-law character of the interactions, exhibits power-law decaying two-point functions, also in the high-temperature phase, although with the same exponent of the coupling $\langle \mathbf{S}(\mathbf{r}) \cdot \mathbf{S}(0) \rangle \sim r^{-2-\sigma}$ [25, 89, 90]. The qualitative form of the phase diagram of the model is shown in Fig. 2.2.

2.7 | Quantum long-range XXZ chain

In the nearest-neighbors case, a rigorous mapping can be established between the classical two-dimensional XY model and the quantum XXZ chain at $T = 0$ [92]. As the mapping between the two models relies on the local nature of the couplings, however, the extension of the equivalence in presence of long-range couplings is not obvious. Indeed, the original derivation in Ref. [92], neglects the z-z interaction terms with a range ≥ 4 lattice sites in the resulting Hamiltonian and introduces a suitable, averaged, interaction term for distances smaller than three lattice sites. This allows introducing a bosonic hard-core condition and the mapping onto the $1d$ quantum XXZ Hamiltonian. This approach cannot be straightforwardly applied to the case of the $2d$ XY model with long-range interactions, as one should show the RG irrelevance of terms violating the hard-core condition.

Therefore, an interesting question is to ascertain whether and how the $T = 0$

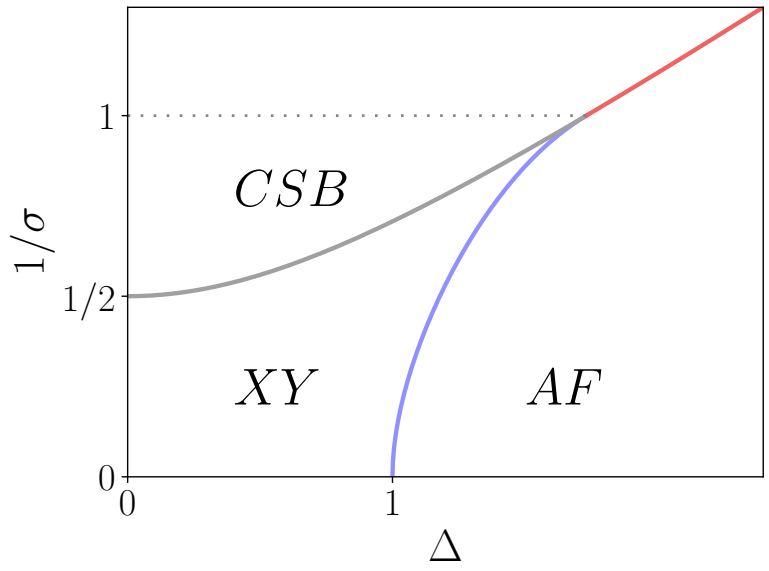

FIGURE 2.3: Qualitative phase diagram of the long-range XXZ quantum chain studied in Ref. [91]. The CSB (continuous simmetry breaking) phase corresponds to the SSB phase of the long-range XY model, the AF (anti-ferromagnetic) phase to the disordered one, the gapless XY phase to the BKT phase. The topology of the phase diagram is the same of the long-range XY case (Fig. 2.2), but here the border between the new broken phase and the gapless XY phase of the chain goes from $\sigma = 2$ to $\sigma = 1$, as discussed in the text. In the region $\sigma < 1$ the intermediate phase disappears.

phase diagram of the $1d$ XXZ Hamiltonian with long-range interactions

$$H = -\sum_{i,r} \frac{1}{r^{1+\sigma}} \left(S_i^x S_{i+r}^x + S_i^y S_{i+r}^y - \Delta S_i^z S_{i+r}^z \right) \tag{2.60}$$

(where $\sigma > 0$ and $S^{x,y,z}$ are the components of the spin $1/2$ operators) is related to that of the $2d$ classical XY model. It is worth noting that Hamiltonian (2.60) has been studied in Ref. [91] through the bosonization technique and numerical simulations. The effective action derived there describing the XXZ model bears a strong resemblance to the one of Eq. (2.33). The resulting RG flow is therefore similar to the one of Eq. (2.52) indicating that the long-short-range crossover of the two models is somehow analogous. In particular, identifying in Eqs. (4) and (8) of Ref. [91] $K, g_{\rm LR}, g$ with $\pi J/4, g, y$ respectively, these flow equations become

$$\begin{aligned} \frac{dy_\ell}{d\ell} &= (2 - \pi J) y \\ \frac{dg_\ell}{d\ell} &= \left(2 - \sigma - \frac{2}{\pi J_\ell}\right) g_\ell \\ \frac{dJ_\ell}{d\ell} &= A(J) g_\ell \end{aligned} \tag{2.61}$$

$A(J)$ being a function of J, depending on the RG-scheme. The similarity between Eq. (2.52) and Eq. (2.61) can be traced back both to the fact that the z-z long-range interaction is actually irrelevant (for $\sigma > 0$) and to the fact that the coefficient of the time derivative in the bosonized action does not renormalize (see the corresponding discussion for $\sigma < 0$ in Ref. [93]). This also explains why both phase diagrams feature three phases: the SSB, the disorder and the BKT one, which are called in Ref. [91] continuous symmetry breaking (CSB) phase, anti-ferromagnetic (AF) phase and gapless XY phase, respectively.

Let us notice that in the long-range regime, the usual mapping based on the coherent spin states, would result in a highly anisotropic action, due to the fact that one still has short-range interactions along the Euclidean time direction [94]. In principle, a similar anisotropy would be present in the bosonized action of Ref. [91] due to the presence of the z-z long-range contribution. As already noticed, however, this term turns out to be irrelevant so that the effective infrared action is actually isotropic.

Notice that Eqs. (2.61) predict that the BKT phase extends here up to $\sigma = 1$, rather than $\sigma = 7/4$. This difference boils down to the fact that, in the short-range regime, in correspondence to the border between the XY and the anti-ferromagnetic phase ($\Delta = 1$), the correlation functions of the x,y components decay as r^{-1}, rather than $r^{-1/4}$, so that the corresponding anomalous dimension is $\eta_{\rm sr} = 1$ and therefore, using the formalism introduced with Sak's criterion, the smallest value of σ_* is 1 and

σ_* ranges between 1 and 2. This has to be compared with the range for σ_* between $7/4$ and 1 for the classical long-range XY at finite temperature in $d = 2$.

Even if the ranges of σ_* do not coincide, the qualitative form of the phase diagrams of the two models is, therefore, the same, as it is possible to see from Fig. 2.3. This is similar to the results in Fig. 1 of Ref. [91] (let us notice that $1/\alpha \equiv 1/(1+\sigma)$ on the vertical axis is replaced by $1/\sigma$ in our Fig. 2.3). In that figure two lines, one separating the BKT and the SSB phases, and the other separating the BKT and the disordered phases, are drawn as extracted from numerical DMRG simulations. It is not clear by the figure whether and where the two lines are going to merge in correspondence of $\sigma = 1$, as foreseen by Eqs. (2.61) and in agreement with the picture presented in this paper. Therefore, more extensive numerical simulations are needed to confirm the predictions from Eqs. (2.61) in the vicinity of $\sigma = 1$.

Moreover, the substantial similarity between the field theory descriptions of the two models implies that the magnetization $m_{\|}$ in the x-y plane of the XXZ chain, scales as

$$\ln m_{\|} \sim -e^{B(\Delta_c - \Delta)^{-1/2}} \tag{2.62}$$

i.e. it follows the same scaling of Eq (2.59). This scaling (which eludes the current classification [95]) is, to the best of our knowledge, a new prediction for the XXZ long-range model.

The present result fits within the effective-dimensionality picture described in Ref. [12], for long-range quantum systems. In particular, the crossover between various long-range regimes of the quantum $O(n)$ model in dimension d can be described within the picture of the effective dimension introduced in section Sec. (1.2.4)

$$D_{eff} = \frac{2 - \eta_{\rm sr}(D_{eff})}{\sigma} d + 1 \tag{2.63}$$

valid for any $\sigma < 2 - \eta_{\rm sr}(d)$, $\eta_{\rm sr}(D)$ being the anomalous dimension of the D-dimensional action which describes the short-range version of our model. For the case the long-range $d = 1$ XXZ phase-diagram, when $D_{eff} = 2$, we know that the system undergoes a BKT transition, for which $\eta_{\rm sr}$ is not defined. If, however, we take $\eta_{\rm sr} \in [0, 1]$, rather than a single value, we find, from Eq. (2.63) we have

$$2 > \sigma > 1 \tag{2.64}$$

that is, exactly the range of coexistence of the SSB and the BKT phases.

For $\sigma < 2/3$, we find $D_{eff} > 4$ (with $\eta_{\rm sr}(D_{eff}) = 0$), so that the order-disorder transition is expected to be captured by the mean-field picture. The same thing it is supposed to happen for the $d = 2$ classical XY model in the $\sigma < 1$ region. Therefore one could expect that the critical behavior of the quantum chain in the $2/3 < \sigma < 1$ interval can be related to the one of the classical model for $1 < \sigma < 7/4$. However,

$2d$ XY	$1d$ XXZ
$\sigma < 1$	$\sigma < 2/3$
$1 < \sigma < 7/4$	$2/3 < \sigma < 1$
$7/4 < \sigma < 2$	$1 < \sigma < 2$
$\sigma > 2$	$\sigma > 2$

TABLE 2.1: Correspondence between the phases of the $2d$ XY long-range model at finite temperature (left) and in the $1d$ XXZ long-range model at zero temperature (right). For the values of σ corresponding to the first line we have a mean-field SSB transition; in correspondence of the second line an interacting SSB transition; in correspondence of the third we have both the order-disorder phase transition and the BKT one; in correspondence of the fourth, finally, only the BKT transition is present.

given that Eqs. (2.61) and Eq. (2.52) do not, respectively, apply in these regimes, further studies would be necessary to clarify this point. While the mapping between the two models is well established in the nearest-neighbors case [92], the similarity between the phase diagrams of the classical and quantum models in the long-range case is remarkable. A table summarizing the analogous phases of the quantum XXZ and the classical XY model is presented, see Tab. 2.1.

References

[11] N. DEFENU, A. TROMBETTONI, and A. CODELLO. "Fixed-point structure and effective fractional dimensionality for $O(N)$ models with long-range interactions". *Phys. Rev. E* 92(5) (Nov. 2015), p. 052113.

[12] N. DEFENU, A. TROMBETTONI, and S. RUFFO. "Criticality and phase diagram of quantum long-range $O(N)$ models". *Phys. Rev. B* 96(10) (Sept. 2017), p. 104432. DOI: 10.1103/PhysRevB.96.104432.

[25] H. SPOHN and W. ZWERGER. "Decay of the Two-Point Function in One-Dimensional $O(N)$ Spin Models with Long-Range Interactions". *J. Stat. Phys.* 94(5-6) (Mar. 1999), pp. 1037–1043. DOI: 10.1023/A:1004595419419.

[31] J. M. KOSTERLITZ and D. J. THOULESS. "Ordering, metastability and phase transitions in two-dimensional systems". *J. Phys. C* 6(7) (Apr. 1973), pp. 1181–1203. DOI: 10.1088/0022-3719/6/7/010.

[32] V. L. BEREZINSKII. "Destruction of Long-range Order in One-dimensional and Two-dimensional Systems Possessing a Continuous Symmetry Group. II. Quantum Systems". *Sov. Phys. JETP* 34 (1972), p. 610.

[33] J. SAK. "Recursion Relations and Fixed Points for Ferromagnets with Long-Range Interactions". *Phys. Rev. B* 8(1) (July 1973), pp. 281–285. ISSN: 0556-2805. DOI: 10.1103/PhysRevB.8.281.

[47] P. W. ANDERSON and G. YUVAL. "Exact Results in the Kondo Problem: Equivalence to a Classical One-Dimensional Coulomb Gas". *Phys. Rev. Lett.* 23 (2 July 1969), pp. 89–92. DOI: 10.1103/PhysRevLett.23.89.

[49] J. L. CARDY. "One-dimensional models with $1/r^2$ interactions". *Journal of Physics A: Mathematical and General* 14(6) (June 1981), pp. 1407–1415. DOI: 10.1088/0305-4470/14/6/017.

[69] G. GIACHETTI, N. DEFENU, S. RUFFO, and A. TROMBETTONI. "Self-consistent harmonic approximation in presence of non-local couplings(a)". *EPL* 133(5) (Apr. 2021), p. 57004. DOI: 10.1209/0295-5075/133/57004.

[70] G. GIACHETTI, N. DEFENU, S. RUFFO, and A. TROMBETTONI. "Berezinskii-Kosterlitz-Thouless Phase Transitions with Long-Range Couplings". *Phys. Rev. Lett.* 127 (Oct. 2021), p. 156801. DOI: 10.1103/PhysRevLett.127.156801.

[71] G. GIACHETTI, A. TROMBETTONI, S. RUFFO, and N. DEFENU. "Berezinskii-Kosterlitz-Thouless transitions in classical and quantum long-range systems". *Phys. Rev. B* 106 (1 July 2022), p. 014106. DOI: 10.1103/PhysRevB.106.014106.

[72] P. MINNHAGEN. "The two-dimensional Coulomb gas, vortex unbinding, and superfluid-superconducting films". *Rev. Mod. Phys.* 59 (4 Oct. 1987), pp. 1001–1066. DOI: 10.1103/RevModPhys.59.1001.

[73] Z. GULACSI and M. GULACSI. "Theory of phase transitions in two-dimensional systems". *Adv. Phys.* 47(1) (1998), pp. 1–89.

[74] AMIT, Y. Y. GOLDSCHMIDT, and S. GRINSTEIN. "Renormalisation group analysis of the phase transition in the 2D Coulomb gas, Sine-Gordon theory and XY-model". *J. Phys. A: Math. Gen.* 13 (2 1980), pp. 585–620. DOI: 10.1088/0305-4470/13/2/024.

[75] R. SAVIT. "Duality in field theory and statistical systems". *Rev. Mod. Phys.* 52 (2 Apr. 1980), pp. 453–487. DOI: 10.1103/RevModPhys.52.453.

[76] J. Villain. "Theory of one-dimensional and two-dimensional magnets with an easy magnetization plane. 2. The Planar, classical, two-dimensional magnet". *J. Phys. France* 36 (1975), pp. 581–590. DOI: 10.1051/jphys:01975003606058100.

[77] J. V. José, L. P. Kadanoff, S. Kirkpatrick, and D. R. Nelson. 16(3) (Aug. 1977), pp. 1217–1241. DOI: 10.1103/PhysRevB.16.1217.

[78] S. Bramwell and P. Holdsworth. "Magnetization and universal sub-critical behaviour in two-dimensional XY magnets". *Journal of Physics: Condensed Matter* 5(4) (1993), p. L53.

[79] S. Bramwell and P. Holdsworth. "Magnetization: A characteristic of the Kosterlitz-Thouless-Berezinskii transition". *Physical Review B* 49(13) (1994), p. 8811.

[80] S. Bramwell and P. Holdsworth. "Can the universal jump be observed in two-dimensional XY magnets?" *Journal of Applied Physics* 75(10) (1994), pp. 5955–5957.

[81] V. Pokrovsky and G. Uimin. "Magnetic properties of two-dimensional and layered systems". *Phys. Lett. A* 45(6) (1973), pp. 467–468. ISSN: 0375-9601. DOI: https://doi.org/10.1016/0375-9601(73)90711-1.

[82] A. S. T. Pires. "A quantum self-consistent harmonic approximation". *Solid State Commun.* 104(12) (Dec. 1997), pp. 771–773. DOI: 10.1016/S0038-1098(97)10025-4.

[83] J. M. Kosterlitz. "The critical properties of the two-dimensional xy model". *J. Phys. C* 7 (1974), p. 1046.

[84] H. Kunz and C. E. Pfister. "First order phase transition in the plane rotator ferromagnetic model in two dimensions". *Comm. Math. Phys.* 46(3) (Oct. 1976), pp. 245–251. DOI: 10.1007/BF01609121.

[85] D. J. Thouless. "Long-Range Order in One-Dimensional Ising Systems". *Phys. Rev.* 187 (2 Nov. 1969), pp. 732–733. DOI: 10.1103/PhysRev.187.732.

[86] F. J. Dyson. "An Ising ferromagnet with discontinuous long-range order". *Communications in Mathematical Physics* 21(4) (Dec. 1971), pp. 269–283. DOI: 10.1007/BF01645749.

[87] M. Aizenman, J. T. Chayes, L. Chayes, and C. M. Newman. "Discontinuity of the magnetization in one-dimensional $1/|x-y|^2$ Ising and Potts models". *Journal of Statistical Physics* 50(1-2) (Jan. 1988), pp. 1–40. DOI: 10.1007/BF01022985.

[88] M. BARMA, S. N. MAJUMDAR, and D. MUKAMEL. "Fluctuation-dominated phase ordering at a mixed order transition". *Journal of Physics A: Mathematical and Theoretical* 52(25) (May 2019), p. 254001. DOI: 10.1088/1751-8121/ab2064.

[89] A. KARGOL. "Decay of correlations in multicomponent ferromagnets with long-range interaction". *Rep. Math. Phys.* 56(3) (Dec. 2005), pp. 379–386. DOI: 10.1016/S0034-4877(05)80092-8.

[90] A. KARGOL. "Decay of correlations in N-vector ferromagnetic quantum models with long-range interactions". *J. Stat. Mech.: Theory Exp.* 2014(10), 10006 (Oct. 2014), p. 10006. DOI: 10.1088/1742-5468/2014/10/P10006.

[91] M. F. MAGHREBI, Z.-X. GONG, and A. V. GORSHKOV. "Continuous Symmetry Breaking in 1D Long-Range Interacting Quantum Systems". *Phys. Rev. Lett.* 119 (2 July 2017), p. 023001. DOI: 10.1103/PhysRevLett.119.023001.

[92] D. C. MATTIS. "Transfer matrix in plane-rotator model". *Phys. Lett. A* 104(6) (1984), pp. 357–360. ISSN: 0375-9601. DOI: https://doi.org/10.1016/0375-9601(84)90816-8.

[93] T. BOTZUNG *et al.* *Phys. Rev. B* 103 (15 Apr. 2021), p. 155139. DOI: 10.1103/PhysRevB.103.155139.

[94] N. DEFENU, A. TROMBETTONI, and S. RUFFO. "Anisotropic long-range spin systems". *Phys. Rev. B* 94(22), 224411 (Dec. 2016), p. 224411. DOI: 10.1103/PhysRevB.94.224411.

[95] A. RAJU *et al.* "Normal Form for Renormalization Groups". *Phys. Rev. X* 9 (2 Apr. 2019), p. 021014. DOI: 10.1103/PhysRevX.9.021014.

3 | The long-range Villain model

The study of the nearest-neighbors XY model is made easier by the introduction of the so-called Villain model, introduced in [76], i.e. a simplified version of the original Hamiltonian (2.1), which shares the same universality class. In this Chapter we address the long-range equivalent of the Villain model and derive its phase diagram. We find a phenomenology with is different with respect to the one of the long-range XY model discussed in Chapter 2, but it is rather close to the one of the one-dimensional Ising model with $1/r^2$ interactions.

In particular, after introducing the long-range Villain model in Sec. 3.1, in 3.2 we discuss the reason why we expect the long-range XY model to be in a different universality class. In Sec. 3.3 we derive the vortex-gas description of the model, analogous to the Coulomb gas one, in Sec. 3.4 we derive the corresponding real-space RG equations, and in Sec. 3.5 we describe the corresponding phase-diagram. Finally, in Sec. 3.6 we comment on our result in the light of the field-theoretical description of the model.

3.1 | Definition of the model

In the nearest-neighbors case, the Villain model consists of a series of plane rotators

$$H = \frac{J}{2} \sum_{\langle \mathbf{i},\mathbf{j} \rangle} \left(\theta_{\mathbf{i}} - \theta_{\mathbf{j}} - 2\pi n_{\mathbf{i},\mathbf{j}} \right)^2 , \tag{3.1}$$

where $\mathbf{i}, \mathbf{j} \in \mathbb{Z}^2$, the $\theta_{\mathbf{j}} \in \mathbb{R}$ are continuous lattice variables while $n_{\mathbf{i},\mathbf{j}} \in \mathbb{Z}$ are discrete link variables which couples nearest-neighbors pairs and obey the relation $n_{\mathbf{i},\mathbf{j}} = -n_{\mathbf{j},\mathbf{i}}$.

The main advantage of the model is that the presence of this auxiliary integer link variables is able to restore the periodicity of the XY Hamiltonian, without introducing a direct interaction between the angular variable. This can be seen explicitly by noticing that Hamiltonian (3.1) is invariant under the local transformation

$$\begin{aligned} \theta_{\mathbf{j}} &\to \theta_{\mathbf{j}} + 2\pi N_{\mathbf{j}} \\ n_{\mathbf{i},\mathbf{j}} &\to N_{\mathbf{j}} - N_{\mathbf{i}}, \end{aligned} \tag{3.2}$$

with $N_{\mathbf{i}} \in \mathbb{Z}$, which can be thought of as a discrete gauge symmetry on the lattice [75, 96]. On the continuous variables $\theta_{\mathbf{j}}$ this is exactly the local symmetry (2.3) of the original XY model, so that the model can account for its non-trivial critical properties [97].

Here we want to introduce the generalization of the Villain model to the case of long-range, power-law decaying couplings, i.e.

$$J(\mathbf{r}) \sim Jr^{-2-\sigma} \tag{3.3}$$

for $r \gg 1$ ($\sigma > 0$ in order to preserve the extensive nature of the thermodynamic quantities [2]). Before going on let us notice how, beyond its link to the XY universality class, the physics of the Villain model *per se* has drown considerable attention in the last decades, proving interesting both from the theoretical [98–100] and numerical [101–103] point of views, with applications running from the study of quantum-phase transitions [104] and superconductivity [105] to lattice gauge theories [96, 106–108] and deconfinement in high-energy physics [109]. The fate of the model in presence of long-range couplings is thus an interesting problem in itself.

First, we notice how the naive generalization of the Hamiltonian (3.1), in which the sum runs all over the lattice sites $\mathbf{i},\mathbf{j}$ and J is replaced by Eq. (3.3), is problematic. Indeed in this case we would have to deal with link variables whose number grows super-extensively (as $O(N^2)$).

In order to overcome this problem, and define a sensitive generalization of the model, we have to give a more general definition of the Villain model. For our purposes, thus, we define the Villain model as a quadratic model in the $\theta_{\mathbf{j}}$, which preserves both the global $O(2)$ and the local symmetry of Eq. (2.3).

We now see how to explicitly construct the Villain Hamiltonian corresponding to an XY model with a generic choice of the couplings $J(r)$. To better understand the procedure is, however, more convenient to address firstly the continuous version (2.35) of the XY Hamiltonian, in which $\theta_{\mathbf{j}}$ is replaced by a continuous field $\theta(\mathbf{x})$. We already see that the Berezinskii approximation alone, i.e. the substitution

$$1 - \cos\left(\theta(\mathbf{x}+\mathbf{r}) - \theta(\mathbf{x})\right) \to \frac{1}{2}\left(\theta(\mathbf{x}+\mathbf{r}) - \theta(\mathbf{x})\right)^2, \tag{3.4}$$

breaks the local symmetry (2.3), which accounts for the periodicity of $\theta(\mathbf{x})$. In the continuum limi, this property can be stated by saying that $\theta(\mathbf{x})$ is not a single-valued function (but rather is defined up to integer multiples of 2π) so that for each closed path ∂A on the plane

$$\oint_{\partial A} \nabla\theta(\mathbf{x}) \cdot d\mathbf{x} = \int_A \nabla \times \nabla\theta(\mathbf{x})\, d^2\mathbf{x} = 2\pi M(A) \tag{3.5}$$

with $M(A) \in \mathbb{Z}$ and $\nabla \times \mathbf{a} = \epsilon_{j,k}\partial_j a_k$. If we divide the region of the plane A enclosed by ∂A into two subregions A_1, A_2 we will have that $M(A) = M(A_1) + M(A_2)$ so that

$M(A)$ has the meaning of the total topological charge enclosed into the region of the plane A. Accordingly, Eq. (3.5) can also be put in a local form, namely

$$\nabla \times \nabla\theta(\mathbf{x}) = 2\pi \sum_k m_k \delta(\mathbf{x} - \mathbf{x}_k), \tag{3.6}$$

where $m_k \in \mathbb{Z}$ and $\mathbf{x}_k$ can be interpreted as vortex charges and their positions respectively. In the continuum limi, then, the Villain model can be defined as a boson $\theta(\mathbf{x})$, interacting with point-like charges m_k through the constraint (3.6). In formal terms

$$Z = \sum_{\{m_i\}} \int \mathcal{D}(\nabla\theta)\, e^{-\beta H_0(\theta)} \delta(\nabla \times \nabla\theta - 2\pi n(\mathbf{x})), \tag{3.7}$$

where the sum represents the trace over all the possible vortex configurations, βH_0 the quadratic Hamiltonian

$$\beta H_0 = \frac{1}{4} \int d^2\mathbf{x} d^2\mathbf{r}\; J(r)\, (\theta(\mathbf{x}+\mathbf{r}) - \theta(\mathbf{x}))^2\,, \tag{3.8}$$

and we introduced the vortex density

$$n(\mathbf{x}) = \sum_k m_k \delta(\mathbf{x} - \mathbf{x}_k). \tag{3.9}$$

Let us notice how we are now integrating over the configurations of $\nabla\theta$, which are single-valued, instead of $\theta(\mathbf{x})$.

Let us now see how we can built the Villain model directly on lattice. Once again, the quadratic approximation alone, namely

$$1 - \cos(\theta_{\mathbf{j}+\mathbf{r}} - \theta_{\mathbf{j}}) \to \frac{1}{2}(\theta_{\mathbf{j}+\mathbf{r}} - \theta_{\mathbf{j}})^2, \tag{3.10}$$

would break the local symmetry of Eq. (2.3), and thus the possibility of correctly describing topological configurations. Indeed, let us notice that, given a closed loop of P points on the lattice $\mathbf{j}_1, \mathbf{j}_2, \ldots, \mathbf{j}_P, \mathbf{j}_{P+1} \equiv \mathbf{j}_1$ the lattice equivalent of the integral in Eq.(3.5) is given by

$$\sum_{p=1}^{P} \left(\theta_{\mathbf{j}_{p+1}} - \theta_{\mathbf{j}_p}\right) \equiv 0. \tag{3.11}$$

In order to overcome this problem, we follow the original idea of the seminal Villain's work, i.e. we introduce an integer-valued link variable $n_{\mathbf{i},\mathbf{j}}$ ($n_{\mathbf{i},\mathbf{j}} = -n_{\mathbf{j},\mathbf{i}}$) for each pair of lattice points and we make the further replacement

$$\theta_{\mathbf{j}+\mathbf{r}} - \theta_{\mathbf{j}} \to \theta_{\mathbf{j}+\mathbf{r}} - \theta_{\mathbf{j}} + 2\pi n_{\mathbf{i},\mathbf{j}+\mathbf{r}}. \tag{3.12}$$

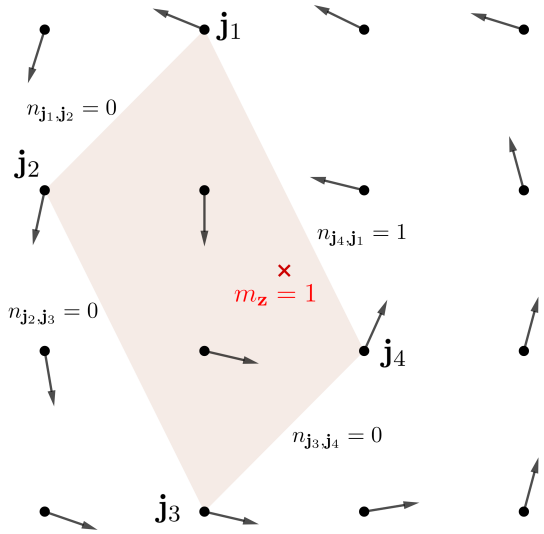

FIGURE 3.1: A topological configuration, namely a vortex with charge $m_{\mathbf{z}} = 1$, and a corresponding choice of the Villain link variables which encircle a parallelogram in such a way to satisfy the constraint (3.16). In agreement with the symmetry (3.2) the choice of the $n_{\mathbf{i},\mathbf{j}}$ which is different from zero is arbitrary.

As a consequence, the Villain Hamiltonian becomes

$$\beta H_0 = \frac{1}{4} \sum_{\mathbf{i} \neq \mathbf{j}} J(r) \left(\theta_{\mathbf{i}} - \theta_{\mathbf{j}} - 2\pi n_{\mathbf{i},\mathbf{j}}\right)^2 , \tag{3.13}$$

(with $r = |\mathbf{j} - \mathbf{i}|$) while the closed-loop integral of Eq.(3.5) is now

$$\sum_{p=1}^{P} \left(\theta_{\mathbf{i}_{p+1}} - \theta_{\mathbf{j}_p} - 2\pi n_{\mathbf{j}_p,\mathbf{j}_{p+1}}\right) = 2\pi \sum_{p=1}^{P} n_{\mathbf{j}_p,\mathbf{j}_{p+1}} . \tag{3.14}$$

In this language, the lattice-analogous of the constraint Eq.(3.5) imposes that the charge enclosed in the region A defined by the $\mathbf{j}_p$,

$$M(A) = \sum_{\partial A} n_{\mathbf{i},\mathbf{j}} \equiv \sum_{p=1}^{P} n_{\mathbf{j}_p,\mathbf{j}_{p+1}} , \tag{3.15}$$

is extensive, such that for any bipartition of the region in two sub-regions A_1, A_2 $M(A) = M(A_1) + M(A_2)$. As a consequence, we can introduce for each point of the dual lattice $\mathbf{z}$ its corresponding vortex charge $m_{\mathbf{z}}$ so that the constraint finally reads as

$$\sum_{\partial A} n_{\mathbf{i},\mathbf{j}} = \sum_{\mathbf{z} \in A} m_{\mathbf{z}} . \tag{3.16}$$

See Fig. 3.1 for a graphical interpretation of the constraint (3.16) within a prototypical topological configuration. Let us notice how, strictly speaking, one or more of the $\mathbf{z}$ could lie on the boundary ∂A of the region A. This could, in principle, cause some problems. However, as we are going to see, this boundary issue is not a problem in the thermodynamic limit as only the large loops are going to contribute to the critical behavior.

Finally, the partition function of the model takes the form

$$Z = \sum_{\{m_i\}} \int \prod_{\mathbf{j}} d\theta_{\mathbf{j}}\, e^{-\beta H_0} \delta \left(\sum_{\partial A} n_{\mathbf{i},\mathbf{j}} = \sum_{\mathbf{z} \in A} m_{\mathbf{z}} \right), \tag{3.17}$$

with H_0 given by (3.13) and we assume $J(r)$ to have the form of Eq. (3.3).

3.2 | Can the Villain model reproduce the XY phase diagram?

Before going on with the study of the long-range version (3.17) of the Villain model, let us briefly discuss, on very general grounds, whether the latter can fall in the same universality class of the corresponding XY model. As already mentioned, this is the case for the nearest-neighbors ($\sigma \to \infty$) regime: this comes from the fact that, once the $\theta_{\mathbf{i}}$ are integrated out, the Villain Hamiltonian can be exactly mapped into the Coulomb gas Hamiltonian. While the same calculation can be performed even for the case of long-range-decaying couplings (and it will actually be performed in the next section) there are, in fact, reasons to believe this will not reproduce the XY phenomenology, as we are going to argue.

First, let us notice that, if on the one hand Hamiltonian (3.17) improves the quadratic approximation by taking into account the presence of topological defects, on the other hand it can only account for an interaction between vortices which is quadratic in their charges. Let us instead now try and isolate the topological component in the action (2.33) which describes the continuous version of the long-range XY model. We start by splitting the field into a topological part and a non-topological, spin-waves, part:

$$\theta(\mathbf{x}) = \theta_0(\mathbf{x}) + \theta_{\text{top}}(\mathbf{x}), \tag{3.18}$$

where

$$\nabla \times \nabla \theta_0(\mathbf{x}) = 0 \qquad \nabla \times \nabla \theta_{\text{top}}(\mathbf{x}) = 2\pi n(\mathbf{x}), \tag{3.19}$$

$n(\mathbf{x})$ being the vortex density given by Eq. (3.9). The ambiguity in the decomposition can be lifted if we impose the further constraint $\nabla \cdot \nabla \theta_{\text{top}} = 0$ (see [110, 111]). This allows us to write $\partial_i \theta_{\text{top}} = \epsilon_{ij} \partial_j \bar{\theta}$ where $\bar{\theta}$ is singled valued. It follows that

$$\nabla^2 \bar{\theta}(\mathbf{x}) = 2\pi n(\mathbf{x}), \tag{3.20}$$

that can be solved introducing the $d = 2$ Green function of the Laplacian $G_c(r) = -\frac{1}{2\pi}\ln r$, finding

$$\bar{\theta}(\mathbf{x}) = 2\pi \sum_k m_k G_c(|\mathbf{x} - \mathbf{x}_k|) \tag{3.21}$$

In terms of the decomposition (3.18) then, the kinetic term in action (2.33) decouples into the two terms

$$\begin{aligned} \frac{J}{2}|\nabla\theta|^2 &= \frac{J}{2}|\nabla\theta_0|^2 + \frac{J}{2}|\nabla\theta_{\text{top}}|^2 \\ &= \frac{J}{2}|\nabla\theta_0|^2 + \frac{J}{2}|\nabla\bar{\theta}|^2. \end{aligned} \tag{3.22}$$

By replacing the solution (3.21) in the second term we get the usual Coulomb gas interaction, so that $S[\theta]$ can be written as

$$\begin{aligned} S[\theta] = \frac{J}{2}\int d^2\mathbf{x}\,|\nabla\theta_0|^2 - \pi J \sum_{j\neq k} m_j m_k \ln|\mathbf{x}_k - \mathbf{x}_j| \\ + \varepsilon_c \sum_k m_k^2 + \frac{g}{2}\int d^2x\, e^{-i(\theta_0+\theta_{\text{top}})}\,\nabla^\sigma e^{i(\theta_0+\theta_{\text{top}})}, \end{aligned} \tag{3.23}$$

where ε_c is the core vortex energy, which takes into account the small-distance singular behavior of the topological configurations. For small values of g we can integrate out the non-topological component of the field, θ_0. At the first order in g we find the the cumulant correction

$$\left\langle S_{\text{LR}}[\theta_0 + \theta_{\text{top}}]\right\rangle_0, \tag{3.24}$$

where the average is computed on the quadratic non-topological term. By exploiting the form (2.34) of S_{LR}

$$\begin{aligned} &\int d^2\mathbf{x}\int_{r>a} d^2\mathbf{r}\frac{\langle\cos(\Delta_{\mathbf{r}}\theta_0)\rangle_0}{r^{2+\sigma}}(1-\cos\Delta_{\mathbf{r}}\theta_{\text{top}}) \\ &\sim \int d^2\mathbf{x}\int_{r>a} d^2\mathbf{r}\frac{1-\cos\Delta_{\mathbf{r}}\theta_{\text{top}}(\mathbf{x})}{r^{2+\sigma+\eta_{\text{sr}}(J)}}, \end{aligned} \tag{3.25}$$

up to immaterial additive constants. This has the same form of Eq. (2.34) so that, provided that $\sigma + \eta_{\text{sr}}(J) < 2$, it can be written as well as

$$\frac{g}{2}\int d^2\mathbf{x}\, e^{-i\theta_{\text{top}}}\nabla^{\sigma+\eta_{\text{sr}}(J)} e^{i\theta_{\text{top}}}, \tag{3.26}$$

where $\eta_{\text{sr}}(J) = 1/2\pi J$ and we absorbed some multiplicative proportionality factor into the coupling g. For $\sigma + \eta_{\text{sr}}(J) > 2$, the above operator should be instead replaced with the laplacian (see Appendix B).

Finally, Eq. (3.23) becomes

$$\begin{aligned} S_{\text{efb}} \sim & -\pi J \sum_{j\neq k} m_j m_k \ln|\mathbf{x}_k - \mathbf{x}_j| + \varepsilon_c \sum_k m_k^2 \\ & + \frac{g}{2}\int d^2\mathbf{x}\, e^{-i\theta_{\text{top}}} \nabla^{\sigma+\eta_{\text{sr}}(J)} e^{i\theta_{\text{top}}}. \end{aligned} \tag{3.27}$$

Let us consider the regime $\sigma + \eta_{\text{sr}}(J) > 2$. In this case

$$-e^{-i\theta_{\text{top}}}\nabla^2 e^{i\theta_{\text{top}}} = |\nabla e^{i\theta_{\text{top}}}| = |\nabla\theta_{\text{top}}|^2 \tag{3.28}$$

so that, by replacing θ_{top} with its expression in terms of the m_i, we recover the usual Coulomb gas interaction

$$S_{\text{efb}} \sim -\pi(J+g)\sum_{j\neq k} m_j m_k \ln|\mathbf{x}_k - \mathbf{x}_j| + \varepsilon_c \sum_k m_k^2. \tag{3.29}$$

On the other hand, this is in agreement with the main result of our analysis in Chapter 2, namely, the fact that, for $\sigma + \eta_{\text{sr}}(J) > 2$, the long-range term is not relevant so that the XY model undergoes a BKT transition (which, in turn, can be described in terms of a Coulomb gas).

Let us now analyze the $\sigma + \eta_{\text{sr}}(J) < 2$ regime. Since the fractional Laplacian does not obey the simple Leibnitz rule [112], here it is not possible to derive a simple charge-charge interaction, unless we expand the exponential term in Eq. (3.27). This expansion is actually not easily justified, since the topological configurations θ_{top} are spatially extended. This suggests that the higher-order terms in θ_{top} in the expansion are relevant so that we have to keep in the Hamiltonian higher-order interaction terms in the m_k (e.g. proportional to $m_i m_j m_k m_p$), which cannot be obtained within the Villain approximation. Moreover, as seen in Chapter 2, $\sigma + \eta_{\text{sr}}(J) < 2$ is precisely the condition under which the LR term becomes relevant. In this regime, our RG analysis foresees a boundless growth for the coupling g, so that the integration on θ_0 cannot be performed perturbatively as we did to derive Eq. (3.27).

The fact that spin-waves and topological contributions do not decouple is a hint that the long-range phenomenology cannot be captured by a quadratic model in θ, as the Villain model. As we provided reasons to believe the long-range two-dimensional XY model is in a different universality class with respect to the Villain model (3.17), the remaining part of the present Chapter will be devoted to understanding the critical behavior of the latter. Let us notice, however, that the numerical results obtained in Refs. [113, 114], seem to indicate that the diluted version of the long-range XY model has a different phase diagram with respect to the original model as well (further investigation, however, would be needed in order to confirm this expectation).

3.3 | Vortex-vortex interaction

In this section we derive the effective interaction between topological charges $m_{\mathbf{z}}$ in Eq. (3.17). To this aim, we define the Fourier transformed variables

$$\theta_{\mathbf{j}} = \frac{1}{\sqrt{N}} \sum_{\mathbf{q}} \theta_{\mathbf{q}} e^{i\mathbf{q}\cdot\mathbf{j}} \qquad n_{\mathbf{j},\mathbf{j}+\mathbf{r}} = \frac{1}{\sqrt{N}} \sum_{\mathbf{q}} n_{\mathbf{q},\mathbf{r}} e^{i\mathbf{q}\cdot\left(\mathbf{j}+\frac{\mathbf{r}}{2}\right)}, \tag{3.30}$$

with $\mathbf{q}$ a vector of the reciprocal lattice. The Hamiltonian Eq. (3.13) becomes:

$$\beta H_0 = \frac{1}{4} \sum_{\mathbf{q},\mathbf{r}} J(r) \left| 2i \sin \frac{\mathbf{q}\cdot\mathbf{r}}{2} \theta_{\mathbf{q}} - 2\pi n_{\mathbf{q},\mathbf{r}} \right|^2 . \tag{3.31}$$

In order to integrate out the $\theta_{\mathbf{j}}$, it is useful to introduce the new variables

$$\psi_{\mathbf{q}} = \theta_{\mathbf{q}} + \frac{2\pi i}{\omega(\mathbf{q})} \sum_{\mathbf{r}} J(r) \sin \frac{\mathbf{q}\cdot\mathbf{r}}{2} n_{\mathbf{q},\mathbf{r}} \tag{3.32}$$

where, as in Chapter 2,

$$\omega(\mathbf{q}) = \sum_{\mathbf{r}} J(r)\,(1 - \cos \mathbf{q}\cdot\mathbf{r}) = 2 \sum_{\mathbf{r}} J(r) \sin^2 \frac{\mathbf{q}\cdot\mathbf{r}}{2} \tag{3.33}$$

(the asymptotic behavior of $\omega(\mathbf{q})$ for small q is worked out in Appendix A). In terms of the new variables the Hamiltonian decouples into two pieces, a spin-wave term and a topological term, which only depends on the discrete link variables

$$\beta H_0 = H_{\mathrm{SW}}(\psi) + H_{\mathrm{top}}(m) \tag{3.34}$$

The two pieces are given by:

$$\begin{aligned} H_{\mathrm{SW}} &= \frac{1}{2} \sum_{\mathbf{q}} \omega(\mathbf{q}) |\psi_{\mathbf{q}}|^2 \\ H_{\mathrm{top}} &= \frac{\pi^2}{\omega(\mathbf{q})} \sum_{\mathbf{q}} \left[\omega(\mathbf{q}) \sum_{\mathbf{r}} J(r) |n_{\mathbf{q},\mathbf{r}}|^2 - 2 \sum_{\mathbf{r},\mathbf{r}'} J(r) J(r') \sin \frac{\mathbf{q}\cdot\mathbf{r}}{2} \sin \frac{\mathbf{q}\cdot\mathbf{r}'}{2} n_{\mathbf{q},\mathbf{r}'} n^*_{\mathbf{q},\mathbf{r}'} \right] \end{aligned} \tag{3.35}$$

Let us notice how the spin-wave part of the Hamiltonian exactly corresponds to the quadratic approximation of the original long-range XY Hamiltonian, analyzed in Sec. 2.2.

In order to derive the exact form of the vortex-vortex interaction let us focus now on H_{top}. First, we notice it can be arranged as

$$H_{\text{top}} = \sum_{\mathbf{q}} \frac{\pi^2}{\omega(\mathbf{q})} \sum_{\mathbf{r},\mathbf{r}'} J(r) J(r') \left| \sin \frac{\mathbf{q}\cdot\mathbf{r}'}{2} n_{\mathbf{q},\mathbf{r}} - \sin \frac{\mathbf{q}\cdot\mathbf{r}}{2} n_{\mathbf{q},\mathbf{r}'} \right|^2 . \tag{3.36}$$

Back to the real space this takes the form

$$H_{\text{top}} = \sum_{\mathbf{r},\mathbf{r}'} J(r) J(r') \sum_{\mathbf{j},\mathbf{j}'} f(\mathbf{j}-\mathbf{j}') (\nabla_r n_{\mathbf{j},\mathbf{j}+\mathbf{r}'} - \nabla_{\mathbf{r}'} n_{\mathbf{j},\mathbf{j}+\mathbf{r}}) (\nabla_{\mathbf{r}} n_{\mathbf{j}',\mathbf{j}'+\mathbf{r}'} - \nabla_{\mathbf{r}'} n_{\mathbf{j}',\mathbf{j}'+\mathbf{r}}), \tag{3.37}$$

where

$$f(\mathbf{x}) = \frac{\pi^2}{4N} \sum_{\mathbf{q}} \frac{e^{i\mathbf{q}\cdot\mathbf{x}}}{\omega(\mathbf{q})} \tag{3.38}$$

and we introduced the notation of the discrete curl

$$\nabla_r n_{\mathbf{j},\mathbf{j}+\mathbf{r}'} - \nabla_{\mathbf{r}'} n_{\mathbf{j},\mathbf{j}+\mathbf{r}} \equiv n_{\mathbf{j},\mathbf{j}+\mathbf{r}} + n_{\mathbf{j}+\mathbf{r},\mathbf{j}+\mathbf{r}+\mathbf{r}'} + n_{\mathbf{j}+\mathbf{r}+\mathbf{r}',\mathbf{j}+\mathbf{r}}. \tag{3.39}$$

As expected, once the continuous field has been integrated out, the interaction depends only on gauge invariants. Indeed, we have that:

$$\nabla_r n_{\mathbf{j},\mathbf{j}+\mathbf{r}'} - \nabla_{\mathbf{r}'} n_{\mathbf{j},\mathbf{j}+\mathbf{r}} = \sum_{\partial\mathcal{P}(\mathbf{j},\mathbf{r},\mathbf{r}')} n_{\mathbf{i},\mathbf{i}'}, \tag{3.40}$$

where the $\mathcal{P}(\mathbf{j},\mathbf{r},\mathbf{r}')$ denotes the region of the plane corresponding to a parallelogram with vertices $\mathbf{j}$,$\mathbf{j}+\mathbf{r}$,$\mathbf{j}+\mathbf{r}+\mathbf{r}'$, $\mathbf{j}+\mathbf{r}$ (and thus sides $\mathbf{r}$,$\mathbf{r}'$). As a consequence, the symmetry of Eq. (3.2) leaves these quantities invariant.

By means of the constraint (3.16) finally, we can express the Hamiltonian in terms of the topological charges enclosed in each parallelogram

$$H_{\text{top}} = \sum_{\mathbf{r},\mathbf{r}'} J(r) J(r') \sum_{\mathbf{j},\mathbf{j}'} f(\mathbf{j}-\mathbf{j}') \left(\sum_{\mathbf{z}\in\mathcal{P}(\mathbf{j},\mathbf{r},\mathbf{r}')} m_{\mathbf{z}} \right) \left(\sum_{\mathbf{z}'\in\mathcal{P}(\mathbf{j},\mathbf{r},\mathbf{r}')} m_{\mathbf{z}'} \right). \tag{3.41}$$

Remarkably, only the congruent parallelograms (which share the same $\mathbf{r}$ and $\mathbf{r}'$) do interact. Reshuffling the sums we finally find the vortex-vortex potential

$$H_{\text{top}} = \sum_{\mathbf{z},\mathbf{z}'} m_{\mathbf{z}} m_{\mathbf{z}'} U(\mathbf{z}-\mathbf{z}'), \tag{3.42}$$

with

$$U(\mathbf{z}-\mathbf{z}') = \sum_{\mathbf{r},\mathbf{r}'} J(r) J(r') \sum_{\mathbf{j},\mathbf{j}' | \mathbf{z}\in\mathcal{P}(\mathbf{j},\mathbf{r},\mathbf{r}') \mathbf{z}'\in\mathcal{P}(\mathbf{j}',\mathbf{r},\mathbf{r}')} f(\mathbf{j}-\mathbf{j}'). \tag{3.43}$$

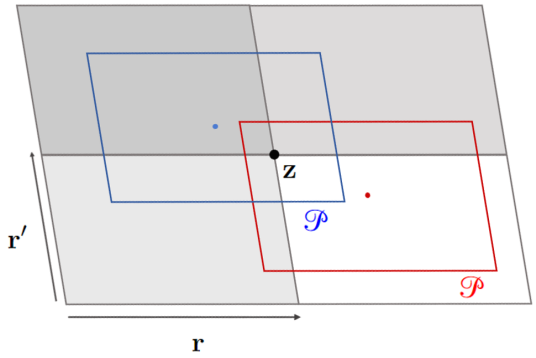

FIGURE 3.2: For a given point of the plane $\mathbf{z}$, all the parallelograms $\mathcal{P}$ of sides $\mathbf{r}$, $\mathbf{r}'$ such that $\mathbf{z} \in \mathcal{P}$ (as the red and the blue one in Figure) are such that their internal points belong to a parallelogram of sides $\mathbf{2r}$, $\mathbf{2r}'$, centered in $\mathbf{z}$.

3.3.1 | Large-distance limit

We want now to derive an approximate expression for the potential (3.43) valid for large distances. In this limit, we can as well replace the sum in Eq. (3.43) with an integral. Since only congruent parallelograms interact we can replace $\mathbf{j} - \mathbf{j}'$ with the distance between the centers of the two. To correctly parametrize the integral we note that, fixed $\mathbf{z}$ and fixed $\mathbf{r}$, $\mathbf{r}'$ the parallelograms such that $\mathbf{z} \in \mathcal{P}$ are those which center belongs to a parallelogram centered in $\mathbf{z}$ of sides $\mathbf{r}$, $\mathbf{r}'$ (see Fig 3.2). In turn, each point of this parallelogram can be written as $\mathbf{j} = \mathbf{z} + \lambda\mathbf{r} + \mu\mathbf{r}'$ with λ, $\mu \in [-1/2, 1/2]$. By choosing λ, μ as our coordinates we have to carry a factor $|\mathbf{r} \times \mathbf{r}'|$ due to the jacobian. Finally, we can express U as

$$U(\mathbf{z} - \mathbf{z}') = \int d^2\mathbf{r} \int d^2\mathbf{r}' (\mathbf{r} \times \mathbf{r}')^2 J(r) J(r') \int_{-1/2}^{1/2} d\lambda d\lambda' \int_{-1/2}^{1/2} d\mu d\mu' f\left(\mathbf{z} - \mathbf{z}' + (\lambda - \lambda')\mathbf{r} + (\mu - \mu')\mathbf{r}'\right). \tag{3.44}$$

So far, all our considerations are equally valid for any choice of $J(r)$. In what follows we are going to replace $J(r)$ with its asymptotic form $J(r) \sim J r^{-2-\sigma}$ valid for $r \gg 1$. This is safe, as we are interested in the large-distance limit.

By exploiting the definition (3.38) of $f(\mathbf{x})$, which in the continuum limi becomes

$$f(\mathbf{x}) = \frac{\pi^2}{4} \int \frac{d^2\mathbf{q}}{(2\pi)^2} \frac{e^{i\mathbf{q}\cdot\mathbf{x}}}{\omega(\mathbf{q})}, \tag{3.45}$$

we find the expression for the Fourier transform of $U(\mathbf{q})$ of $U(\mathbf{z}-\mathbf{z}')$

$$\begin{aligned} U(\mathbf{q}) &= \frac{(\pi J)^2}{4\omega(q)} \int \frac{d^2\mathbf{r}}{r^{2+\sigma}} \int \frac{d^2\mathbf{r}'}{r'^{2+\sigma}} (\mathbf{r}\times\mathbf{r}')^2 \int_{-1/2}^{1/2} d\lambda d\lambda' d\mu d\mu' e^{i\mathbf{q}\cdot((\lambda-\lambda')\mathbf{r}+(\mu-\mu')\mathbf{r}')} \\ &= \frac{(2\pi J)^2}{\omega(q)} \int \frac{d^2\mathbf{r}}{r^{2+\sigma}} \int \frac{d^2\mathbf{r}'}{r'^{2+\sigma}} (\mathbf{r}\times\mathbf{r}')^2 \frac{\sin^2(\mathbf{q}\cdot\mathbf{r}/2)}{(\mathbf{q}\cdot\mathbf{r})^2} \frac{\sin^2(\mathbf{q}\cdot\mathbf{r}'/2)}{(\mathbf{q}\cdot\mathbf{r}')^2}. \end{aligned} \tag{3.46}$$

By switching to the polar coordinates on the plane, for $\mathbf{r}$ and $\mathbf{r}'$, we have

$$\mathbf{r}\times\mathbf{r}' = rr'\sin(\theta-\theta') \qquad \mathbf{q}\cdot\mathbf{r} = qr\cos\theta \tag{3.47}$$

(and similarly for $\mathbf{q}'\cdot\mathbf{r}'$). Through the further substitution $\rho = qr\cos\theta/2$, we get then

$$\begin{aligned} U(q) =& \omega(q)^{-1} \left(2^{1-\sigma}\pi J q^{\sigma-2} \int \frac{d\rho}{\rho^{1+\sigma}} \sin^2\rho\right)^2 \\ & \int d\theta' d\theta |\cos\theta|^{\sigma-2} |\cos\theta'|^{\sigma-2} \sin^2(\theta-\theta'). \end{aligned} \tag{3.48}$$

In Appendix A we derive the asymptotic expression of $\omega(q)$ in the regime $0<\sigma<2$ to be q to be $\omega(q)\sim Jc_\sigma q^\sigma$, with

$$c_\sigma = 2^{1-\sigma} \int_0^\infty \frac{d\rho}{\rho^{1+\sigma}} \sin^2\rho \int_0^{2\pi} d\theta |\cos\theta|^\sigma. \tag{3.49}$$

As a consequence we have that

$$U(q) = I(\sigma)\frac{\omega(q)}{q^4}, \tag{3.50}$$

where

$$\begin{aligned} I(\sigma) &= \pi^2 \left(\int d\theta'' |\cos\theta''|^\sigma\right)^{-2} \int d\theta d\theta' \sin^2(\theta-\theta') |\cos\theta|^{\sigma-2} |\cos\theta'|^{\sigma-2} \\ &= 2\pi^2 \frac{\int d\theta \sin^2\theta |\cos\theta|^{\sigma-2}}{\int d\theta' |\cos\theta'|^\sigma} \\ &= \frac{2\pi^2}{\sigma-1} \end{aligned} \tag{3.51}$$

We see then the that proportionality constant $I(\sigma)$ converges as long as $\sigma>1$. If we carefully insert an infrared cutoff L it is easy to see that the divergence for $\sigma\leq 1$ is

actually an infrared divergence ($\propto L^{1-\sigma}$, L being the linear size of the system). This mean that, as $\sigma \to 1^+$, in the thermodynamic limit we cannot excite the vortices for any temperature, so that only the spin wave part $H_{\rm SW}$ of the Hamiltonian survives, and the system exhibits a finite magnetization at any temperature.

For $1 < \sigma < 2$ the vortex-vortex potential should be taken into account. In Fourier space, for $q \ll 1$, it takes the form:

$$U(q) \propto \frac{\omega(q)}{q^4} \sim J q^{\sigma-4} + O(q^{-2}) \tag{3.52}$$

In turn, this implies that for $R \gg 1$ (R being the distance between a pair of vortices):

$$U(R) \sim J \int_{1/L}^{1/R} q^{\sigma-3} dq = \frac{J}{2-\sigma}\left(L^{2-\sigma} - R^{2-\sigma}\right) \tag{3.53}$$

The additive constant $L^{2-\sigma}$ brings a term $\propto L^{2-\sigma}\,(\sum_i m_i)^2$ in the Hamiltonian (3.42), which kills all the non neutral configurations, exactly as in the short-range case. Then,

$$\begin{aligned} H_{\rm top} &= \sum_{i,j} m_i m_j U(\mathbf{r}_i - \mathbf{r}_j) \\ &= U(0)\sum_i m_i^2 + \sum_{i\neq j} m_i m_j U(\mathbf{r}_i - \mathbf{r}_j) \\ &= \sum_{i\neq j} m_i m_j \left(U(\mathbf{r}_i - \mathbf{r}_j) - U(0)\right) \end{aligned} \tag{3.54}$$

where now we denoted with $\{\mathbf{r}_i\}$ and $\{m_i\}$ respectively the position and the charge of the vortices of a given configuration, and noticed that, for any neutral configuration $\sum_{i\neq j} m_i m_j = -\sum_i m_i^2$. We can thus write

$$U(R) - U(0) \sim J \int \frac{d^2\mathbf{q}}{(2\pi)^2} \frac{e^{i\mathbf{q}\cdot\mathbf{r}} - 1}{q^{4-\sigma}} \sim -J\, R^{2-\sigma}. \tag{3.55}$$

Let us notice that, now that the sum runs only on $i \neq j$, $U(r)$ is no longer defined up to additive constants. It is customary however to define the energy so that it is zero for $r = 1$, which is the minimum distance at which a pair can be created. This means that in the Hamiltonian we can write:

$$H_{\rm top} = \sum_{i\neq j} m_i m_j \left(U(\mathbf{r}_i - \mathbf{r}_j) - U(1)\right) + (U(0) - U(1)) \sum_i m_i^2 \tag{3.56}$$

Now we can finally introduce:

$$V(\mathbf{r}) = U(\mathbf{r}) - U(1) = g \int \frac{d^2\mathbf{q}}{2\pi} \frac{e^{i\mathbf{q}\cdot\mathbf{r}} - e^{i\mathbf{q}\cdot\mathbf{n}}}{q^{4-\sigma}} = -\gamma\left(r^{2-\sigma} - 1\right) \tag{3.57}$$

(with $g, \gamma \propto J$) and the finite quantity $\varepsilon_c = U(0) - U(1) > 0$, which physically represents the core energy associated with the creation of a vortex pair at the minimum distance possible. In terms of those the Hamiltonian becomes

$$H_{\text{top}} = \sum_{i \neq j} m_i m_j V(\mathbf{r}_i - \mathbf{r}_j) + \varepsilon_c \sum_i m_i^2 \tag{3.58}$$

while, the (topological part of the) partition function is given by

$$Z_{\text{top}} = \sum_{\{m_j\}} \int \prod_j d^2\mathbf{r}_j e^{-H_{\text{top}}}. \tag{3.59}$$

Finally, let us notice how in the $\sigma > 2$ case we recover the usual logarithmic interaction of the two-dimensional Coulomb gas as

$$U(R) \sim J \int_{1/L}^{1/R} q^{-1} dq = J(\ln L - \ln r). \tag{3.60}$$

Since in this case, as noticed, the dispersion relation $\omega(q)$ of the spin waves has the same form of the nearest-neighbours one, we can safely conclude that the Villain model is in the same universality class of the nearest-neighbours case for all $\sigma > 2$.

3.4 | Real-space renormalization group procedure

In this are now going to carry out the renormalization group procedure in the vortex gas representation. To this extent we then introduce the renormalization parameter ℓ such that the effective lattice spacing a_ℓ is given by $a_\ell = e^\ell$. Our picture is the following: at scale ℓ the vortex-antivortex pairs with scale $< a_\ell$ renormalizes the vortex-vortex potential. Let us notice that, while the ultra-violet (UV) potential $V_{\ell=0}(r)$ is given by Eq. (3.57), there is no reason for the effective potential at scale ℓ, $V_\ell(r)$, to have the same functional form.

Since in the UV the potential grows as a power law a simple energy-entropy scaling argument would suggest that the fugacity $y \equiv e^{-\varepsilon_c}$ is not relevant at any temperature. However, as we are going to see, these naive expectations are defied by the renormalization group calculations, which shows that, for every finite value of ℓ, the behavior at large distances of the potential is no longer given by the power law of Eq. (3.57). The renormalization procedure we present here is the straightforward generalization of those introduced for the short-range case by Kosterlitz and Thouless [31] to arbitrary (well-behaved) interaction potential and it is similar to those present in [72] for a screened Coulomb interaction. However, up to our knowledge, the corresponding treatment for the case of a confining interaction as Eq. (3.67) is absent in the literature.

In order to carry out the renormalization process, we assume $y \ll 1$: in this regime only the vortices with charge ± 1 will actually contribute to the renormalization procedure. Then, by the neutrality condition, every possible configuration will have the same number of positive and negative charges, and the partition function takes the form:

$$Z_{\text{top}} = \sum_{p=0}^{\infty} \frac{y_\ell^{2p}}{p!^2} \int_{|\mathbf{r}_i - \mathbf{r}_j|>1} \prod_{i=1}^{p} d\mathbf{r}_i^+ d^2\mathbf{r}_i^- \; e^{-\sum_{i\neq j} m_i m_j V_\ell(\mathbf{r}_i - \mathbf{r}_j)} \tag{3.61}$$

where $\mathbf{r}_i^\pm$ are the positions of the vortices with positive/negative charge respectively.

To perform the renormalization we integrate all over the pair such that $1 < |\mathbf{r}_i - \mathbf{r}_j| < e^{\delta\ell}$. In order to do so, let us consider the sector with p pairs of vortices in the partition function of Eq. (3.61). There are p^2 equivalent ways to choose the pair to trace out. Then, assuming the coordinates of this couple to be $\mathbf{r}_p^\pm \equiv \mathbf{r}^\pm$ we have an additional term given by:

$$\begin{aligned}
&\frac{y^{2p}p^2}{p!^2} \int_{|\mathbf{r}_i - \mathbf{r}_j|>e^{\delta\ell}} \prod_{i=1}^{p} d^2\mathbf{r}_i^+ d^2\mathbf{r}_i^- \int_{1<|\mathbf{r}_i - \mathbf{r}_j|<e^{\delta\ell}} d\mathbf{r}_p^+ d\mathbf{r}_p^- e^{-\sum'_{i\neq j} m_i m_j V(\mathbf{r}_i - \mathbf{r}_j)} \\
&= \frac{y^{2p}}{(p-1)!^2} \int_{|\mathbf{r}_i - \mathbf{r}_j|>e^{\delta\ell}} \prod_{i=1}^{p-1} d\mathbf{r}_i^+ d\mathbf{r}_i^- e^{-\sum'_{i\neq j} m_i m_j V(\mathbf{r}_i - \mathbf{r}_j)} \\
&\int_{1<|\mathbf{r}^+ - \mathbf{r}^-|<e^{\delta\ell}} d^2\mathbf{r}^+ d^2\mathbf{r}^- e^{-V(\mathbf{r}^+ - \mathbf{r}^-) - \sum'_i m_i (V(\mathbf{r}_i - \mathbf{r}^+) - V(\mathbf{r}_i - \mathbf{r}^-))},
\end{aligned}$$

where we are denoting with $\sum'$ the summation all over the remaining charges, namely $i, j \neq p$ and we are dropping the subscript ℓ in $V(r)$ and y in order to keep the notation easy. This gives nothing but a $p-1$-pair term with the additional interaction:

$$\begin{aligned}
&\frac{y^{2(p-1)}}{(p-1)!^2} \int_{|\mathbf{r}_i - \mathbf{r}_j|>e^{\delta\ell}} \prod_{i=1}^{p-1} d^2\mathbf{r}_i^+ d^2\mathbf{r}_i^- e^{-\sum'_{i\neq j} m_i m_j V(\mathbf{r}_i - \mathbf{r}_j)} (1 + \mathcal{A}) \\
&\approx \frac{y^{2(p-1)}}{(p-1)!^2} \int_{|\mathbf{r}_i - \mathbf{r}_j|>e^{\delta\ell}} \prod_{i=1}^{p-1} d^2\mathbf{r}_i^+ d^2\mathbf{r}_i^- e^{-\sum'_{i\neq j} m_i m_j V(\mathbf{r}_i - \mathbf{r}_j) + \mathcal{A}}
\end{aligned} \tag{3.62}$$

where we introduced the quantity:

$$\mathcal{A} = y^2 \int_{1<|\mathbf{r}^+ - \mathbf{r}^-|<e^{\delta\ell}} d^1\mathbf{r}^+ d^2\mathbf{r}^- e^{-V(\mathbf{r}^+ - \mathbf{r}^-) - \sum'_i m_i (V(\mathbf{r}_i - \mathbf{r}^+) - V(\mathbf{r}_i - \mathbf{r}^-))}. \tag{3.63}$$

We now introduce $\boldsymbol{\xi} = \mathbf{r}_+ - \mathbf{r}_-$, $\mathbf{x} = \frac{\mathbf{r}_+ + \mathbf{r}_-}{2}$. Moreover, since $\xi = 1 + O(\delta\ell)$ and $V(1) = 0$, we have that $V(\mathbf{r}^+ - \mathbf{r}^-) = O(\delta\ell^2)$ and can be neglected. At the same

time, since the potential is supposed to vary slowly at large distance, we can expand $V(\mathbf{r}_i - \mathbf{r}^+) - V(\mathbf{r}_i - \mathbf{r}^-) = \boldsymbol{\xi} \cdot \nabla V(\mathbf{r}_i - \mathbf{x}) + O(\xi^3)$. Then we obtain

$$\begin{aligned} \mathcal{A} &= y^2 \int_{1<\xi<e^{\delta\ell}} d^2\boldsymbol{\xi}\, d^2\mathbf{x} e^{-\boldsymbol{\xi}\cdot\sum_i' m_i \nabla V(\mathbf{x}-\mathbf{r}_i)} \\ &= y^2 \int_{1<\xi<e^{\delta\ell}} d^2\boldsymbol{\xi}\, d^2\mathbf{x} \left(1 - \boldsymbol{\xi}\cdot\mathbf{E} + \frac{1}{2}\xi_a\xi_b E_a E_b + O(\xi^4)\right) \end{aligned} \tag{3.64}$$

where we introduced the electric filed $\mathbf{E}(\mathbf{x}) = \sum_i m_i \nabla V(\mathbf{x} - \mathbf{r}_i)$. Performing the integral over $\boldsymbol{\xi}$:

$$\mathcal{A} = \text{const} + y^2(e^{\delta\ell} - 1)\frac{\pi}{2}\int d^2\mathbf{x}\, \mathbf{E}^2 = \delta\ell\, \frac{\pi y^2}{2}\int d^2\mathbf{x}\, \mathbf{E}^2 + O(\delta\ell^2) \tag{3.65}$$

where we got rid of the additive constant which has no physical meaning. Now we have to compute the electrostatic energy: let us notice that, in the ultraviolet, the electric field of a single charge goes as $\nabla V \sim r^{1-\sigma}$ for $r \gg 1$; taking into account the global neutrality we have $E \sim r^{-\sigma}$ and $E^2 \sim r^{-2\sigma}$ so that the integral is convergent only for $\sigma > 1$, which is exactly the range of the parameter we are interested in. In this case we can write

$$\begin{aligned} \int d^2\mathbf{x}\, \mathbf{E}^2(\mathbf{x}) &= \sum_{i,j}' m_i m_j \int d^2\mathbf{x} \nabla V(\mathbf{x} + \mathbf{r}_i)\cdot\nabla V(\mathbf{x} + \mathbf{r}_j) \\ &= \sum_{i,j}' m_i m_j \int d^2\mathbf{x} \nabla V(\mathbf{x})\cdot\nabla V(\mathbf{x} + \mathbf{r}_j - \mathbf{r}_i) \\ &= \sum_{i\neq j}' m_i m_j \int d^2\mathbf{x} \left(\nabla V(\mathbf{x})\cdot\nabla V(\mathbf{x} + \mathbf{r}_j - \mathbf{r}_i) - |\nabla V(\mathbf{x})|^2\right) \end{aligned} \tag{3.66}$$

where we once again used the charge neutrality to write all in terms of the sum with $i \neq j$. Thus, setting $p' = p - 1$, we end up with a partition function with the same form of Eq. (3.61) with a renormalized two-body interaction given by $V_\ell(r) \to V(r) - \frac{\pi^2}{2} y_\ell^2 \Delta V(r)$, with

$$\Delta V(r) = \int d^2\mathbf{x} \left(\nabla V_\ell(\mathbf{x})\cdot\nabla V_\ell(\mathbf{x} + \mathbf{r}) - |\nabla V_\ell(\mathbf{x})|^2\right). \tag{3.67}$$

Finally, in order to correctly write the change of the partition function under the renormalization procedure we have to change the length-scale $\tilde{r} = re^{-\delta\ell}$ so that the new cutoff length $a_{\ell+\delta\ell}$ is 1 as well. Let us notice that, from the integration measure of Eq. (3.61) we get a factor $e^{4p\delta\ell}$ which can be reabsorbed into a renormalization

of the fugacity, $y_\ell \to y_\ell e^{2\delta\ell}$. In terms of $\tilde{r}$ the potential becomes $V_\ell(r) = V_\ell(\tilde{r}) + \tilde{r}\, V'_\ell(\tilde{r})\delta\ell + O(\delta\ell^2)$. From now on we will rename $\tilde{r}, r$. Thus, up to higher orders in $\delta\ell$, we can write $V_\ell(r) \to V_\ell(r) + \delta V(r)$ where

$$\delta V(r) = \delta\ell \left(r V'_\ell(r) - \frac{\pi y^2}{2} \Delta V(r) \right) \tag{3.68}$$

Let us notice that the new interaction energy no longer respects the condition $V(1) = 0$, so that the procedure cannot be properly repeated. To make up for it we can exploit once again the neutrality condition to have:

$$\begin{aligned} H_{\text{top}} &= \sum_{i \neq j} m_i m_j \left(V_\ell(\mathbf{r}_i - \mathbf{r}_j) + \delta V(\mathbf{r}_i - \mathbf{r}_j) \right) \\ &= \sum_{i \neq j} m_i m_j V_{\ell+\delta\ell}(\mathbf{r}_i - \mathbf{r}_j) - \delta V(1) \sum_i m_i^2 \end{aligned} \tag{3.69}$$

with $V_{\ell+\delta\ell}(r) = V_\ell(r) + \delta V(r) - \delta V(1)$. The last term can be absorbed into the renormalization of the fugacity:

$$y_{\ell+\delta\ell} = y_\ell e^{2\delta\ell} e^{\delta V(1)} \tag{3.70}$$

Summarizing we have been able to put the partition function in the same form of the original one, with a different fugacity $y_{\ell+\delta\ell}$ and a different vortex interaction energy $V_{\ell+\delta\ell}(r)$, given by

$$\begin{aligned} \partial_\ell V_\ell(r) &= r V'_\ell(r) - V'_\ell(1) - \frac{\pi}{2} y_\ell^2 \left(\Delta V_\ell(r) - \Delta V_\ell(1) \right) \\ \frac{dy_\ell}{d\ell} &= y_\ell \left(2 + V'_\ell(1) \right) + O(y^3) \end{aligned} \tag{3.71}$$

with ΔV from Eq. (3.67). These are the renormalization equations we are interested in.

3.5 | Phase diagram of the model

We now want to derive the phase diagram of the model, discussing the behavior of the renormalization flow described by Eqs. (3.71). Quite surprisingly, in spite of the fact that we are dealing with a non-linear functional set of equations, it is possible to solve them analytically.

Let us start by noticing that, since ΔV_ℓ in Eq. (3.67) involves a convolution, it is natural to write $V_\ell(r)$ as

$$V_\ell(r) = \int \frac{d^2q}{(2\pi)^2} U_\ell(q) \left(e^{i\mathbf{q}\cdot\mathbf{n}} - e^{i\mathbf{q}\cdot\mathbf{r}} \right), \tag{3.72}$$

with $\mathbf{n}^2 = 1$ and $U_{\ell=0}(q) = -gq^{-4-\sigma}$, in agreement with Eq. (3.57). In terms of $U_\ell(q)$ the first equation of Eq. (3.71) becomes

$$\partial_\ell U_\ell(q) = -\left(2 + q\partial_q\right) U_\ell(q) + \frac{\pi}{2} y_\ell^2 q^2 U_\ell(q)^2, \tag{3.73}$$

which, in turn, can be rewritten as

$$\partial_\ell U_\ell^{-1}(q) = \left(2 - q\partial_q\right) U_\ell^{-1}(q) - \frac{\pi}{2} y_\ell^2 q^2. \tag{3.74}$$

Taking into account our initial condition we can solve this equation by using the ansatz:

$$U_\ell^{-1}(q) = -A_\ell q^{4-\sigma} - B_\ell q^2, \tag{3.75}$$

finding:

$$\begin{aligned} \frac{dA_\ell}{d\ell} &= -(2-\sigma)A_\ell \\ \frac{dB_\ell}{d\ell} &= \frac{\pi}{2} y_\ell^2 \end{aligned} \tag{3.76}$$

along with the initial condition $A_0 = g^{-1}$, $B_0 = 0$. We have then that $A_\ell \to 0$ in the infrared, while B_0 grows as long as $y_\ell \neq 0$. The vortex-vortex potential becomes then:

$$V_\ell(r) = -\int \frac{d^2\mathbf{q}}{(2\pi)^2} \frac{e^{i\mathbf{q}\cdot\mathbf{n}} - e^{i\mathbf{q}\cdot\mathbf{r}}}{A_\ell q^{4-\sigma} + B_\ell q^2} = -\int \frac{dq}{2\pi} \frac{1 - \mathcal{J}_0(qr)}{A_\ell q^{3-\sigma} + B_\ell q}, \tag{3.77}$$

($\mathcal{J}_k(qr)$ being the k-th order Bessel function of the first kind). By computing $V'(r)$ we can derive the equation for y which, together with Eqs. (3.76), gives the reduced RG set of equations of the model

$$\frac{dy_\ell}{d\ell} = y_\ell \left(2 - \int \frac{dq}{2\pi} \frac{\mathcal{J}_1(q)}{B_\ell + A_\ell q^{2-\sigma}}\right) \tag{3.78}$$

From Eqs. (3.76) it follows that for any finite ℓ we have $B_\ell > 0$, so that the second term in the denominator of Eq. (3.77) dominates for $q \ll 1$ and $V_\ell(r) \sim -\ln r$ for $r \gg 1$. As announced then, the infrared behavior of the vortex-vortex potential is, for any finite value of ℓ, qualitatively different from the ultraviolet behavior. In particular, let us notice that the infrared, as $A_\ell \to 0$, the RG equations (3.71) and (3.78) can be approximated as

$$\begin{aligned} \frac{dB_\ell}{d\ell} &= \frac{\pi}{2} y_\ell^2 \\ \frac{dy_\ell}{d\ell} &= y_\ell \left(2 - \frac{1}{2\pi B_\ell}\right), \end{aligned} \tag{3.79}$$

i.e. exactly the form of the BKT RG flow for the short-range XY model.

As a consequence, we also have here a line of stable fixed points $y = 0$, $B < \frac{1}{4\pi}$, corresponding to a phase in which the vortices are not relevant. At the same time it will exist a transition temperature T_{BKT} such that, for $T > T_{BKT}$, the vortices unbind so that the system flows toward a disordered phase.

Let us notice, however, how here the low-temperature phase ($T < T_{BKT}$) does not correspond to a quasi-long-range-ordered phase. Indeed, since the vortices are irrelevant and it is not possible to excite vortex-antivortex pair, the constraint (3.16) tells us that in the infrared the link variables $n_{\mathbf{i},\mathbf{j}}$ are suppressed as well. As a consequence, from Eq. (3.32), in the infrared we have the identification

$$\theta(x) \to \psi(x). \tag{3.80}$$

Since H_{SW} is a quadratic Gaussian model, with the dispersion relation $\omega(q) \sim q^{\sigma}$, we once again find the low-temperature effective Hamiltonian

$$S \sim -\frac{1}{2}\int d^2\mathbf{x}\, \theta \nabla^{\sigma} \theta \tag{3.81}$$

which, in turn, foresees a finite magnetization for the order parameter $\mathbf{s} = (\cos\theta, \sin\theta)$ (see Sec. 2.2 and 2.6 of Chapter 2).

Unlike the case of the long-range XY model, however, here we do not find any intermediate quasi-long-range-order phase. Instead, our analysis foresees a non-universal jump in the magnetization between the ordered and the disordered phase. We expect, however, the correlation length ξ in the disorder phase ($T > T_{BKT}$) to exhibit the usual BKT scaling, namely

$$\ln \xi \sim (T - T_{BKT})^{-1/2}, \tag{3.82}$$

as the set of RG Eqs. (3.79) has the same form of the standard BKT one.

We can thus conclude unambiguously that the Villain model and the XY model are not in the same universality class for $\sigma < 2$.

In summarizing, we find the following phase diagram for the Villain model:

- For $\sigma > 2$, the long-range Villain model exhibits the same phases as its nearest-neighbors counterpart, i.e. it undergoes a BKT phase transition between a low-temperature quasi-long-range ordered phase and a high-temperature disordered one. The phase diagram is thus analogous to the one of the XY model with $\sigma > 2$.

- For $1 < \sigma < 2$ the model undergoes a phase transition which falls as well under the BKT universality. In this regime, however, we have spontaneous symmetry breaking, and a first-order phase transition in the order parameter

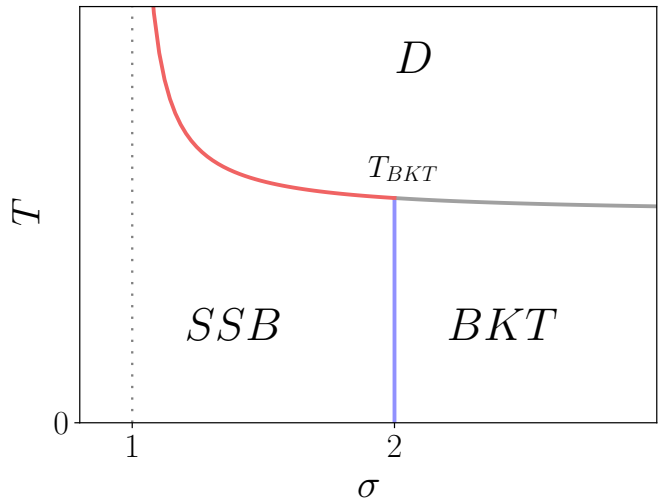

FIGURE 3.3: Qualitative phase diagram of the long-range Villain model. For $\sigma > 2$ the system exhibits a BKT transition between the quasi-long-range-ordered BKT phase and the disordered (D) one (grey line). For $1 < \sigma < 2$, for low temperature the model exhibit a low-temperature spontaneous-symmetry-broken (SSB) phase with a finite magnetization. As the temperature increases, we have a transition (red line) to the disordered (D) phase, with a jump in the order parameter. This transition, however, still falls within the BKT universality class. For $\sigma \to 1^+$ the transition temperature diverges, so that only the SSB phase survives for $\sigma < 1$.

as the temperature is increased. The phase diagram is analogous to the one of the one-dimensional Ising model with $1/r^2$ interactions ($\sigma = 1$) [49, 115, 116], in which we have, as well coexistence of first-order and *BKT* features in the transition.

- For $0 < \sigma < 1$ the topological defects cannot be excited at any temperature, so that the model does not undergo any phase transition and exhibits spontaneous-symmetry breaking at any temperature.

A qualitative depiction of the phase diagram of the model is presented in Fig. 3.3. Depending whether we are looking at the behavior of the order parameter or to the universality class of the phase transition, we can thus say that the model has $\sigma^* = 1$ or $\sigma^* = 2$.

3.6 | Field-theory representation of the model

In this section we see how some of the results obtained rigorously through the lattice Villain model (3.17) can be understood in terms of its continuum limit (3.7) within the field theory formalism.

Let us start by expressing the quadratic action in terms of its Fourier modes

$$\beta H_0 = \frac{J}{4}\int d^2\mathbf{q}\;\omega(q)\;|\theta(\mathbf{q})|^2 \sim J\int d^2\mathbf{q}\;q^\sigma|\theta(\mathbf{q})|^2, \tag{3.83}$$

or, in terms of the single-valued, vector field $\mathbf{v} = \nabla\theta(\mathbf{x})$:

$$\beta H_0 \sim J\int d^2\mathbf{q}\;q^{\sigma-2}|\mathbf{v}(\mathbf{q})|^2. \tag{3.84}$$

It is now possible to solve the constraint in Eq. (3.7) by introducing an auxiliary field $\varphi(\mathbf{x})$ so that

$$Z \sim \sum_{\{m_i\}}\int \mathscr{D}(\mathbf{v})\int \mathscr{D}(\varphi)\; e^{-J\int d^2\mathbf{q}\;q^{\sigma-2}|\mathbf{v}(\mathbf{q})|^2}\; e^{-i\int d^2\mathbf{x}\;\varphi(\mathbf{x})(\nabla\times\mathbf{v}-2\pi n(\mathbf{x}))}. \tag{3.85}$$

After noticing that

$$-i\int d^2\mathbf{x}\;\varphi(\mathbf{x})\;\nabla\times\mathbf{v} = \int d^2\mathbf{q}\;\mathbf{v}(\mathbf{q})\times\varphi(\mathbf{q}), \tag{3.86}$$

we can trace out the $\mathbf{v}$, obtaining, for the topological part of the partition function

$$Z_{\text{top}} \sim \sum_{\{m_i\}}\int \mathscr{D}(\varphi)\; e^{-J^{-1}\int d^2\mathbf{q}\;q^{4-\sigma}|\varphi(\mathbf{q})|^2} e^{-2\pi i\int d^2x\;\varphi(\mathbf{x})n(\mathbf{x})} \tag{3.87}$$

From here, by integrating out the auxiliary field as well we get

$$Z_{\text{top}} \sim \sum_{\{m_i\}}\; e^{-J\int d^2\mathbf{q}\;q^{\sigma-4}|n(\mathbf{q})|^2} \sim \sum_{\{m_i\}} e^{-\sum_{j,k} m_j m_k U(\mathbf{r}_j-\mathbf{r}_k)} \tag{3.88}$$

with $U(q) \sim Jq^{\sigma-4}$, which is precisely the form of the (large-distance) vortex-vortex interaction we worked out in Sec. 3.3. Let us notice, however, how this field theory approach is not able to predict the divergence in the coupling constant for $\sigma \to 1$.

On the other hand, from Eq. (3.87), one could trace out the vortices, obtaining an effective field theory of the model in terms of the field φ. To this extent, it is necessary to introduce by hand the core energy of the vortices, whose presence is not captured by the long-distance, field-theoretical description. We get

$$Z_{\text{top}} \sim \sum_{\{m_i\}}\int \mathscr{D}(\varphi)\; e^{-J^{-1}\int d^2\mathbf{q}\;q^{4-\sigma}|\varphi(\mathbf{q})|^2} e^{-2\pi i\int d^2x\;\varphi(\mathbf{x})n(\mathbf{x})} e^{-\varepsilon_c\sum_i m_i^2}. \tag{3.89}$$

Working in the limit of low fugacity $y = e^{-\varepsilon_c}$, we sum over the configurations such that $m_i = \pm 1$. This means that, for each point of the space we get a term of the form

$$\sum_{m=-1}^{1} y^m e^{-2\pi i \varphi(\mathbf{x}) m} = 1 + y \cos 2\pi\varphi \approx e^{y \cos 2\pi\varphi} \tag{3.90}$$

obtaining

$$Z_{\text{top}} \sim \int \mathscr{D}(\varphi)\, e^{-S}, \tag{3.91}$$

with

$$S = J^{-1} \int d^2\mathbf{q}\, q^{4-\sigma} |\varphi(\mathbf{q})|^2 - y \int d^2\mathbf{x} \cos(2\pi\varphi). \tag{3.92}$$

This is a Sine-Gordon action with a peculiar dispersion relation of the kinetic term $\sim U^{-1}(q)$. Within this field-theoretical picture, it is the latter that is responsible for the peculiar form of the RG flow. Let us notice, indeed, how $q^{4-\sigma}$ is less relevant than the usual q^2 short-range dispersion relation. On the other hand, if we perform a perturbative renormalization group for small y (e.g. in the Wilson picture) it is known that the Sine-Gordon term, would generate, at the second order in y, short-range kinetic terms $\sim q^2|\varphi(q)|^2$ in the Lagrangian (see e.g. [117, 118]). This means that the action (3.92) would flow in the infrared to the usual Sine-Gordon theory, which falls in the universality class of the BKT transition.

References

[2] A. Campa, T. Dauxois, D. Fanelli, and S. Ruffo. *Physics of Long-Range Interacting Systems*. Oxford Univ. Press, 2014.

[31] J. M. Kosterlitz and D. J. Thouless. "Ordering, metastability and phase transitions in two-dimensional systems". *J. Phys. C* 6(7) (Apr. 1973), pp. 1181–1203. DOI: 10.1088/0022-3719/6/7/010.

[49] J. L. Cardy. "One-dimensional models with $1/r^2$ interactions". *Journal of Physics A: Mathematical and General* 14(6) (June 1981), pp. 1407–1415. DOI: 10.1088/0305-4470/14/6/017.

[72] P. Minnhagen. "The two-dimensional Coulomb gas, vortex unbinding, and superfluid-superconducting films". *Rev. Mod. Phys.* 59 (4 Oct. 1987), pp. 1001–1066. DOI: 10.1103/RevModPhys.59.1001.

[75] R. Savit. "Duality in field theory and statistical systems". *Rev. Mod. Phys.* 52 (2 Apr. 1980), pp. 453–487. DOI: 10.1103/RevModPhys.52.453.

[76] J. VILLAIN. "Theory of one-dimensional and two-dimensional magnets with an easy magnetization plane. 2. The Planar, classical, two-dimensional magnet". *J. Phys. France* 36 (1975), pp. 581–590. DOI: 10.1051/jphys:01975003606058100.

[96] H. KLEINERT. *Gauge fields in condensed matter*. Vol. 2. World Scientific, 1989.

[97] J. V. JOSÉ, L. P. KADANOFF, S. KIRKPATRICK, and D. R. NELSON. "Renormalization, vortices, and symmetry-breaking perturbations in the two-dimensional planar model". *Phys. Rev. B* 16 (3 Aug. 1977), pp. 1217–1241. DOI: 10.1103/PhysRevB.16.1217.

[98] J. FRÖHLICH and T. SPENCER. "The Kosterlitz-Thouless transition in two-dimensional abelian spin systems and the Coulomb gas". *Communications in Mathematical Physics* 81(4) (1981), pp. 527–602.

[99] O. KAPIKRANIAN, B. BERCHE, and Y. HOLOVATCH. "Interplay of topological and structural defects in the two-dimensional XY model". *Physics Letters A* 372(35) (2008), pp. 5716–5721. ISSN: 0375-9601. DOI: https://doi.org/10.1016/j.physleta.2008.06.087.

[100] J. T. HARALDSEN and R. S. FISHMAN. "Spin rotation technique for non-collinear magnetic systems: application to the generalized Villain model". *Journal of Physics: Condensed Matter* 21(21) (Apr. 2009), p. 216001. DOI: 10.1088/0953-8984/21/21/216001.

[101] M. HASENBUSCH. "The two-dimensional XY model at the transition temperature: a high-precision Monte Carlo study". *Journal of Physics A: Mathematical and General* 38(26) (2005), p. 5869.

[102] W. JANKE. "Logarithmic corrections in the two-dimensional XY model". *Phys. Rev. B* 55 (6 Feb. 1997), pp. 3580–3584. DOI: 10.1103/PhysRevB.55.3580.

[103] T. SURUNGAN, S. MASUDA, Y. KOMURA, and Y. OKABE. "Berezinskii–Kosterlitz–Thouless transition on regular and Villain types of q-state clock models". *Journal of Physics A: Mathematical and Theoretical* 52(27) (2019), p. 275002.

[104] W. WITCZAK-KREMPA, E. S. SØRENSEN, and S. SACHDEV. "The dynamics of quantum criticality revealed by quantum Monte Carlo and holography". *Nature Physics* 10(5) (2014), pp. 361–366.

[105] C. DASGUPTA and B. I. HALPERIN. "Phase Transition in a Lattice Model of Superconductivity". *Phys. Rev. Lett.* 47 (21 Nov. 1981), pp. 1556–1560. DOI: 10.1103/PhysRevLett.47.1556.

[106] E. ONOFRI. "$SU(N)$ lattice gauge theory with Villainâs action". *Nuovo Cimento* 66(7644) (Dec. 1981), pp. 217–220. DOI: 10.1007/BF02731690.

[107] M. Romo and M. Tierz. "Unitary Chern-Simons matrix model and the Villain lattice action". *Phys. Rev. D* 86 (4 Aug. 2012), p. 045027. DOI: 10.1103/PhysRevD.86.045027.

[108] Y. Choi *et al.* "Noninvertible duality defects in 3+1 dimensions". *Phys. Rev. D* 105 (12 June 2022), p. 125016. DOI: 10.1103/PhysRevD.105.125016.

[109] O. Borisenko, V. Chelnokov, M. Gravina, and A. Papa. "Deconfinement and universality in the 3D U (1) lattice gauge theory at finite temperature: study in the dual formulation". *Journal of High Energy Physics* 2015(9) (2015), pp. 1–17.

[110] H. Helmholtz. "Uber Integrale der hydrodynamischen Gleichungen". *Journal fur die reine und angewandte Mathematik* 55 (1858).

[111] O. Heaveside. *Electromagnetic theory, vol. I.* The Electrician Publishing, 1893.

[112] V. E. Tarasov. "No violation of the Leibniz rule. No fractional derivative". *Communications in Nonlinear Science and Numerical Simulation* 18(11) (2013), pp. 2945–2948. ISSN: 1007-5704. DOI: https://doi.org/10.1016/j.cnsns.2013.04.001.

[113] M. I. Berganza and L. Leuzzi. "Critical behavior of the X Y model in complex topologies". *Physical Review B* 88(14) (2013), p. 144104.

[114] F. Cescatti, M. Ibáñez-Berganza, A. Vezzani, and R. Burioni. "Analysis of the low-temperature phase in the two-dimensional long-range diluted XY model". *Phys. Rev. B* 100(5), 054203 (Aug. 2019), p. 054203. DOI: 10.1103/PhysRevB.100.054203.

[115] J. Fröhlich and T. Spencer. "Massless phases and symmetry restoration in abelian gauge theories and spin systems". *Commun. Math. Phys.* 83(3) (Dec. 1982), pp. 411–454. DOI: 10.1007/BF01213610.

[116] P. W. Anderson, G. Yuval, and D. R. Hamann. "Exact Results in the Kondo Problem. II. Scaling Theory, Qualitatively Correct Solution, and Some New Results on One-Dimensional Classical Statistical Models". *Phys. Rev. B* 1(11) (June 1970), pp. 4464–4473. DOI: 10.1103/PhysRevB.1.4464.

[117] A. O. Gogolin, A. A. Nersesyan, and A. M. Tsvelik. *Bosonization and strongly correlated systems*. Cambridge university press, 2004.

[118] T. Giamarchi. *Quantum Physics in One-Dimension*. Clarendon Press, 2004.

Part II

4 | Quench dynamics in the long-range $O(n)$ model

In this Chapter we address the study of the dynamics of closed quantum systems in presence of strong-long range (non-additive) interactions, using as a prototypical example the quantum $O(n)$ model in the large n limit. The peculiar properties of the spectrum analyzed in Sec. 1.3.1 give rise to a complete new phenomenology that manifests itself on mesoscopic timescales.

The Chapter is based on Ref. [119] and it is structured as follows: after introducing the model in Sec. 4.1 and discussing its large n limit, in Sec. 4.2 and Sec. 4.3 we discuss the solution of the effective equations of motion for short and mesoscopic timescales respectively. Finally, in Sec. 4.4 we discuss the characteristics of the entanglement spreading in the model and how they can be used to tell apart the different dynamical phases of the model.

4.1 | The quantum $O(n)$ model

The quantum $O(n)$ rotor model, constitutes a prototypical tool in the context of quantum many-body physics. In the large n limit, it provides one of the simplest instances of an interacting model [120, 121]. Let us consider a one dimensional lattice of N sites. For any lattice sites j we introduce a pair of n-component variables Φ_j^a,Π_j^a (with $a = 1, \cdots n$) which are canonically conjugate $[\Phi_{\mathrm{j}}^a, \Pi_{\mathrm{j}'}^{a'}] = i\delta_{\mathrm{j},\mathrm{j}'}\delta_{a,a'}$ and interact though the Hamiltonian

$$H = \frac{1}{2}\sum_j \left(|\vec{\Pi}_j|^2 + r|\vec{\Phi}_j|^2 + \frac{\lambda}{2n}|\vec{\Phi}_j|^4 \right) + \frac{1}{2}\sum_{j,j'} J(r)|\vec{\Phi}_j - \vec{\Phi}_j|^2 \tag{4.1}$$

with $r = |j - j'|$. The model exhibits a global $O(n)$ symmetry which justifies its name; in the classical limit ($[\Phi_{\mathrm{j}}^a, \Pi_{\mathrm{j}'}^{a'}] = 0$), moreover, the model can be interpreted as a straightforward discretization of the $O(n)$ field-theory in Eq. (1.16).

In the strong-long range case, the quadratic coupling $J(r)$ takes the form

$$J(r) = \frac{1}{N_\alpha} r^{-\alpha}, \tag{4.2}$$

with $0 < \alpha < 1$ (strong long-range regime) and

$$N_\alpha = \sum_{r \neq 0} r^{-\alpha} \tag{4.3}$$

the Kac scaling [2, 10], crucial to ensure energy extensivity. Although we are here working in $d = 1$, in this regime the qualitative features of the evolution shall not depend on the dimension d. In the following we will also assume periodic boundary conditions.

An appropriate solution for the model dynamics after a global quench on any of the Hamiltonian parameters can be achieved, in the limit $n \to \infty$. There, the quartic term in Eq. (4.1) can be decoupled via the self-consistent relation

$$|\vec{\Phi}_j|^4 \to \left\langle |\vec{\Phi}|^2 \right\rangle |\vec{\Phi}_j|^2. \tag{4.4}$$

Formally, this means that the correlation function involving a finite number of components, at any time t, are the same for the two theories, up to $O(1/n)$ terms [121]. In conclusion, the Hamiltonian in Eq. (4.1) at $n \to \infty$ can be replaced by its quadratic counterpart with a self-consistent effective mass [17]

$$\mu(t) = r + \frac{\lambda}{2} \left\langle \Phi^2(t) \right\rangle. \tag{4.5}$$

The dynamical properties of the model in the case of short-range couplings have been deeply investigated(finding dynamical transitions [17, 122], aging [123]) as well as the first finite-n corrections [124] and its extension to weak long-range regime [125].

The solution of the dynamics of the model passes through the introduction of the Fourier modes, labeled by the momentum $q = \frac{2\pi m}{N}$ with $m = -N/2 + 1, \ldots, N/2$, in terms of which we have

$$H = \sum_{q \geq 0} \left(\Pi_q^\dagger \Pi_q + (\omega^2(q) + \mu(t)) \Phi_q^\dagger \Phi_q \right) \tag{4.6}$$

where $\mu(t)$ is determined self-consistently as

$$\mu(t) = r + \frac{\lambda}{N} \sum_q |f_q|^2, \tag{4.7}$$

while

$$\omega^2(q) = 1 - \sum_{r \neq 0} J(r) \cos(qr). \tag{4.8}$$

As seen in Sec. 1.3.1 (or in Ref. [61]), in the thermodynamic limit, a spectrum of the form of Eq. (4.8) does not converge to a continuous function of q as the short-range case (and in the weak long-range regime $\alpha > 1$, see Eq. (1.14)). Rather, we can derive the expression

$$\omega^2(q) = 1 - \frac{1}{u_\alpha}\int_0^\pi ds \frac{\cos(sm)}{\mathbf{s}^\alpha}, \tag{4.9}$$

with

$$u_\alpha = \frac{\pi^{1-\alpha}}{1-\alpha}, \tag{4.10}$$

valid up to order $N^{\alpha-1}$ terms (see Sec. 4.9). The spectrum exhibits a finite gap between the ground state $\epsilon_0 = 0$ and the first-excited states ($|m| = 1$), while the states accumulate around $\omega_\infty = 1$ for $|m| >> 1$, so that a thermodynamic large number of single-particle states is in a neighbourhood of $\omega = 1$.

The Hamiltonian in Eq. (4.6), as well as its dynamics, is readily diagonalized in terms of

$$\Phi_q = \frac{1}{\sqrt{2}}\left(f_q(t)a_q + f^*_{-q}(t)a^\dagger_{-q}\right), \tag{4.11}$$

$$\Pi_q = \frac{1}{\sqrt{2}}\left(\dot{f}^*_q(t)a^\dagger_q + \dot{f}_{-q}(t)a_{-q}\right). \tag{4.12}$$

where a_q, $a^\dagger_q$ and a_{-q}, $a^\dagger_{-q}$ are two independent sets of ladder operators which do not depend on time (see Ref. [17]). The canonical commutation relations introduce the constraints $f_q(t) = f_{-q}(t)$, $\mathrm{Im}(f^*_q\dot{f}_q) = 1$. Let us notice that, in terms of the f_q, we can express the equal-time correlators of the model as

$$\begin{aligned}
\left\langle \Phi_q(t)\Phi_{q'}(t)^\dagger \right\rangle &= \frac{\mathcal{N}_q}{2}|f_q(t)|^2\delta_{qq'},\\
\left\langle \Pi_q(t)\Pi_{q'}(t)^\dagger \right\rangle &= \frac{\mathcal{N}_q}{2}|\dot{f}_q(t)|^2\delta_{qq'},\\
\left\langle \Phi_q(t)\Pi_{q'}(t) \right\rangle &= \frac{\delta_{qq'}}{2}\left(\mathcal{N}_q\mathrm{Re}(f_q(t)\dot{f}^*_q(t)) + i\mathcal{S}_q\right),
\end{aligned} \tag{4.13}$$

where $\mathcal{N}_q = 1 + \left\langle n_q \right\rangle + \left\langle n_{-q} \right\rangle$, $\mathcal{S}_q = 1 + \left\langle n_q \right\rangle - \left\langle n_{-q} \right\rangle$, $\left\langle n_q \right\rangle = \left\langle a^\dagger_q a_q \right\rangle$ being the *initial* occupation numbers of the corresponding mode.

The evolution equations of the amplitude functions $f_q(t)$ are obtained by the Heisenberg equations of motion of Hamiltonian (4.6)

$$\dot{\Phi}_q = \Pi^\dagger_q, \qquad \dot{\Pi}_q = -(\omega^2(q) + \mu(t))\Phi^\dagger_q, \tag{4.14}$$

which, once expressed in terms of the creation and annihilation operators, give

$$\ddot{f}_q(t) + \left(\omega^2(q) + \mu(t)\right)f_q(t) = 0. \tag{4.15}$$

In turn, once written in terms of the real and imaginary part of f_q, they can be seen as the equations of motion for a set of two-dimensional isotropic harmonic oscillators. The frequency varies in time, and it is determined self consistently by Eq. (4.5). The evolution respects the constraints $\mathrm{Im}(f_q^* \dot{f}_q) = 1$, as they correspond to the conserved angular momenta of the oscillators. The single oscillator energy is instead not conserved. However, one can verify that the energy per particle

$$\epsilon = \frac{\lambda}{2N} \sum_q \mathcal{N}_q \left(|\dot{f}_q|^2 + \omega^2(q) |f_q|^2 \right) + \frac{1}{2}\mu^2 \tag{4.16}$$

is a constant of motion. Let us notice that, by definition $\mu > r$ and $\mu^2 < 2\epsilon$ must hold.

In the following, we will focus on the dynamics of the model after a quench in the bare mass parameter r ($r^- \to r^+$) at $t = 0$, assuming the system is in the ground state for $t < 0$.

4.1.1 | Ground state properties

Let us now analyze the ground state properties of the model (4.6) and compute the ground-state energy per particle ϵ_{gs} and the corresponding value of μ_{gs}. In our protocol, those will coincide with the state of the model at $t = 0^-$.

Since each oscillator Φ_q is now in the ground state, we have

$$\begin{aligned} \left\langle \Phi_q(0) \Phi_{q'}(0)^\dagger \right\rangle &= \frac{1}{2\sqrt{\omega^2(q) + \mu_{\mathrm{gs}}}}\, \delta_{q'q}, \\ \left\langle \Pi_q(0) \Pi_{q'}(0)^\dagger \right\rangle &= \frac{1}{2} \sqrt{\omega^2(q) + \mu_{\mathrm{gs}}}\, \delta_{q'q}, \\ \left\langle \Phi_q(0) \Pi_{q'}(0) \right\rangle &= \frac{i}{2}\, \delta_{q'q} \end{aligned} \tag{4.17}$$

from which, we find

$$f_q(0) = \left(\omega^2(q) + \mu_{\mathrm{gs}} \right)^{-1/4}, \qquad \dot{f}_q(0) = i \left(\omega^2(q) + \mu_{\mathrm{gs}} \right)^{1/4}, \tag{4.18}$$

valid up to an immaterial phase factor. Since μ_{gs} is a positive constant, the solution of the corresponding equations of motion (4.15) is given by

$$f_q(t) = \left(\omega^2(q) + \mu_{\mathrm{gs}} \right)^{-1/4} e^{i\sqrt{\omega^2(q) + \mu_{\mathrm{gs}}}\, t}. \tag{4.19}$$

Finally, from Eq. (4.5),

$$\mu_{\mathrm{gs}} = r + \frac{\lambda}{2N} \sum_q \frac{1}{\sqrt{\omega^2(q) + \mu_{\mathrm{gs}}}}. \tag{4.20}$$

Let us remind that in the strong-long range regime we can replace $\sqrt{\omega^2(q)+\mu_{\rm gs}}$ with $\sqrt{1+\mu_{\rm gs}}$, up to $O(N^{-\zeta})$ corrections, with $\zeta = \max(1, 2-2\alpha)$ (see Sec. 1.3.1). We thus get

$$\mu_{\rm gs} = r^- + \frac{1}{2}\frac{\lambda}{\sqrt{1+\mu_{\rm gs}}}, \tag{4.21}$$

which always has a unique solution. Since we are implicitly assuming $\mu_{\rm gs} > 0$, in order to have an oscillatory behavior for the $q = 0$ mode, we have to require $r^- > -\lambda/2$. For $r^- < -\lambda/2$ the $q = 0$ mode acquires a non-zero occupation number, signaling a finite magnetization in the system (the fact that the system undergoes a phase transition even in one dimension is not surprising, since the Mermin-Wanger theorem [30] no longer holds). The corresponding energy per particle is, up to $O(N^{-\zeta})$ corrections, given by

$$\begin{aligned}\epsilon_{\rm gs} &= \frac{\lambda}{2N}\sum_q \frac{1}{\sqrt{\omega^2(q)+\mu_{\rm gs}}}\left(2\omega^2(q)+\mu_{\rm gs}\right) + \frac{1}{2}\mu_{\rm gs}^2 \\ &= \frac{1}{2}\frac{\lambda}{\sqrt{1+\mu_{\rm gs}}}\left(2+\mu_{\rm gs}\right) + \frac{1}{2}\mu_{\rm gs}^2.\end{aligned} \tag{4.22}$$

For the sake of simplicity, in the following, we will always assume to be at $t = 0^-$ in the disordered phase $r_- > -\lambda/2$, in which all the modes have a finite occupation number.

4.2 | Solution of the equation of motion

Now we are going to solve the equations of motion (4.15) in order to describe the dynamics for $t > 0$. The entire model dynamics is crucially dependent on the evolution of the effective mass $\mu(t)$, which can be thought of as a classical degree of freedom. In turn, the dynamics of quantum degrees of freedom (parameterized by the f_q) is forced by $\mu(t)$

Due to the peculiar spectral properties of the model, here we are able to derive a closed equation for the $\mu(t)$ which becomes exact in the thermodynamic limit. Indeed, by taking the time derivative of both sides of Eq. (4.5)

$$\begin{aligned}\dot{\mu} &= \frac{\lambda}{2N}\sum_q \mathcal{N}_q \dot{f}_q f_q^* + c.c. \\ \ddot{\mu} &= \frac{\lambda}{2N}\sum_n \mathcal{N}_q\left(|\dot{f}_n|^2 + \ddot{f}_n f_n^* + c.c.\right) \\ &= \frac{\lambda}{N}\sum_q \mathcal{N}_q |\dot{f}_q|^2 - \frac{\lambda}{N}\sum_q \mathcal{N}_q\left(\mu+\omega^2(q)\right)|f_q|^2\,,\end{aligned} \tag{4.23}$$

from which, exploiting once again Eq. (4.5) together with the conservation of energy, we can write

$$\ddot{\mu} = 2\epsilon + 2r\mu - 3\mu^2 - 2(\mu - r) + g(t) \tag{4.24}$$

where we introduced

$$g(t) = \frac{1}{2}\sum_q m_q |f_q(t)|^2, \tag{4.25}$$

and $m_q = 4\lambda \mathcal{N}_q(1-\omega^2(q))/N$. Now, as discussed in Sec. 1.3.1, because of the peculiar structure of the spectrum, in the strong-long-range limit we have

$$g(t) \sim \left\langle 1 - \omega^2(q) \right\rangle \sim O(N^{-\zeta}) \tag{4.26}$$

as long as $f_q = O(1)$, so that its contribution to the equations of motion of $\mu(t)$ is negligible. In this limit, we can thus set $f_q = 0$ in the above Hamiltonian and consider the single particle dynamics

$$H = \frac{P_\mu^2}{2} + V(\mu), \tag{4.27}$$

which conserves the quantity

$$\mathscr{E} = \frac{\dot{\mu}^2}{2} + V(\mu). \tag{4.28}$$

Within the same approximation

$$\epsilon = \frac{\lambda}{2N}\sum_q \mathcal{N}_q |\dot{f}_q|^2 + \mu - r + \frac{1}{2}\mu^2. \tag{4.29}$$

The aforementioned classical dynamics only applies as long as the external force $g(t)$ remains negligible, this condition may be violated in two cases

1. The initial state at $t = 0$ contains at least one macroscopically populated mode leading to some extensive n_q.
2. The external drive $g(t)$ may become extensive due to one (or more) q modes undergoing a parametric resonance.

Scenario 1) occurs for any dynamics beginning in the magnetized ground-states at $r < -\lambda/2$, where the $q = 0$ mode acquires a macroscopic occupation. We ruled out this possibility as we restricted ourselves to the region $r^- > \lambda/2$ in the parameter space. On the other hand, even for an initially negligible external drive $g(t)$, one or more of the q modes can resonate with the unperturbed, classical dynamics of $\mu(t)$, leading to scenario 2) at later times.

Before examining the possibility of resonances, let us now consider the short-time behavior of the model, in which we can safely ignore the forcing $g(t)$ in Eq. (4.24). First, we notice that the assumption that the system is in the ground state at $t = 0^-$ has a simple physical interpretation in terms of the dynamics of the fictitious particle $\mu(t)$. Indeed it is easy to verify that, for $r = r^-$, $\mu = \mu_{\rm gs}$ and $\epsilon = \epsilon_{\rm gs}$, we have $V'(\mu_{\rm gs}) = 0$, so that the ground state corresponds to the stable equilibrium for the fictitious particle in the potential $V(\mu)$.

After the quench $r^- \to r^+$, the fictitious particle is no longer in the stable equilibrium, and starts moving in the potential $V(\mu)$. In spite of the fact that the potential $V(\mu)$ is cubic, let us notice, however, that its motion within the bounded region of the potential, and it is thus given by a periodic oscillation, as $\mathscr{E}$ can only be negative. To see this, we exploit the Cauchy-Schwartz inequality in Eq. (4.23), finding

$$\begin{aligned}\dot{\mu}^2 &= \left(\mathrm{Re}\left(\frac{\lambda}{N}\sum_q \mathcal{N}_q \dot{f}_q f_q^*\right)\right)^2 \leq \left|\frac{\lambda}{N}\sum_q \mathcal{N}_q \dot{f}_q f_q^*\right|^2 \\ &\leq \left(\frac{1}{N}\sum_q \mathcal{N}_q |f_q|^2\right)\left(\frac{1}{N}\sum_q \mathcal{N}_q |\dot{f}_q|^2\right).\end{aligned} \tag{4.30}$$

Now, putting together Eq. (4.29) and Eq. (4.15) and we find the constraint

$$\dot{\mu}^2 \leq 2\left(2\epsilon - 2(\mu - r) - \mu^2\right)(\mu - r) = -V(\mu), \tag{4.31}$$

from which the condition $\mathscr{E} < 0$ follows.

4.3 | Fate of the quantum degrees of freedom

Let us now explore the fate of the quantum modes f_q which may, at later times, lead to the breakdown of our classical, single-particle picture. Since for early times $g(t)$ is negligible and $\mu(t)$ is periodic with some period T, the equation of motion (4.15) for each of f_q is in the form of a Hill equation so that the Floquet theory applies. Indeed let us now consider the two independent solutions $f_1(t)$ and $f_2(t)$ of Eq. (4.15), such that $f_1(0) = 1$, $\dot{f}_1(0) = 0$ and $f_2(0) = 0$, $\dot{f}_2(0) = 1$ respectively. Let us notice that the Wronskian of the solutions $W = f_1\dot{f}_2 - f_2\dot{f}_1$ of the system is such that $\dot{W} = 0$. Now we notice that, being $a(t)$ periodic of period T, $f_1(t+T)$, $f_2(t+T)$ can be seen as a new pair of independent solutions, and thus expressed as a linear combination of $f_1(t)$, $f_2(t)$ namely

$$\begin{pmatrix} f_1(t+T) \\ f_2(t+T) \end{pmatrix} = C \begin{pmatrix} f_1(t) \\ f_2(t) \end{pmatrix}, \tag{4.32}$$

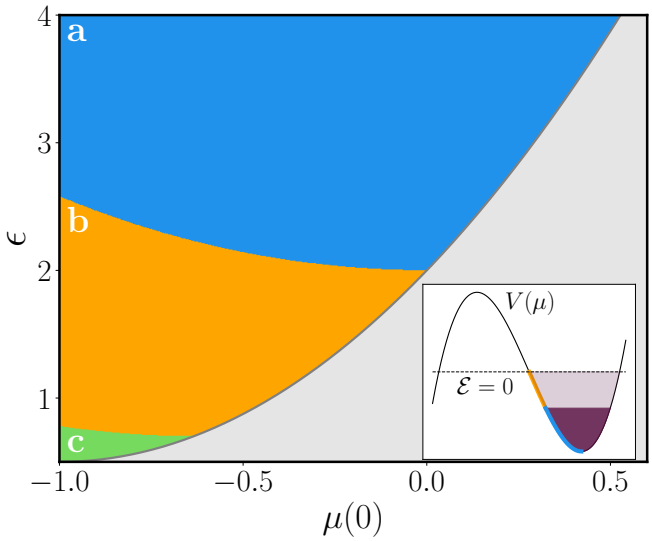

FIGURE 4.1: Phase diagram of the model for $r^+ = -1$, $\alpha = 0.5$ as a function of the energy per particle ϵ and the initial effective mass $\mu(0)$, assuming $\dot{\mu}(0) = 0$. Only the region with $\mu(0)$ between r and the minimum of $V(\mu)$ is shown, being all the other initial conditions nonphysical or redundant. In blue we have the resonance-free region (in which $\mu(t)$ is periodic); in orange the region in which the mode $q = 0$ is resonant; in green the region, where multiple modes above $q = 0$ are resonant as well. *Inset:* the potential $V(\mu)$ for $\epsilon = 2.25$, in which the values of $\mu(0)$ corresponding to different phases and the relative values of the classical energy $\mathcal{E}$, see Eq. (4.28), are outlined.

where C is a constant square matrix of order 2. In particular, imposing $W(t) = W(t+T)$ we find $\det C = 1$. Let us now consider two independent linear combinations $f_\pm(t)$, of $f_{1,2}(t)$ such that $f_\pm(t+T) = \Lambda_\pm f_\pm(t)$, $\Lambda_\pm$ being the eigenvalues of C. On the other hand, since C is real and $\det C = 1$ we have that only two cases are possible: either

$$f_q^\pm(t+T) = e^{\pm i\mu T} f_q^\pm(t) \tag{4.33}$$

with $\mu > 0$, or

$$f_q^\pm(t+T) = e^{\pm\kappa T} f_q^\pm(t) \tag{4.34}$$

with $\kappa > 0$. In the former case we are dealing with a quasi periodic pair of solutions, in the latter, instead, we have a so-called parametric resonance in which the generic solution $f_q(t)$ grows boundlessly.

As long as no resonance occurs for all the f_q, we have that for any time $f_q \sim O(1)$, so that the effect of the external drive $g(t)$ is suppressed in the thermodynamic limit, up to $t_Q \sim N^\zeta$. If, however, we have a resonance for a given mode f_q, the whole picture breaks down on a timescale $t \sim \ln N$, after which $f_q = O(N)$. Thus, the time-scale for the external drive $g(t)$ to become relevant is reduced as well to $t_Q \sim \ln N$. If we compare the latter with $t \sim N^\zeta$ of the non-resonant case we can see that, while strictly speaking in both cases this time-scale diverges in the thermodynamic limit, in the resonant case we will never reach, in practice, values of N so large to get rid of this phenomenon.

Although it is very difficult, in general, to say something about the condition under which such resonances occur, here we can derive some stability conditions. Indeed let us notice that, even if we do not neglect $g(t)$ in Eq. (4.24), the equation of motion for $\mu(t)$ and the corresponding Eq. (4.15) for the f_q, can be derived from the classical Hamiltonian

$$H = \frac{P_\mu^2}{2} + V(\mu) - \sum_q \left(\frac{|p_q|^2}{2m_q} + \frac{m_q}{2}(\mu + \omega^2(q))|f_q|^2 \right). \tag{4.35}$$

It follows that we, even when taking into account the contribution of the quantum mode f_q, we still have a conserved fictitious energy, namely

$$\mathscr{E} = \frac{P_\mu^2}{2} + V(\mu) - \sum_q \frac{m_q}{2} \left(|\dot{f}_q|^2 + (\mu + \omega^2(q))|f_q|^2 \right). \tag{4.36}$$

(see Ref. [126] for an analogous picture in the classical case). This differs from the single-particle energy (4.28) by a quantity of order $N^{-\zeta}$, as it can be seen by computing both quantities at $t = 0$, when $f_q = O(1)$ for all q. On the other hand, we know that for small times the system will follow the trajectory $\mu^{\mathrm{sp}}(t)$ defined by Eq. (4.24). It follows that, for $t \ll t_Q$

$$\frac{m_q}{2} \left(|\dot{f}_q|^2 + (\mu^{\mathrm{sp}}(t) + \omega^2(q))|f_q|^2 \right) = \text{const} \tag{4.37}$$

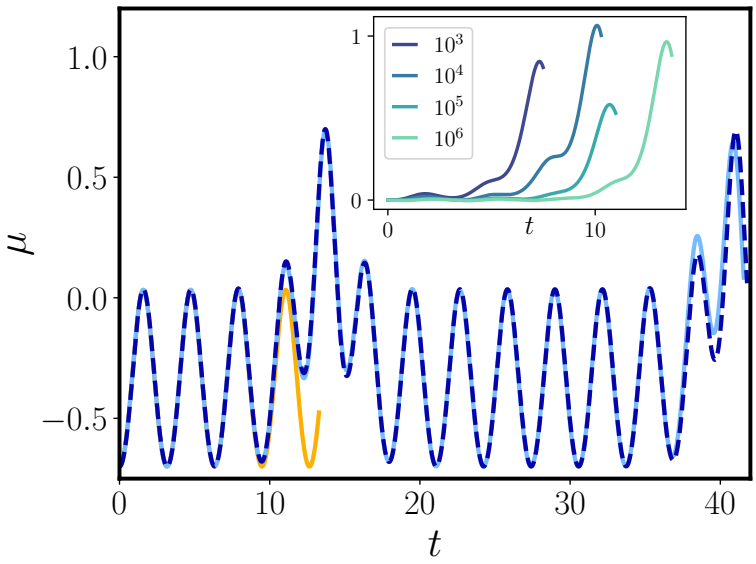

FIGURE 4.2: Behavior of $\mu(t)$ with $r^+ = -1$, $\lambda = 1.24$, $N = 10^6$ for the initial conditions $\mu(0) = -0.7$, $\dot{\mu}(0) = 0$, $\epsilon = 1.2$ (dotted blue line) compared with the corresponding single-particle classical picture (continuous orange) and the two-particle one (continuous cyan line). Since for this initial conditions only the $q = 0$ mode is resonant, the latter reproduces the right evolution, while the former fails on a finite timescale. *Inset:* difference between $\mu(t)$ and the single-particle picture for different values of N, showing how the time-scale on which the approximation breaks down grows as $\ln N$.

of order $N^{-\zeta}$. Now if, along this trajectory, $\mu^{\rm sp}(t) + \omega^2(q) > 0$ for every t and for every q, then f_q cannot be resonant, since a growth to $|f_q|^2 = O(N)$ is not compatible with the above constraint. We conclude that in this case $\mu(t)$ has to remain in the vicinity of $\mu^{\rm sp}(t)$, i.e. the single particle dynamics described by Eq. (4.24). In particular, since $\mu(t) > r$, we can rule out the possibility of a resonance as long as $r^+ > 0$.

Since $\omega(q)$ grows with q, the first mode that can become resonant is $q = 0$: if $\mu^{\rm sp}(t)+\omega^2(0) = \mu(t) < 0$ for some $t \in [0, T]$, then the trajectory constraint at short-times by Eq. (4.37) can escape, as the energy landscape has a hyperbolic structure. As $\mu^{\rm sp}(t)+\omega^2(q)$ becomes negative for some $t \in [0, T]$ the other modes can become resonant as well. However, even in this case, looking at the form of Eq. (4.35), we have that the condition $r^+ + \omega^2(q) > 0$ is sufficient in order to prevent the q-th modes from resonating. It is worth noting that the fact that the spectrum is discrete and bounded both from above and below is crucial in order to allow for the existence of resonance-free regions in the parameter space.

Our picture is indeed confirmed by the numeric phase diagram for $r^+ = -1$, $\alpha = 0.5$ is shown in Fig. 4.1. In particular, at small enough ϵ, large oscillations of $\mu(t)$ begin triggering the resonance in the $q = 0$ mode (as $\mu(t)$ becomes negative during the oscillation); while, further decreasing ϵ, an increasing number of resonant modes emerges (as $\mu^{\rm sp}(t) + \omega(q)$ becomes negative).

Since we can always neglect non-resonant excitations, in the Hamiltonian (4.35), the latter reduces to the contribution of resonant modes only. It follows that the system is described in terms of a finite number of degrees of freedom. This is the case shown in Fig. 4.2, where the single-particle picture (orange line) applicable in the non-resonant phase is shown to fail on a time-scale $t_Q \sim \ln N$, while a two-mode approximation (cyan line) faithfully reproduces the numerical results (dotted blue line). On timescale $t > t_Q$ the resonant mode grows large, and then becomes again negligible, resulting in a periodic oscillation of $\mu(t)$, punctured with periodic bursts, corresponding to the resonances.

4.4 | Entanglement Production

So far we saw how, due to the discrete nature of the spectrum, the contribution of the quantum degrees of freedom to the dynamics is suppressed in the thermodynamic limit, at least for non-condensed initial states. Yet, for any finite size N the spreading of quantum correlations may still occur at time-scales t_Q which are radically different for the non-resonant and resonant cases, as t_Q scales as N^ζ or $\ln N$ respectively. To grasp the qualitative difference between those phases, it is instructive to look at the entanglement production. As a measure of entanglement, it is convenient to choose the Von Neumann entropy relative to the partition of the chain in two intervals, of

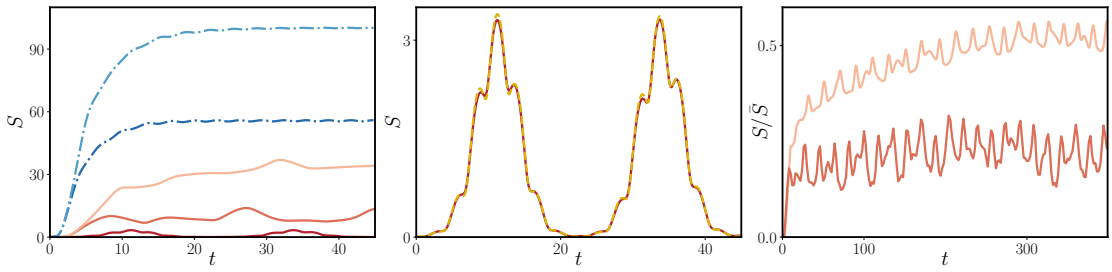

FIGURE 4.3: *Left panel:* behavior of the Von Neumann entropy $S(t)$ relative to a $\ell = 10$ interval after a ground state quench of r from 1 to -1, for $N = 10^4$. The dark red, red and orange curves are relative to different values of λ ($\lambda = 1.24$, $\lambda = 0.028$, $\lambda = 0.0028$) and $\alpha = 0.5$, which in turn corresponds to have 1, 116 and 221 resonant modes respectively. The dotted dark blue and blue curves correspond to the short-range counterpart ($\alpha = \infty$) of the $\lambda = 0.028$, $\lambda = 0.0028$ cases. *Central panel:* Behavior of $S(t)$ in the single-resonance phase (red), characterized by periodic bursts, compared with the analytical prediction of Eq. (4.51) (dashed yellow line). *Right panel:* Production of entanglement for larger times in the multi-resonant phase, compared with the correspondent limiting value $\bar{S}$ for the same quench in the short-range limit ($\alpha \to \infty$).

length ℓ and $N - \ell$, namely

$$S = -\operatorname{Tr}\{\rho_\ell \ln \rho_\ell\}, \tag{4.38}$$

ρ_ℓ being the reduced density matrix of the system to the subspace relative to the lattice sites belonging to an interval of length ℓ.

Entanglement, which has indeed been called *the characteristic trait of quantum mechanics*[127], plays a major role in the understanding of many-body quantum systems, as their collective out-of-equilibrium dynamics, from thermalization and excitation confinement, to the complexity of numerical simulations can be witnessed by entanglement propagation [128–133]. In the case of one-dimensional short-range interacting systems, linear growth in time of bipartite von Neumann entropy, followed by a saturation to an equilibrium value, has been observed. This behavior has been traced back to the presence of entangled pairs of quasi-particle excitations[129, 134–136], which propagate ballistically. For the consistency of this picture, the presence of finite speed in information spreading and excitation propagation is crucial, guaranteed for short-range-interacting systems by the Lieb-Robinson bound[137].

At the same time, the breakdown of the locality concept induced by long-range interactions is known to yield a strong impact on the traditional picture for correlations and entanglement spreading, breaking down the description of entanglement spreading in terms of quasi-particle propagation. Several numerical simulations have indeed shown that the growth of entanglement entropy is dramatically slowed

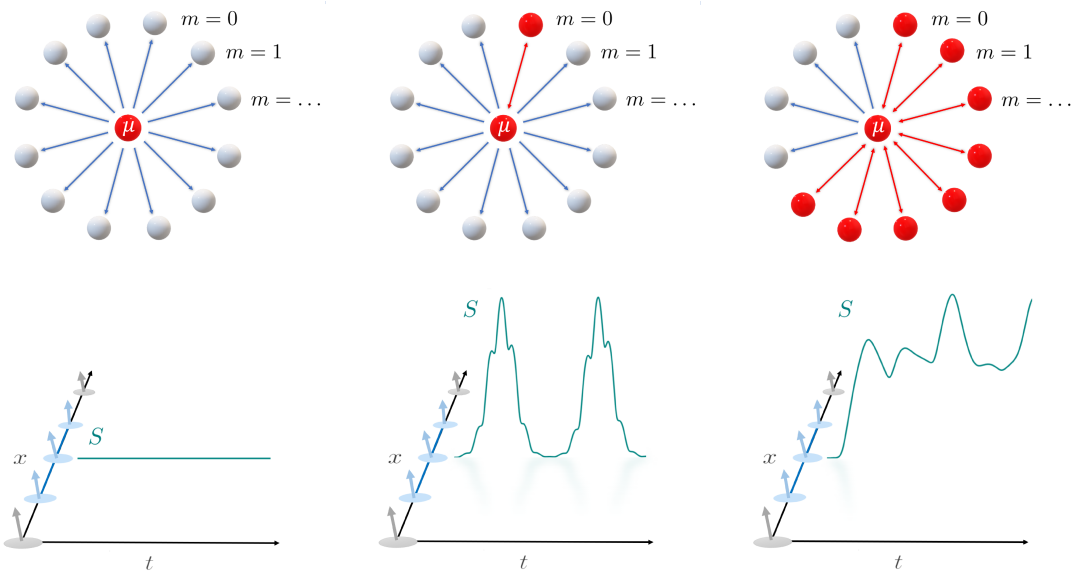

FIGURE 4.4: Schematic depiction of the phases of our model along with the behavior of the bipartite Von Neumann entropy $S(t)$. *Left:* the classical phase, in which the classical dynamics of $\mu(t)$ is not influenced by the presence of the quantum bath up until $t_Q \sim N^{\zeta}$ so that there is no production of entanglement. *Center:* the resonant phase, in which the $m = 0$ mode becomes resonant and affects the dynamics of the system on a timescale $t_Q \sim \ln N$, causing periodic bursts in $S(t)$. *Right:* the multi-resonant phase, in which a larger number of modes resonate, causing a more complex oscillatory behavior with a finite production of entanglement.

down [138–140], this in spite of the fact that quantum correlations between far-apart degrees of freedom could build up quickly [18, 141].

The picture developed in the present Chapter for the quantum $O(n)$ model is able to substantiate these findings, giving an analytical picture of such entanglement spreading in terms of the parametric resonances.

Let us, then, consider the growth of entanglement entropy in an interval of length ℓ. Due to the factorisation of the rotor models interaction term at large-n, and to the fact that the initial state is described by a Gaussian density matrix, one can apply the formalism developed in Ref. [142] for computing the entanglement entropy starting from the momentum and position two-point functions. Following this procedure we introduce the matrix of the correlations

$$\gamma = \mathrm{Re}\begin{pmatrix} \langle \Phi_x(t)\Phi_{x'}(t)\rangle & \langle \Phi_x(t)\Pi_{x'}(t)\rangle \\ \langle \Pi_x(t)\Phi_{x'}(t)\rangle & \langle \Pi_x(t)\Pi_{x'}(t)\rangle \end{pmatrix}. \tag{4.39}$$

The bipartite Von Neumann entropy $S(t)$ can be expressed in terms of the symplectic spectrum $\{\sigma_n\}$ of $\gamma_{\rm red}$, i.e. the matrix reduced to the subspace $x, x' \in (0, \ell)$. The symplectic spectrum is defined such that $\{\sigma_n^2\}$ is the spectrum of $-(J\gamma_{\rm red})^2$, J being the symplectic unity

$$J = \begin{pmatrix} 0 & \mathbb{I}_\ell \\ -\mathbb{I}_\ell & 0 \end{pmatrix}. \tag{4.40}$$

In terms of the σ_n, we have

$$S = \sum_n s(\sigma_n), \tag{4.41}$$

where:

$$s(\sigma) = \left(\sigma + \frac{1}{2}\right) \ln\left(\sigma + \frac{1}{2}\right) - \left(\sigma - \frac{1}{2}\right) \ln\left(\sigma - \frac{1}{2}\right). \tag{4.42}$$

For simplicity, we first restrict to the case in which the $q = 0$ mode only may be resonant. Once again, up to corrections of order $O(N^{-\zeta})$, we can discard the q dependence of all modes at $q > 0$. Therefore, we can replace $f_q(t)$ and $\dot{f}_q(t)$ with their high energy limit $f_\pi(t)$, $\dot{f}_\pi(t)$. As a result, the dynamical theory reduces to the one of a classical particle coupled to the resonant $q = 0$ mode plus a $\sim N$ times degenerate high energy mode. The corresponding correlators are thus given by

$$\begin{aligned} \langle \Phi_x(t)\Phi_{x'}(t)\rangle &= \frac{\delta_{x'x}}{2}|f_\pi(t)|^2 + \frac{1}{2N}|f_0(t)|^2, \\ \langle \Pi_x(t)\Pi_{x'}(t)\rangle &= \frac{\delta_{x'x}}{2}|\dot{f}_\pi(t)|^2 + \frac{1}{2N}|\dot{f}_0(t)|^2, \\ \langle \Phi_x(t)\Pi_{x'}(t)\rangle &= \frac{\delta_{x'x}}{2}\left(\mathrm{Re}(f_\pi(t)\dot{f}_\pi^*(t)) + i\right) \\ &\quad + \frac{1}{2N}\mathrm{Re}(f_0(t)\dot{f}_0^*(t)). \end{aligned} \tag{4.43}$$

It is worth noting that the latter expressions approximate the actual correlations of the system up to $O(N^{-\zeta})$ terms, which may become relevant if the length of the considered interval ℓ becomes of order N.

The resulting expression for the matrix of Eq. (4.39), reduced to the interval, is thus given by

$$\gamma_{\rm red} = \frac{1}{2}\begin{pmatrix} Q(t) & R(t) \\ R(t) & P(t) \end{pmatrix}, \tag{4.44}$$

where $Q(t)$,$P(t)$,$R(t)$ are ℓ by ℓ matrices defined as

$$\begin{aligned} Q(t) &= |f_\pi(t)|^2 \mathbb{I}_\ell + \frac{\ell}{N}|\dot{f}_\pi(t)|^2 \mathbb{P}, \\ P(t) &= |\dot{f}_0(t)|^2 \mathbb{I}_\ell + \frac{\ell}{N}|\dot{f}_\pi(t)|^2 \mathbb{P}, \\ R(t) &= \mathrm{Re}\left(f_\pi(t)\dot{f}_\pi^*(t)\mathbb{I}_\ell + \frac{\ell}{N} f_0(t)\dot{f}_0^*(t)\mathbb{P} \right), \end{aligned} \tag{4.45}$$

with $\mathbb{P}_{j,k} = \frac{1}{\ell},\ \forall\, j,k = 1,\ldots \ell$. Since $[P,R] = 0$ and $[Q,R] = 0$ we find

$$-(J\gamma_{\mathrm{red}})^2 = \frac{1}{4}\begin{pmatrix} PQ - R^2 & 0 \\ 0 & PQ - R^2 \end{pmatrix}. \tag{4.46}$$

Using the fact that $\mathrm{Im}(f_q(t)\dot{f}_q^*(t)) = 1$ and $\mathbb{P}^2 = \mathbb{P}$ we have

$$PQ - R^2 = \mathbb{I} + \ell\Delta(t)\mathbb{P} + \ell^2 N^{-2}\,\mathbb{P}, \tag{4.47}$$

with $\Delta(t)$ given by

$$\begin{aligned} N\Delta(t) = {} & |f_\pi(t)\dot{f}_0(t)|^2 + |f_0(t)\dot{f}_\pi(t)|^2 \\ & - 2\mathrm{Re}\left(f_0(t)\dot{f}_0^*(t)\right)\mathrm{Re}\left(f_\pi(t)\dot{f}_\pi^*(t)\right). \end{aligned} \tag{4.48}$$

For a finite interval, the last term on the r.h.s. of Eq. (4.47) is negligible while the second one may become $O(1)$ on a timescale $t_Q \sim \ln(N)$. Then all the eigenvalues of $-(J\gamma_{\mathrm{red}})^2$ are $\frac{1}{4}$ but two which are

$$\frac{1}{4} + \frac{\ell}{4}\Delta(t). \tag{4.49}$$

The symplectic spectrum is finally given by

$$\begin{aligned} \sigma_1 = \sigma_2 &= \frac{1}{2}\sqrt{1 + \ell\Delta(t)}, \\ \sigma_n &= \frac{1}{2} \quad \forall\, n = 3,\ldots 2\ell. \end{aligned} \tag{4.50}$$

Substituting in Eq. (4.42), we notice that only the first two eigenvalues, coming from the resonant mode, do actually contribute to $S(t)$, so that we find a closed expression for the bipartite Von Neumann Entropy:

$$\begin{aligned} S(t) = {} & \left(\sqrt{1 + \ell\Delta(t)} + 1\right)\ln\frac{\sqrt{1 + \ell\Delta(t)} + 1}{2} \\ & - \left(\sqrt{1 + \ell\Delta(t)} - 1\right)\ln\frac{\sqrt{1 + \ell\Delta(t)} - 1}{2}. \end{aligned} \tag{4.51}$$

As expected, the $1/N$ factor included in the definition of $\Delta(t)$ suppresses the propagation of entanglement unless the $q = 0$ mode is resonant. Thus, the parametric resonance results in the production of entanglement on an intermediate time-scale $t_Q \sim \ln N$ (which, has been noticed, remains however accessible even for large many-particle experiments). The behavior of $S(t)$ in the resonant phase is shown in Fig. 4.3. $S(t)$ is characterized by periodic bursts on a time-scale $t_q \sim \ln N$, after which it comes back to its initial value. Lack of equilibration in the system is signaled by the $S(t)$ function not saturating. This periodic generation of entanglement and its complete loss due to long-range interactions is evidenced here for the first time. Moreover, Eq. (4.51) implies that the larger ℓ is, the faster quantum correlations will be established. This is in antithesis to the case of local and weak long-range systems, where the short-time growth of entanglement is independent of ℓ, due to the light-cone-like structure of the Lieb-Robinson bound [143].

The impact of the number of resonant modes (and thus of effective degrees of freedom) on the evolution of $S(t)$ is evident as we consider the case of multiple resonant modes beyond the $q = 0$ one. In this case, the analytic expression for the correlation functions in Eq. (4.51) does not apply, and only numerical estimates are here accessible, as shown in Fig. 4.3. There, the quasi-periodic oscillations of $S(t)$ are accompanied by the generation of a finite amount of entropy at large times, which is however smaller than the short-range counterpart. Even though the situation is way more similar to the short-range one, the quasi-periodic oscillations persist at any large time, so that no actual equilibration occurs even in the multi-resonant phase.

In summarizing, we can characterize the dynamical phase diagram of the quantum $O(n)$ model after a ground-state quench in terms of the behavior of the bipartite Von Neumann entropy. We can identify three main phases

1. *Classical phase:* in the thermodynamic limit, the many-body dynamics corresponds to the one of a single classical particle, representing the effective mass $\mu(t)$. Correspondingly, at finite sizes, no entanglement emerges in the system up to a scale $t_q \sim N^{\zeta}$.

2. *Resonant phase:* for larger initial energies the oscillations of the effective mass $\mu(t)$ trigger a resonance in the lowest $q = 0$ mode. As a consequence, the entanglement entropy grows in quasi-periodic bursts, the first of which occurs at a time-scale $t_q \sim \ln(N)$. Yet, following each burst, the amount of entanglement vanishes, and classical dynamics is restored.

3. *Multi-resonant phase:* at high energy, the effective mass oscillations generated by the instantaneous quench are strong enough to generate multiple resonances, leading to a mosaic of different phases, each characterized by a different number of active modes in the dynamics. The phenomenology of all these phases

is analogous to the single resonance one. However, in the long-time limit, the amount of entanglement generated is finite.

As the present picture can be traced back to the discreteness of the single-particle spectrum (see Sec. 1.3.1), we expect this picture to apply to generic many-body systems with non-additive long-range interactions. While this slow growth of entanglement may be confused with the one found in finite range and weak long-range systems [144], the latter is generated by quasi-particle confinement [145] or Bloch oscillations [146] and, due to its prethermal character, can only be observed at short times. On the contrary, the current picture follows from the collective character of long-range interactions, which produces an effective global coupling among the degrees of freedom in the thermodynamic limit, see Fig. 4.4, stabilizing the aforementioned phases even at large times.

Along the same lines, the collective character of long-range interactions prevents the divergence of low-energy excitations and stabilizes the $1/n$ approach employed to study the dynamics, making it trustworthy also in the thermodynamic limit. As a result, the effective mass $\mu(t)$ acts in all respects as a global drive and generates the resonant phases in analogy with previous studies of bosonic theories subject to an external periodic force [147]. Nevertheless, in the present case, the back action of the resonant modes on the drive prevents the linear growth of the entropy with time. This is consistent with the isolated nature of the system and, consequently, with the absence of any external energy source.

References

[2] A. Campa, T. Dauxois, D. Fanelli, and S. Ruffo. *Physics of Long-Range Interacting Systems*. Oxford Univ. Press, 2014.

[10] M. Kac, G. E. Uhlenbeck, and P. C. Hemmer. "On the van der Waals Theory of the Vapor-Liquid Equilibrium. I. Discussion of a One-Dimensional Model". *Journal of Mathematical Physics* 4(2) (Feb. 1963), pp. 216–228. DOI: 10.1063/1.1703946.

[17] A. Chandran, A. Nanduri, S. Gubser, and S. Sondhi. "Equilibration and coarsening in the quantum O (N) model at infinite N". *Physical Review B* 88 (Apr. 2013). DOI: 10.1103/PhysRevB.88.024306.

[18] P. Hauke and L. Tagliacozzo. "Spread of correlations in long-range interacting quantum systems". *Physical review letters* 111(20) (2013), p. 207202.

[30] N. D. Mermin and H. Wagner. "Absence of ferromagnetism or antiferromagnetism in one-or two-dimensional isotropic Heisenberg models". *Physical Review Letters* 17(22) (1966), p. 1133.

[61] N. DEFENU. "Metastability and discrete spectrum of long-range systems". *Proceedings of the National Academy of Sciences* 118(30) (2021). ISSN: 0027-8424. DOI: 10.1073/pnas.2101785118.

[119] G. GIACHETTI and N. DEFENU. "Entanglement propagation and dynamics in non-additive quantum systems". *arXiv preprint arXiv:2112.11488* (2021).

[120] M. MOSHE and J. ZINN-JUSTIN. "Quantum field theory in the large N limit: a review". *Physics Reports* 385(3) (2003), pp. 69–228. ISSN: 0370-1573. DOI: https://doi.org/10.1016/S0370-1573(03)00263-1.

[121] R. SERRAL GRACIÀ and T. M. NIEUWENHUIZEN. "Quantum spherical spin models". *Phys. Rev. E* 69 (5 May 2004), p. 056119. DOI: 10.1103/PhysRevE.69.056119.

[122] P. SMACCHIA, M. KNAP, E. DEMLER, and A. SILVA. "Exploring dynamical phase transitions and prethermalization with quantum noise of excitations". *Phys. Rev. B* 91 (20 May 2015), p. 205136. DOI: 10.1103/PhysRevB.91.205136.

[123] A. MARAGA, A. CHIOCCHETTA, A. MITRA, and A. GAMBASSI. "Aging and coarsening in isolated quantum systems after a quench: Exact results for the quantum O(N) model with $N \to \infty$". *Phys. Rev. E* 92 (4 Oct. 2015), p. 042151. DOI: 10.1103/PhysRevE.92.042151.

[124] B. SCIOLLA and G. BIROLI. "Quantum quenches, dynamical transitions, and off-equilibrium quantum criticality". *Physical Review B* 88(20) (Nov. 2013). DOI: 10.1103/physrevb.88.201110.

[125] J. C. HALIMEH and M. F. MAGHREBI. "Quantum aging and dynamical universality in the long-range $O(N \to \infty)$ model". *Phys. Rev. E* 103 (5 May 2021), p. 052142. DOI: 10.1103/PhysRevE.103.052142.

[126] G. GIACHETTI and L. CASETTI. "Violent relaxation in the Hamiltonian mean field model: I. Cold collapse and effective dissipation". *Journal of Statistical Mechanics: Theory and Experiment* 2019(4) (Apr. 2019), p. 043201. DOI: 10.1088/1742-5468/ab0c19.

[127] E. SCHRODINGER. *Discussion of probability relations between separated systems*. Mathematical Proceedings of the Cambridge Philosophical Society, 1935.

[128] L. AMICO, R. FAZIO, A. OSTERLOH, and V. VEDRAL. "Entanglement in many-body systems". *Rev. Mod. Phys.* 80 (2 Apr. 2008), pp. 517–576. DOI: 10.1103/RevModPhys.80.517.

[129] V. Alba and P. Calabrese. "Entanglement and thermodynamics after a quantum quench in integrable systems". *Proceedings of the National Academy of Sciences* 114(30) (2017), pp. 7947–7951. ISSN: 0027-8424. DOI: 10.1073/pnas.1703516114.

[130] M. Serbyn, Z. Papi ć, and D. A. Abanin. "Universal Slow Growth of Entanglement in Interacting Strongly Disordered Systems". *Phys. Rev. Lett.* 110 (26 June 2013), p. 260601. DOI: 10.1103/PhysRevLett.110.260601.

[131] G. Vidal. "Efficient Classical Simulation of Slightly Entangled Quantum Computations". *Phys. Rev. Lett.* 91 (14 Oct. 2003), p. 147902. DOI: 10.1103/PhysRevLett.91.147902.

[132] F. Verstraete, V. Murg, and J. Cirac. "Matrix product states, projected entangled pair states, and variational renormalization group methods for quantum spin systems". *Advances in Physics* 57(2) (2008), pp. 143–224. DOI: 10.1080/14789940801912366.

[133] M. C. Bañuls, M. B. Hastings, F. Verstraete, and J. I. Cirac. "Matrix Product States for Dynamical Simulation of Infinite Chains". *Phys. Rev. Lett.* 102 (24 June 2009), p. 240603. DOI: 10.1103/PhysRevLett.102.240603.

[134] H. Kim and D. A. Huse. "Ballistic Spreading of Entanglement in a Diffusive Nonintegrable System". *Phys. Rev. Lett.* 111 (12 Sept. 2013), p. 127205. DOI: 10.1103/PhysRevLett.111.127205.

[135] A. Nahum, J. Ruhman, S. Vijay, and J. Haah. "Quantum Entanglement Growth under Random Unitary Dynamics". *Phys. Rev. X* 7 (3 July 2017), p. 031016. DOI: 10.1103/PhysRevX.7.031016.

[136] A. Chan, A. De Luca, and J. T. Chalker. "Solution of a Minimal Model for Many-Body Quantum Chaos". *Phys. Rev. X* 8 (4 Nov. 2018), p. 041019. DOI: 10.1103/PhysRevX.8.041019.

[137] E. Lieb and D. Robinson. "The finite group velocity of quantum spin systems". *Communications in Mathematical Physics* 28(3) (1972), pp. 251–257. DOI: cmp/1103858407.

[138] J. schachenmayer, B. P. Lanyon, C. F. Roos, and A. J. Daley. "Entanglement Growth in Quench Dynamics with Variable Range Interactions". *Phys. Rev. X* 3 (3 Sept. 2013), p. 031015. DOI: 10.1103/PhysRevX.3.031015.

[139] S. Pappalardi *et al.* "Scrambling and entanglement spreading in long-range spin chains". *Phys. Rev. B* 98 (13 Oct. 2018), p. 134303. DOI: 10.1103/PhysRevB.98.134303.

[140] A. LEROSE and S. PAPPALARDI. "Origin of the slow growth of entanglement entropy in long-range interacting spin systems". *Phys. Rev. Research* 2 (1 Feb. 2020), p. 012041. DOI: 10.1103/PhysRevResearch.2.012041.

[141] L. LEPORI, A. TROMBETTONI, and D. VODOLA. "Singular dynamics and emergence of nonlocality in long-range quantum models". *Journal of Statistical Mechanics: Theory and Experiment* 2017(3) (Mar. 2017), p. 033102. DOI: 10.1088/1742-5468/aa569d.

[142] H. CASINI and M. HUERTA. "Entanglement entropy in free quantum field theory". *Journal of Physics A: Mathematical and Theoretical* 42(50) (Dec. 2009), p. 504007. DOI: 10.1088/1751-8113/42/50/504007.

[143] M. C. TRAN *et al.* "Lieb-Robinson Light Cone for Power-Law Interactions". *Phys. Rev. Lett.* 127 (16 Oct. 2021), p. 160401. DOI: 10.1103/PhysRevLett.127.160401.

[144] S. SCOPA, P. CALABRESE, and A. BASTIANELLO. "Entanglement dynamics in confining spin chains". *arXiv* (2021), p. 2111.11483.

[145] M. KORMOS, M. COLLURA, G. TAKÁCS, and P. CALABRESE. "Real-time confinement following a quantum quench to a non-integrable model". *Nature Physics* 13(3) (Mar. 2017), pp. 246–249. DOI: 10.1038/nphys3934.

[146] O. POMPONIO, M. A. WERNER, G. ZARAND, and G. TAKACS. "Bloch oscillations and the lack of the decay of the false vacuum in a one-dimensional quantum spin chain". *arXiv* (2021), p. 2105.00014.

[147] E. BIANCHI, L. HACKL, and N. YOKOMIZO. "Linear growth of the entanglement entropy and the Kolmogorov-Sinai rate". *JHEP* 03 (2018), p. 025. DOI: 10.1007/JHEP03(2018)025.

5 | Higher-order time-crystalline phases

Strong long-range interacting systems subjected to a periodic (Floquet) driving are known to exhibit a spontaneous breaking of the discrete time-translation symmetry, i.e. to exhibit so-called time-crystalline phases. In this Chapter, we will focus on the physics of the so-called higher-order time crystals, introducing a new order parameter, ζ, able to give a full characterization of the phases of the model.

The Chapter is based on Ref. [148] and it is structured as follows: in Sec. 5.1 we introduce the concept of discrete Floquet time-crystal, in Sec. 5.2 we introduce ζ in the context of the paradigmatic fully-connect Ising Model and in Sec. 5.3 we draw the corresponding phase diagram. In Sec. 5.4 we show how properties of this phase diagram for high-frequency driving can be captured analytically, while in Sec. 5.5 we discuss numerically the robustness of our picture against finite size effects.

5.1 | Discrete Floquet Time Crystals

Among the several non-trivial dynamical phases of long-range-interacting systems, we now focus on the possibility of the emergence of Discrete Floquet Time Crystalline (DFTC) phases. Those arise in systems subjected to an external periodic driving $H(t) = H(t+T)$, in which the discrete time-translation symmetry is spontaneously broken, so that the expectation values display oscillations with a period being an integer multiple of T [149–156].

More precisely, in such a driven system a DFTC phase exists if, taken a class of states $|\Psi\rangle$ with short-ranged connected correlations [151], it always exists an observable $\hat{O}$ such that the time-evolved expectation value in the thermodynamic limit $N \to \infty$,

$$O(t) = \lim_{N\to\infty} \langle \Psi(t)|O|\Psi(t)\rangle, \tag{5.1}$$

satisfies the following conditions [157]:

1. Time-translation symmetry breaking: $O(t+T) \neq O(t)$, although $H(t) = H(t+T)$.

2. Rigidity: $O(t)$ must display periodic oscillations, with some period τ, in a finite and connected region of the Hamiltonian parameters space.

3. Persistence: in the large system size limit $N \to \infty$, the oscillations of $O(t)$ must persist for infinitely long time.

We refer to $O(t)$ as the order parameter of the time-crystal. The order p of a DFTC phase is defined as

$$O(t + pT) = O(t), \tag{5.2}$$

$p = 1$ corresponding to the trivial non-broken phase, $p = 2$ to the so-called period doubling phase.

Let us notice that, being the driving periodic, one can define a Floquet propagator as

$$U_F = U(t, t + T), \tag{5.3}$$

$U(t)$ being the evolution operator of the system. As a consequence, at stroboscopic times $t = nT$, we have that

$$|\Psi(nT)\rangle = U_F^n \, |\Psi(0)\rangle \, . \tag{5.4}$$

The condition of time-translation symmetry breaking can be expressed in terms of U_F by requesting the eigenstates of the Floquet eigenstates to be long-range correlated in space [151].

For generic many-body systems, the conditions above are not satisfied, as the presence of an external driving would lead to the relaxation toward an completely mixed state (corresponding to heating toward infinite temperature), ruling out long-lived oscillations. Protecting ordering against relaxation necessitates a mechanism to keep the impact of dynamically generated excitations under control, as it seems the case for strongly disordered systems, subject to localization [151, 153, 155, 158–160].

As seen in Sec. 1.3.3 and in Chapter 4, strong long-range interaction are able to provide as well such a mechanism, as they are known to enhance the robustness of collective oscillations [67, 161], avoiding the proliferation of local defects. The presence of DFTC phases have been actually established in the strong long-range regime ($\alpha < d$) [157, 159, 162, 163], while for $\alpha > d$ the oscillations are not persistent in the $N \to \infty$ limit [155, 156, 164, 165].

In order to be more concrete, let us introduce the long-range kicked Ising Model, which we will use from now on as a paradigmatic example of long-range time-crystalline behavior. Given a chain of N spin 1/2 particles, interacting through the $\mathbb{Z}_2$-symmetric Ising Hamiltonian:

$$H = -\frac{1}{4N_\alpha} \sum_{j>j'} r^{-\alpha} \hat{\sigma}_x^j \hat{\sigma}_x^{j'} + h(t) \sum_j \hat{\sigma}_z^j \, , \tag{5.5}$$

where $\hat{\sigma}_x^i$, $\hat{\sigma}_y^i$, $\hat{\sigma}_z^i$ are the components of the Pauli operators relative to the site j, $r = |j - j'|$ and

$$N_\alpha = \sum_{j \neq 0} |j|^{-\alpha}. \tag{5.6}$$

is the Kac scaling factor [2, 10]. The driving is given by a periodic instantaneous pulse in the transverse field $h(t)$

$$h(t) = \psi \sum_{n=1}^{\infty} \delta(t - nT) \ . \tag{5.7}$$

Let us notice how the instantaneous pulse in the magnetic field $h(t)$ has the effect of rotating each spin along the z axis of an angle 2ψ. If at $t = 0$, the system is initialized in one of the ground states of the $h(t) = 0$ Hamiltonian, e.g. $|\Psi_0\rangle = |\rightarrow \cdots \rightarrow\rangle$, and we choose ψ to be exactly $\pi/2$, then we have that the dynamics simply interpolates between $|\Psi_0\rangle$ and the other ground state $|\leftarrow \cdots \leftarrow\rangle$. We thus have trivially period doubling, as for any $\mathbb{Z}_2$-odd observable, $O(nT) = (-1)^n O(0)$. At the same time, for any $\psi = \pi/2 + \epsilon$ with $\epsilon \neq 0$, local excitations will be generated by the dynamics. It has been shown [165] that, for any $\alpha > 1$, theese will spread, resulting in a damping in the oscillations of $O(nT)$, so that the rigidity property requested for the definition of a time-crystalline phase is not met.

The situation is different for $\alpha < 1$. In this regime, the spin-wave propagation is hindered due to the peculiar structure of their dispersion relation, analyzed in Sec. 1.3.1. It means that the behavior of the system is expected to converge to the one of $\alpha = 0$ in the thermodynamic limit. The presence of resonances, as analyzed in Chapter 4, can lead to the breakdown of this picture on mesoscopic timescales. This possibility has been analyzed in Ref. [166], finding that the time crystalline phase is robust under such a mechanism.

5.2 | An order parameter for higher-order time crystals

For a long time, the presence of time crystals has been related to the symmetry of the Hamiltonian, as in the aforementioned case of the Ising model. As a consequence the possibility of a DFTC phase of order $p > 2$, was thought to be connected with the underlying $\mathbb{Z}_p$ symmetry of the model [157, 159], as one can engineer a Floquet driving which approximately interpolates between $\mathbb{Z}_p$-connected vacua. Recently, however, high-order ($p > 2$) DFTCs were recently observed also in long-range systems with only $\mathbb{Z}_2$ symmetry [163, 166, 167] such the kicked Ising model. This phenomenon was deeper investigated in Ref. [162], where it was pointed out how higher-order DFTC phases are associated with an emergent $\mathbb{Z}_p$ symmetry which is not apparent

in the original model. Despite these preliminary studies, the understainding of high-order time crystal phases has been fundamentally hindered by the lack of a unique order parameter capable of detecting all the DFTC phases simultaneously.

Here we propose a possible candidate for such an order parameter, which has the advantage to be blind to the order p of the DFTC phase while being easily accessible from the experimental point of view. To this extent, we consider the fully-connected ($\alpha = 0$) limit of the kicked Ising model (5.5)

$$H = -\frac{1}{4N}\sum_{j,j'}\hat{\sigma}_x^j\hat{\sigma}_x^{j'} + h(t)\sum_j \hat{\sigma}_z^j \,, \tag{5.8}$$

i.e. the kicked LMG model [26], and we choose to investigate the evolution of the observables

$$m_a(t) = \frac{1}{N}\sum_j \left\langle \hat{\sigma}_a^j \right\rangle \tag{5.9}$$

(with $a = x, y, z$) which correspond to the components of the magnetization of the system. In the $N \to \infty$ limit, it is possible to write a closed evolution equation for $\mathbf{m}(t)$ [66, 124], which leads, in terms of the stroboscopic magnetization $\mathbf{m}_n \equiv \mathbf{m}(nT)$, to the map

$$\mathbf{m}_{n+1} = f(\mathbf{m}_n) \equiv R_z(2\psi)R_x(-m_{x,n}T)\mathbf{m}_n \,, \tag{5.10}$$

where $R_{x,y,z}(\xi)$ is the rotation matrix of an angle ξ around the corresponding axis (see Appendix C for the details of the derivation). If at $t = 0$ we start from the $h = 0$ ground state $|\Psi_0\rangle = |\rightarrow \cdots \rightarrow\rangle$ we have $\mathbf{m}_0 = (1, 0, 0)$. The constraint $\mathbf{m}^2 = 1$ is preserved, as consequence of the global angular momentum conservation, so that the motion takes place on a Bloch sphere [124]. The $\mathbb{Z}_2$ symmetry of the model is instead encoded into the dynamical symmetry of Eq. (5.10)

$$\begin{aligned} \psi &\to \psi + \pi/2 \\ \mathbf{m}_n &\to R_z(\pi n)\mathbf{m}_n \end{aligned} \tag{5.11}$$

Depending on the values of T and ψ we observe different dynamical phases.

In particular, we can pinpoint three different phases:

1. A chaotic phase in which $\mathbf{m}_n$ shows an erratic behavior, with a strong sensitivity to initial conditions.

2. A quasi-periodic phase, in which $\mathbf{m}_n$ has a non-integer period, sensitive to small changes in ψ.

3. A periodic phase in which $\mathbf{m}_n$ exhibits an integer period p, robust with respect to small changes of ψ, with an additional small quasi-periodic modulation (referred to as micromotion in Ref. [166]).

Within the latter scenario we can distinguish the trivial $p = 1$ case (in which the discrete time translation symmetry is not broken) the period-doubling DFTC for $p = 2$, and the higher-order DFTC phases for $p > 2$.

Due to the dynamical $\mathbb{Z}_2$ symmetry of the system, the presence of an order p DFTC for some ψ automatically implies the presence of DFTC in correspondence of $\psi - \pi/2$, of order p if p is even, $2p$ if p is odd.

We want now to introduce a quantity which is able to distinguish between these phases, and in particular to pinpoint the periodic phase, regardless of the order p of the DFTC. To this extent we introduce the quantity

$$\zeta^2 = \frac{1}{n_{\max}} \sum_{n=0}^{n_{\max}} \left(m_{x,n}(\psi + \delta\psi) - m_{x,n}(\psi) \right)^2 , \tag{5.12}$$

in the limit $\delta\psi \to 0$, $n_{\max} \to \infty$ with $n_{\max}\, \delta\psi = O(1)$ fixed.

Before going on let us now examine more in detail the dynamics induced by the map (5.10) in order to justify our choice of the quantity (5.12). We notice first that the map inherits a Hamiltonian structure, which is manifest in the fact that the area of any region on the sphere $\mathbf{m}^2 = 1$ is preserved by the action of $f(\mathbf{m})$. In terms of the usual polar coordinates along the z axis,

$$\mathbf{m} = (\sin\theta\cos\phi, \cos\theta\cos\phi, \cos\theta) \tag{5.13}$$

such area element can be written as $dS = d\cos\theta d\phi$, so that ϕ and $I = \cos\theta$ are natural canonical conjugate variables for our system (see also Sec. (1.3.3)). This is coherent with the picture developed in Ref.[124] and can be intuitively understood by thinking of I as the z component of the angular momentum, and ϕ the coordinate corresponding to a rotation around the z axis.

In particular, in the limit $T = 0$, the map becomes

$$\begin{cases} I_{n+1} &= I_n , \\ \phi_{n+1} &= \phi_n + 2\psi , \end{cases} \tag{5.14}$$

with $I_0 = 0$, $\phi_0 = \pi/2$. This correspond to the stroboscopic section of an integrable dynamics, ϕ and I playing the role of an angle-action pair. In terms of the Floquet phases introduced in our paper, this implies a quasi-periodic evolution of $\mathbf{m}_n$, with period π/ψ.

As a small T is switched on, it can be treated as a perturbation to the map (5.14). In this case, the fate of the system is described by the Kolmogorov-Arnold-Moser theorem [168–170], according to which the torus $I = \text{const}$ is only deformed as long as the corresponding frequency is not resonant. In turn, this means that the quasi-periodic phase survives as long as ψ is not close to a rational multiple of π. In the

case of ψ close to a $q : p$ resonance, i.e. $\psi = \psi_r \equiv r\pi$, with $r = q/p$ and p and q coprime integers, according to the Poincare-Birkhoff theorem, pairs of elliptic and unstable fixed points are expected to arise. In this case the action of the p-iterated map $f^p(\mathbf{m})$ identifies different regions in the phase space (I, ϕ), corresponding to different possible behaviors of $\mathbf{m}_n$. In particular, if (I_0, ϕ_0) is far from the fixed points, we have rotation dynamics, with ϕ growing from 0 to 2π, and we have a quasi-periodic behavior. If (I_0, ϕ_0) is close to one of the centers instead, we have libration dynamics, with ϕ oscillating around a finite value. As a consequence, m_{n+p} remains close to m_n, and we have a DFTC phase. At the boundaries between these two regions, a chaotic region is expected to arise which, as T increases, grows and possibly swallows the regular ones.

Let us analyze the consequence of this picture on the order parameter ζ: to consider different values of the amplitude, ψ, $\psi + \delta\psi$ it means that we are considering two nearby initial conditions on the phase space. Both in the DFTC phase and in the quasi-periodic one the evolution is not chaotic, so that the two trajectories will diverge linearly in time. As a consequence

$$\begin{aligned} \zeta^2 &= \frac{1}{n_{\max}} \sum_{n=0}^{n_{\max}} \left(m_{x,n}(\psi + \delta\psi) - m_{x,n}(\psi)\right)^2 \\ &\sim \frac{\ell}{n_{\max}} \sum_{n=0}^{n_{\max}} \delta\psi^2 n^2 \sim \ell (\delta\psi\, n_{\max})^2 \,, \end{aligned} \tag{5.15}$$

where ℓ depends on the average distance between two randomly chosen points of the two nearby trajectories. While the r.h.s. of Eq. (5.15) remains finite and $O(1)$ as $n_{\max} \to \infty$, $\delta\psi \to 0$, ℓ jumps discontinuously as we pass from the libration regime (corresponding to a DFTC phase) and the rotation one (corresponding to a quasi-periodic phase). In particular, as we approach the the fixed point of the iterate map, i.e. in the regime in which the micro-motion becomes negligible, $\zeta \to 0$, so that ζ is able to quantify how far away is our system from the pure crystalline regime. Let us notice, however, how the other values of ζ in this two phases are not universal, as they depend on the choice of $\lim_{\delta\psi\to 0} n_{\max}\, \delta\psi$.

In the chaotic phase, instead, the trajectories diverge exponentially, so that after a time-scale $n_{\max} \sim -\ln(\delta\psi)$ the memory of the initial condition is lost. In this case we can assume each $m_{x,n}(\psi)$ and $m_{x,n}(\psi + \delta\psi)$ to be drawn from a set of equally distributed random variables with zero mean. As a consequence, according to the central limit theorem, ζ^2 is distributed as a Gaussian around the value

$$\left\langle \zeta^2 \right\rangle = 2 \left\langle m_x^2 \right\rangle \tag{5.16}$$

with a variance $O(n_{\max}^{-1})$. Assuming furthermore the distribution of the three com-

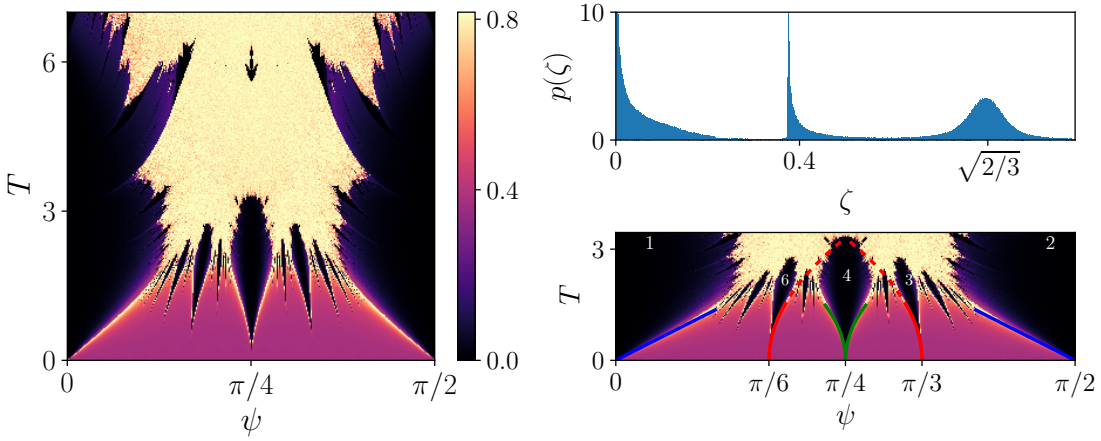

FIGURE 5.1: *Left panel:* Color plot of the order parameter ζ as a function of the amplitude ψ and the period T of the driving, saturated at the value $\zeta = \sqrt{2/3}$, with $n_{\max} = 300$, $\delta\psi = 1,6 \cdot 10^{-3}$. *Top-right panel:* Normalized occurrence frequency $p(\zeta)$ of ζ. The gap between the DFTC phase, localized around $\zeta = 0$, and the quasi-periodic one, localized around $\zeta \approx 0.36$ is apparent. On the right, the profile of the Gaussian distribution around $\zeta = \sqrt{2/3}$, characteristic of the chaotic phase. *Bottom-right panel:* Detail of the $T < 3$ region of the phase diagram. The order of the principal DFTC phases is indicated, along with the theoretical prediction for small T of the boundaries between the phases (blue, red, green solid lines respectively for the $p = 1, 2$, $p = 4$, $p = 3, 6$ islands). The prolongation of the boundaries of the $p = 3$, $p = 6$ islands (dashed red line) gives a good estimate of the onset of caos, which disrupts the time-crystal phases at large T.

ponents to be isotropic, and taking into account the constraint $\mathbf{m}^2 = 1$, we have

$$\langle m_x^2 \rangle = \frac{1}{3} \langle \mathbf{m}^2 \rangle = \frac{1}{3} , \tag{5.17}$$

so that $\langle \zeta^2 \rangle = 2/3$.

This picture is indeed confirmed by the Fig. (5.1) (top-right panel), in which the occurrence frequency of different values of ζ is plotted, showing a gap between the DFTC phase ($\zeta \lesssim 0.25$) and the quasi-periodic one ($\zeta \gtrsim 0.36$), with an additional Gaussian peak around $\zeta = \sqrt{2/3} \approx 0.816$, corresponding to the chaotic phase.

We conclude that ζ is not only a natural choice to define the DFTC and measure its distance from the perfect crystalline case, but it turns out to be a useful choice in chaos diagnostic as well. These considerations are expected to be very general, depending only on the geometrical features of the map.

5.3 | Phase Diagram

Now that we have justified the choice of our order parameter, we can show the corresponding phase diagram of the model as a function of ψ and T (i.e. the amplitude and the period of the motion). The result is shown in Fig. 5.1 (left-panel) showing strikingly complex and convoluted. The symmetry around the $\psi = \pi/4$ is a consequence of the dynamical $\mathbb{Z}_2$ symmetry (5.11). For small values of T the quasi-periodic phase is prevalent, while small islands of the periodic phase appear around the resonant values of ψ which corresponds to rational multiples of π. Initially, the size of these islands grows with T and, as they get closer to each other, chaotic regions start to appear around their boundaries. Finally, all the islands corresponding to a DFTC of order $p > 2$ disappear gradually as they are swallowed by the chaotic phase, the last one being the $p = 4$ one. In correspondence with particular values of the driving period, we have a revival of the higher-order DFTC phases, especially visible in correspondence of $p = 4$.

The boundary between the chaotic and the DFTC phase is not smooth: rather it presents plenty of self-similar patterns which are repeated at smaller and smaller scales. This is particularly clear if we consider the detail of the $p = 3$ island in Fig. 5.2 (left panel). In agreement with the general theory of discrete maps, these boundaries are indeed expected to exhibit a fractal structure. In order to quantify this fractal behavior and check the self-similarity of different parts of the phase diagram, we compute the Minkowski-Bouligand, or box-counting, dimension of the boundary.

This is defined as follows: let us cover our space with and evenly spaced square grid of side ϵ. Said $N(\epsilon)$ the number of boxes which lies on the boundary, then the dimension is defined as [171]

$$d_{MB} \equiv -\lim_{\epsilon \to 0} \frac{\ln N(\epsilon)}{\ln \epsilon} \,. \tag{5.18}$$

Since we are interested in the border between the chaotic and the DFTC phases, we restricted ourselves to the region of Fig. 5.2 (left panel) of the phase diagram in which only these phases are present (in particular $\psi \in (0.94, 1.01)$, $T \in (2.3, 2.8)$). To precisely define our boundary, we have here to define a threshold ζ_* such that a point with $\zeta > \zeta_*$ is considered to belong to the chaotic phase.

Since for any finite $n_{\max}$ the distribution of ζ in the chaotic phase around $\zeta = 0.816$ has a finite width, it is convenient, in this case, to choose $\delta\psi$ such that, $n_{\max}\,\delta\psi << 1$. In this regime, indeed, the distribution of ζ in the DFTC phase is sharply peaked around 0, and the separation of the two phases more pronounced. If, however, we choose $\delta\psi$ to be too small, the diagnostic of the chaotic region will not be accurate, as $\mathbf{m}_n(\psi)$ will not forget its initial condition for $n \sim n_{\max}$. We checked that the choice $n_{\max} = 300$, $\delta\psi = 10^{-4}$ is close to the optimal one. The separation between the different phases, shown in Fig. 5.2, right panel, is clear.

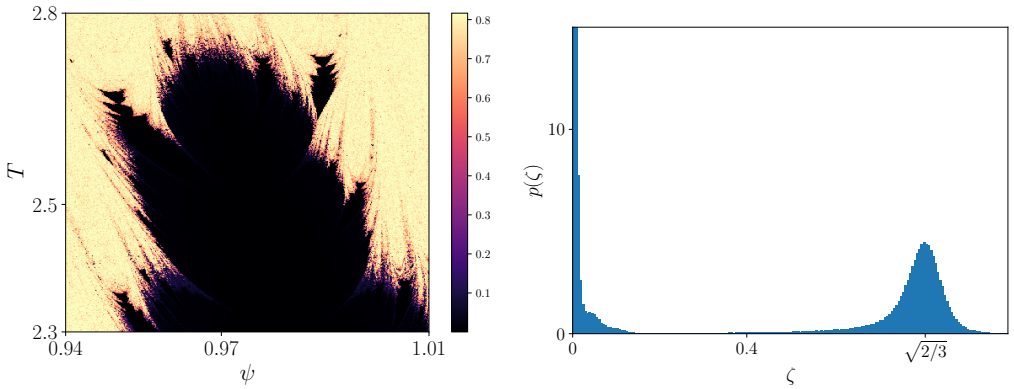

FIGURE 5.2: Color plot of the order parameter ζ saturated at the value $\zeta = \sqrt{2/3}$ with $n_{\max} = 300$, $\delta\psi = 10^{-4}$ (left) and corresponding normalized occurrence frequency $p(\zeta)$ of ζ for this region of the phase diagram.

$$d_{MB} \approx 1.42 > 1. \tag{5.19}$$

By repeating the procedure with slightly different values of $n_{\max}$ and $\delta\psi$ we get an uncertainty of order 10^{-2} on the above result.

In Fig. 5.3 right panel, we reported the behavior of d_{MB} as a function of the threshold ζ_* for the whole phase-diagram of Fig. 1 of the main text. To rule out the effect of the quasi-periodic phase, which is now present, we have to restrict ourselves to the region $\zeta_* \gtrsim 0.36$. As a consequence, the resulting estimate is far less accurate, and the dependence of d_{MB} on ζ_* is more pronounced. We see, however, that our previous, local, estimate is fully compatible with the hypothesis that the fractal dimension of the whole boundary is everywhere given by the value (5.19).

5.4 | Small T limit

As already noticed in Ref. [162], the formation DFTC islands can be understood within the formalism of area-preserving maps [172], and in particular can be linked to the existence of Arnold tongues [173] (see also [174]). By exploiting this picture, here we obtain an analytic description of the structure of the phase diagram for small values of T.

As in Sec. 5.2, it is convenient to parameterise the magnetization as

$$\mathbf{m} = (\sin\theta\cos\phi, \sin\theta\sin\phi, \cos\theta) \tag{5.20}$$

and to introduce the canonical coordinates $I = \cos\theta$, ϕ. Expanding the map (5.10)

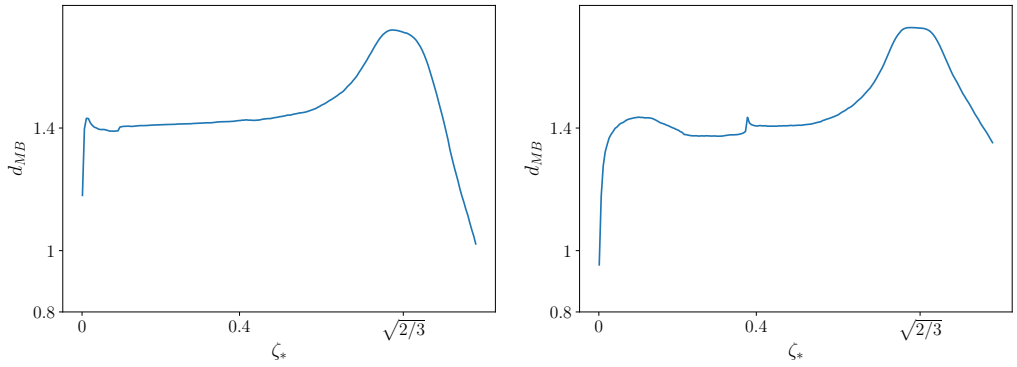

FIGURE 5.3: Behavior of the Minkowski-Bouligan dimension d_{MB} of the boundary between the chaotic DFTC phases as a function of the threshold ζ_* chosen, for the case of the restricted area of Fig. (left) and for the case of the whole phase diagram (right).

at the first order in T we obtain

$$\begin{aligned} I_{n+1} &= I_n - \frac{T}{2}(1 - I_{n+1}^2)\sin 2\phi_n + O(T^2) \,, \\ \phi_{n+1} &= \phi_n + 2\psi + \frac{T}{2} I_{n+1}\,(1 + \cos 2\phi_n) + O(T^2) \,. \end{aligned} \tag{5.21}$$

Let us notice that the $O(T)$ terms on the r.h.s. of the above equations, I_{n+1} can be replaced by I_n up to higher order corrections. This choice guarantees that our approximation preserves the symplectic structure of the original map. Eq. (5.21) is invariant under the discrete translation $\phi_n \to \phi_n + n\pi$; this is a consequence of the dynamical $\mathbb{Z}_2$ symmetry of the original model.

Let us now build the equivalent of the map (5.21) for the generic $\tilde{p}$-iterated map ($\tilde{p}$ being a generic integer). For $T = 0$ we have than that the action of the $\tilde{p}$-iterated map is trivially

$$\begin{cases} \phi_{n+\tilde{p}} &= \phi_n + 2\tilde{p}\psi \\ I_{n+\tilde{p}} &= I_n \end{cases} . \tag{5.22}$$

Then, by exploiting the identity

$$\sum_{n=0}^{\tilde{p}-1} e^{i(2\phi + 4n\tilde{p}\psi)} = \frac{\sin 2\tilde{p}\psi}{\sin 2\psi} e^{i(2\phi_n + 2(\tilde{p}-1)\psi)}, \tag{5.23}$$

we can write $I_{n+\tilde{p}}, \phi_{n+\tilde{p}}$ at the lowest order in T as

$$\begin{aligned} I_{n+\tilde{p}} &= I_n - \frac{\tilde{p}T}{2}(1 - I_{n+p}^2) U_{\tilde{p}}(\psi)\ \sin(2\phi_n + 2(\tilde{p}-1)\psi) \,, \\ \phi_{n+\tilde{p}} &= \phi_n + 2\tilde{p}\psi + \frac{\tilde{p}T}{2} I_{n+\tilde{p}}\left[1 + U_{\tilde{p}}(\psi)\cos(2\phi_n + 2(\tilde{p}-1)\psi)\right] \,, \end{aligned} \tag{5.24}$$

where

$$U_{\tilde{p}}(\psi) = \frac{\sin 2\tilde{p}\psi}{\tilde{p}\sin 2\psi} \ . \tag{5.25}$$

Being T small, in general, the $2\tilde{p}\psi$ term in the r.h.s. of the second equation od Eq(5.24) is going to dominate the evolution so that, we expect to find ourselves in the quasi-periodic phase. However, as $\tilde{p}\psi \sim k\pi$ for some integer k we have that this term becomes small as well, signaling the onset of the Poincaré-Birkhoff mechanism (for k odd, this is due to the $\mathbb{Z}_2$ symmetry, which allows us to reabsorb the term by redefining $\phi_n \to \phi_n + n\pi$).

Let us put ourselves close to a resonance, i.e. let us consider the limit $\psi = \psi_r + \delta\psi$ with $\delta\psi \ll \pi/p$. If p is odd, the smallest choice of $\tilde{p}$ which makes the term $\tilde{p}\psi$ small is $\tilde{p} = p$; if p is even, however, we have to choose $\tilde{p} = p/2$ (and redefine $\phi_n \to \phi_n + n\pi$. In this limit the Eq. (5.24) becomes

$$\begin{aligned} I_{n+\tilde{p}} &= I_n - \frac{\tilde{p}T}{2}(1 - I^2_{n+\tilde{p}})a_r \ \sin(2\phi_n - 2\psi_r) \ , \\ \phi_{n+\tilde{p}} &= \phi_n + 2\tilde{p}\delta\psi + \frac{\tilde{p}T}{2} I_{n+\tilde{p}} \ (1 + a_r \cos(2\phi_n - 2\psi_r)) \ , \end{aligned} \tag{5.26}$$

where

$$a_r = \begin{cases} 1 & \text{if } p = 1, 2 \\ 2(-1)^{\tilde{p}-1} \csc(2\psi_r)\delta\psi & \text{if } p \geq 3 \ . \end{cases} \tag{5.27}$$

Let us notice how in Eq. (5.26) the evolution of both ϕ and I is now slow, signaling that the $\tilde{p}$-iterated map can be approximated by a continuous flow. In order to do so, we have to redefine the time scale $\tilde{p}T \to T$, such that $\phi_{n+\tilde{p}}, I_{n+\tilde{p}} \to \phi_{n+1}, I_{n+1}$ now by introducing the time step $\Delta t = \tilde{p}T$, and expanding

$$\begin{aligned} I_{n+1} &= I_n + \dot{I} \ T + O(T^2) \\ \phi_{n+1} &= \phi_n + \dot{\phi} \ T + O(T^2) \end{aligned} \tag{5.28}$$

We find then

$$\begin{aligned} \dot{I} &= -\frac{a_r}{2}(1 - I^2)\sin(2\phi - 2\psi_r) \ , \\ \dot{\phi} &= 2\tilde{p}\frac{\delta\psi}{T} + \frac{1}{2} I \ (1 + a_r \cos(2\phi - 2\psi_r)) \ . \end{aligned} \tag{5.29}$$

In turn, this can have the form of a Hamiltonian flow, generated by

$$\mathcal{H}_p(\phi, I) = 2\frac{\delta\psi}{T} I - \frac{1}{4}(1 - I^2) \ (1 + a_r \cos(2\phi - 2\psi_r)) \ . \tag{5.30}$$

Let us notice how, for different values of $p > 2$, the effective Hamiltonian (5.30) is the same up to a renormalization of the parameter a_r, further supporting the hypothesis of a self-similar structure in the phase diagram.

By taking into account our initial condition, namely $\phi(0) = \pi/2$, $I(0) = 0$ we have that our p-iterated dynamics takes place along the curve

$$\mathcal{H}_p(I, \phi) = -\frac{1}{4}\left(1 - a_r \cos(2\psi_r)\right) . \tag{5.31}$$

If this curve is bounded between two finite values of the angle ϕ, the dynamics will circle around a fixed point, signaling that we are within the time crystalline phase. If, instead, the curves cover all the $\phi \in [0, 2\pi]$ interval, we have a quasi-periodic motion. Finally, close to the separatrix between these two cases, chaos is expected to arise, so that the boundary between these two regimes in terms of T, ϕ can be taken as an estimate of the edge of the DFTC for small T. For $p = 1, 2$, this criterion gives the condition

$$T = 4|\delta\psi|. \tag{5.32}$$

For $p > 2$, instead, at the lowest order in $\delta\psi$ we find, for any $\psi_r < \pi/2$, the condition

$$T^2 = \begin{cases} 8\,\tilde{p}^2 \tan\psi_r\,|\delta\psi| & \text{if } \delta\psi < 0\ , \\ 8\,\tilde{p}^2 \cot\psi_r\,|\delta\psi| & \text{if } \delta\psi > 0\ . \end{cases} \tag{5.33}$$

Let us notice how Eq.(5.33) captures both the non-analytic behavior of the boundary of the DFTC and its lack of symmetry $\delta\psi \to -\delta\psi$ around the resonant value ψ_r for $r \neq 1/4$. However, in order for the result to be predictable at the quantitative level we have to impose that the term $\delta\psi/T$ in Hamiltonian (5.30) to be small, this implies that the steepest curve between the two of Eq. (5.33) is not a good approximation of the boundary in the whole region $|\delta\psi| \sim \pi/p$, and its coefficient is not reliable. For $r = 1/4$ ($\tilde{p} = 2$) Eq. (5.33) gives

$$T^2 = 32|\delta\psi|\ , \tag{5.34}$$

while for $r = 1/6$ and $r = 1/3$ ($\tilde{p} = 3$) we find that the steepest edge grows respectively as

$$T^2 = \pm 24\sqrt{3}\delta\psi\ . \tag{5.35}$$

Those prediction are checked against the phase diagram of Fig. (5.1). In particular we find that the boundaries corresponding to $r = 0, 1$ are well described for small T by Eq. (5.32) (blue solid lines); the ones of the $r = 1/4$ island by the curve Eq. 5.34; while Eq. (5.35) describes the right/left boundary respectively of the $r = 1/3$, $r = 1/6$ islands (red solid lines).

According to the criterion introduced by Chirikov [175], the value of T at which two of these curves intersect can be taken as an estimate of the threshold T_* beyond which the chaos takes over: this gives the estimate

$$T_* = (12\pi^2)^{1/4} \approx 3.299 \tag{5.36}$$

for the onset of chaos in the $p = 4$ island, which is in excellent agreement with the numerics.

5.5 | Finite size effects

Our description of the DFTC phases is grounded on the solid foundation of dynamical systems theory. This parallelism is granted by the presence of long-range interactions in the Hamiltonian in (5.5), which suppress fluctuations and thermalization effects in the thermodynamic limit. On the other hand, it was estabilished in Ref. [157] that the $p = 2$ DFTC (around $\psi = \pi/2$) survives to finite sizes N. One may wonder if such a picture can be generalized to higher-order DFTC phases, to infer the robustness of our thermodynamic description to finite N. To do so, we performed the exact diagonalization of the $\alpha = 0$ model, explicitly computing the structure of the Floquet eigenstates $|\eta_m\rangle$.

The fact that the modulus of the total spin $\mathbf{S}$ of the system is conserved even for finite N allows us to restrict ourselves to the subspace with $\mathbf{S}^2 = s(s+1)$, with $s = N/2$, and thus to consider larger sizes ($N = 800$) [157, 176]. In Fig. 5.4 we show the projection of the Floquet eigenstates $|\eta_m\rangle$ onto the spin coherent states $|\Omega_{\theta,\phi}\rangle$ with $s = N/2$ (θ, ϕ being again the polar coordinates relative to z-axis introduced in Sec. 5.2) [177].

These eigenstates are qualitatively different in the three different phases of the system: while no structure is present in the chaotic phase (Fig. 5.4, bottom panel), in the quasi-periodic phase the eigenstate is localized in a connected region of the (θ, ϕ) space (Fig. 5.4,top panel: curves (a) and (c)), while in the $p = 4$ DFTC phase it appears localized around four, $\mathbb{Z}_4$ symmetric, points (Fig. 5.4,top panel: curve (b)).

This behavior can be explained within our picture. Indeed, close to a resonance, the Floquet evolution can be interpreted semi-classically as a tight-binding hopping between adjacent wells in the space $(\phi, \cos\theta)$ [167], each one localized around $\psi = k\psi_r$ (with $k = 1, \cdots p-1$), so that the corresponding $|\eta_m\rangle$ will take the form of a Bloch superposition

$$\langle \Omega_{\theta,\phi} | \eta_m \rangle = \sum_{k=0}^{p-1} e^{2i\pi k/p} \, W_m(I, \phi - k\psi_r) \tag{5.37}$$

of the p wavefunctions $W(I, \phi - k\phi_r)$, each localized around $\phi = k\psi_r$ and connected

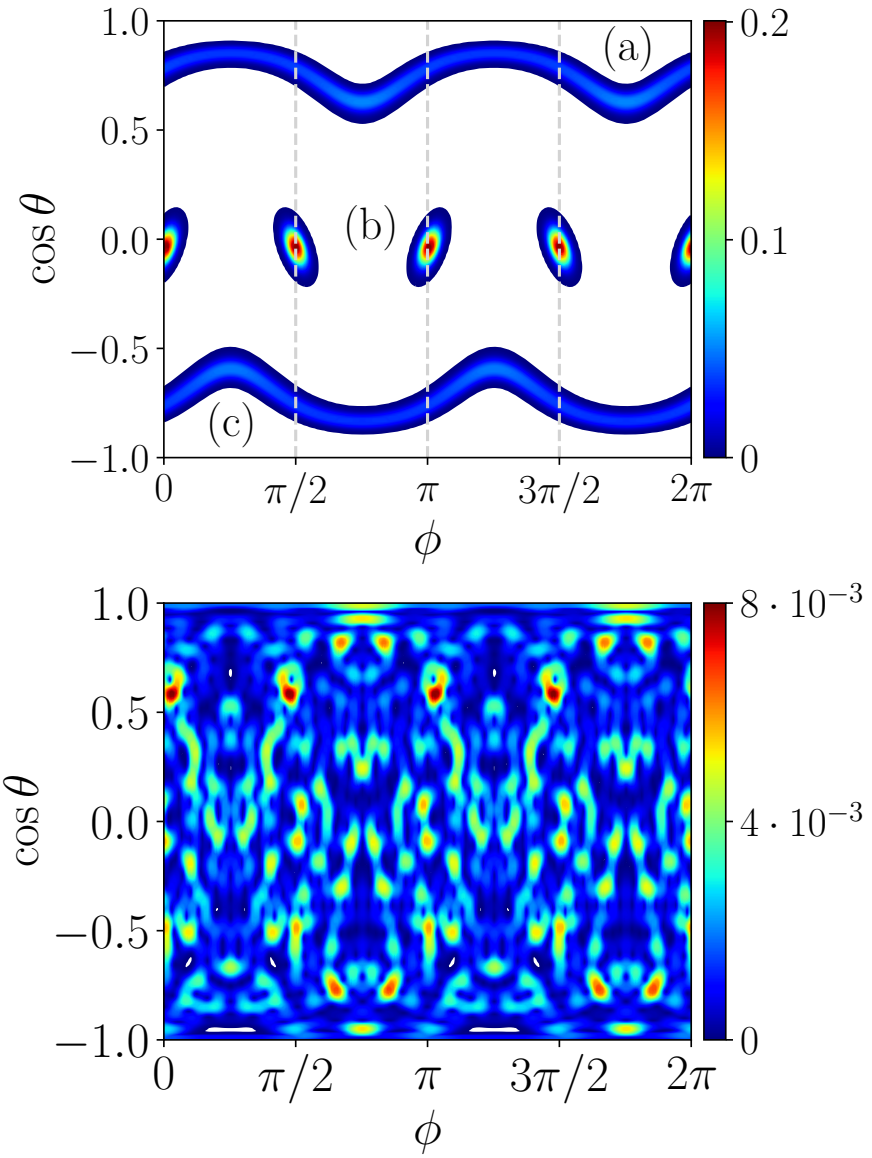

FIGURE 5.4: Color plot of the overlap $|\langle\Omega_{\theta,\phi}|\eta_m\rangle\langle\eta_m|\Omega_{\theta,\phi}\rangle|^2$ with the spin coherent state $|\Omega_{\theta,\phi}\rangle$ for different Floquet eigenstates $|\eta_m\rangle$, corresponding to different phases, for $N = 800$, $\psi = \pi/2 + 0.01$, $T = 1$ (top) and $T = 10$ (bottom). While in the chaotic phase (bottom panel) the eigenstate has no structure, the eigenstate (b) (top panel), which correspond to the DFTC phase with $p = 4$, clearly exhibits the structure of a Bloch wave-function localized around the $\mathbb{Z}_4$ symmetric wells. The eigenstate (b) (top panel) has maximum overlap with the spin coherent state corresponding to the initial conditions $\cos\theta = 0$, $\phi = \pi/2$. Initial conditions localized around the eigenstates (a) and (c) (top panel) instead correspond to a quasi-periodic phase.

to the following by the Floquet propagator:

$$U_F W_m(I, \phi - k\psi_r) = e^{i\beta_m} W_m(I, \phi - (k+1)\psi_r) \tag{5.38}$$

As a consequence, we expect this quantity to be localized around the fixed points of the p-iterated evolution in the time-crystalline phase. The agreement obtained between this semiclassical description and the numerical description obtained by exact diagonalization proves the validity of our analysis also at finite values of N and T.

References

[2] A. Campa, T. Dauxois, D. Fanelli, and S. Ruffo. *Physics of Long-Range Interacting Systems*. Oxford Univ. Press, 2014.

[10] M. Kac, G. E. Uhlenbeck, and P. C. Hemmer. "On the van der Waals Theory of the Vapor-Liquid Equilibrium. I. Discussion of a One-Dimensional Model". *Journal of Mathematical Physics* 4(2) (Feb. 1963), pp. 216–228. DOI: 10.1063/1.1703946.

[26] H. J. Lipkin, N. Meshkov, and A. Glick. "Validity of many-body approximation methods for a solvable model:(I). Exact solutions and perturbation theory". *Nuclear Physics* 62(2) (1965), pp. 188–198.

[66] A. Das, K. Sengupta, D. Sen, and B. K. Chakrabarti. "Infinite-range Ising ferromagnet in a time-dependent transverse magnetic field: Quench and ac dynamics near the quantum critical point". *Physical Review B* 74(14) (2006), p. 144423.

[67] A. Lerose *et al.* "Impact of nonequilibrium fluctuations on prethermal dynamical phase transitions in long-range interacting spin chains". *Physical Review B* 99(4) (2019), p. 045128.

[124] B. Sciolla and G. Biroli. "Quantum quenches, dynamical transitions, and off-equilibrium quantum criticality". *Physical Review B* 88(20) (Nov. 2013). DOI: 10.1103/physrevb.88.201110.

[148] G. Giachetti, A. Solfanelli, L. Correale, and N. Defenu. "High-order time crystal phases and their fractal nature". *arXiv preprint arXiv:2203.16562* (2022).

[149] F. Wilczek. "Quantum Time Crystals". *Phys. Rev. Lett.* 109 (16 Oct. 2012), p. 160401. DOI: 10.1103/PhysRevLett.109.160401.

[150] K. Sacha. "Modeling spontaneous breaking of time-translation symmetry". *Physical Review A* 91(3) (Mar. 2015). DOI: 10.1103/physreva.91.033617.

[151] D. V. ELSE, B. BAUER, and C. NAYAK. "Floquet Time Crystals". *Phys. Rev. Lett.* 117 (9 Aug. 2016), p. 090402. DOI: 10.1103/PhysRevLett.117.090402.

[152] D. V. ELSE, C. MONROE, C. NAYAK, and N. Y. YAO. "Discrete Time Crystals". *Annual Review of Condensed Matter Physics* 11(1) (2020), pp. 467–499. DOI: 10.1146/annurev-conmatphys-031119-050658.

[153] P. BORDIA *et al.* "Periodically driving a many-body localized quantum system". *Nature Physics* 13(5) (Jan. 2017), pp. 460–464. DOI: 10.1038/nphys4020.

[154] J. ZHANG *et al.* "Observation of a discrete time crystal". *Nature* 543(7644) (2017), pp. 217–220.

[155] S. CHOI *et al.* "Observation of discrete time-crystalline order in a disordered dipolar many-body system". *Nature* 543(7644) (2017), pp. 221–225.

[156] J. ROVNY, R. L. BLUM, and S. E. BARRETT. "Observation of discrete-time-crystal signatures in an ordered dipolar many-body system". *Physical review letters* 120(18) (2018), p. 180603.

[157] A. RUSSOMANNO, F. IEMINI, M. DALMONTE, and R. FAZIO. "Floquet time crystal in the Lipkin-Meshkov-Glick model". *Phys. Rev. B* 95 (21 June 2017), p. 214307. DOI: 10.1103/PhysRevB.95.214307.

[158] V. KHEMANI, A. LAZARIDES, R. MOESSNER, and S. L. SONDHI. "Phase Structure of Driven Quantum Systems". *Phys. Rev. Lett.* 116 (25 June 2016), p. 250401. DOI: 10.1103/PhysRevLett.116.250401.

[159] F. M. SURACE *et al.* "Floquet time crystals in clock models". *Phys. Rev. B* 99 (10 Mar. 2019), p. 104303. DOI: 10.1103/PhysRevB.99.104303.

[160] J. ZHANG *et al.* "Observation of a many-body dynamical phase transition with a 53-qubit quantum simulator". *Nature* 551(7682) (Nov. 2017), pp. 601–604. DOI: 10.1038/nature24654.

[161] A. LEROSE, J. MARINO, A. GAMBASSI, and A. SILVA. "Prethermal quantum many-body Kapitza phases of periodically driven spin systems". *Phys. Rev. B* 100 (10 Sept. 2019), p. 104306. DOI: 10.1103/PhysRevB.100.104306.

[162] M. H. MUÑOZ-ARIAS, K. CHINNI, and P. M. POGGI. *Floquet time crystals in driven spin systems with all-to-all p-body interactions*. 2022. arXiv: 2201.10692 [quant-ph].

[163] S. KELLY, E. TIMMERMANS, J. MARINO, and S.-W. TSAI. "Stroboscopic aliasing in long-range interacting quantum systems". *SciPost Physics Core* 4(3) (Sept. 2021). DOI: 10.21468/scipostphyscore.4.3.021.

[164] F. Machado *et al.* "Long-Range Prethermal Phases of Nonequilibrium Matter". *Phys. Rev. X* 10 (1 Feb. 2020), p. 011043. DOI: 10.1103/PhysRevX.10.011043.

[165] M. Collura, A. D. Luca, D. Rossini, and A. Lerose. *Discrete time-crystalline response stabilized by domain-wall confinement*. 2021. arXiv: 2110.14705.

[166] A. Pizzi, J. Knolle, and A. Nunnenkamp. "Higher-order and fractional discrete time crystals in clean long-range interacting systems". *Nature Communications* 12(1) (Apr. 2021), p. 2341. ISSN: 2041-1723. DOI: 10.1038/s41467-021-22583-5.

[167] K. Giergiel, A. Kosior, P. Hannaford, and K. Sacha. "Time crystals: Analysis of experimental conditions". *Physical Review A* 98(1) (July 2018). DOI: 10.1103/physreva.98.013613.

[168] A. Kolmogorov. "On the conservative of conditionally periodic motions for a small change in Hamiltonâs function (in Russ.), Dokl. Acad. Nauk SSSR 98,(1954), 524–530; English transl". *Lecture Notes in Physics* 93 (1979), pp. 51–56.

[169] V. I. Arnold. "Proof of a theorem of AN Kolmogorov on the invariance of quasi-periodic motions under small perturbations of the Hamiltonian". *Collected Works: Representations of Functions, Celestial Mechanics and KAM Theory, 1957–1965* (2009), pp. 267–294.

[170] J. Möser. "On invariant curves of area-preserving mappings of an annulus". *Nachr. Akad. Wiss. Göttingen, II* (1962), pp. 1–20.

[171] S. H. Strogatz. *Nonlinear Dynamics and Chaos*. CRC Press, May 2018. DOI: 10.1201/9780429492563.

[172] R. S. MacKay. *Renormalisation in area preserving maps*. Princeton University, 1982.

[173] M. Cencini, F. Cecconi, and A. Vulpiani. *Chaos: from simple models to complex systems*. WORLD SCIENTIFIC, Sept. 2009. DOI: 10.1142/7351.

[174] H. P. O. Collado *et al.* "Emergent parametric resonances and time-crystal phases in driven Bardeen-Cooper-Schrieffer systems". *Physical Review Research* 3(4) (Nov. 2021). DOI: 10.1103/physrevresearch.3.l042023.

[175] B. V. Chirikov. "A universal instability of many-dimensional oscillator systems". *Physics Reports* 52(5) (May 1979), pp. 263–379. DOI: 10.1016/0370-1573(79)90023-1.

[176] P. Ribeiro, J. Vidal, and R. Mosseri. "Exact spectrum of the Lipkin-Meshkov-Glick model in the thermodynamic limit and finite-size corrections". *Physical Review E* 78(2) (Aug. 2008). DOI: 10.1103/physreve.78.021106.

[177] A. AUERBACH. *Interacting electrons and quantum magnetism*. Springer Science & Business Media, 2012.

Appendices

A | Recurring integrals

We now derive the low-momentum behavior of the integrals of the form

$$\omega(q) = \int_{r>a} d^2\mathbf{r}\, J(r)\Big(1 - \cos(\mathbf{q}\cdot\mathbf{r})\Big). \tag{A.1}$$

and

$$G(r) = \int_{q<\Lambda} \frac{d^2\mathbf{q}}{(2\pi)^2} \frac{\Big(1 - \cos(\mathbf{q}\cdot\mathbf{r})\Big)}{\omega(q)}. \tag{A.2}$$

with $\Lambda = 2\pi/a$. We choose our coupling to be

$$J(r) = J^S(r) + \frac{J}{r^{2+\sigma}} \tag{A.3}$$

where $J^S(r)$ is fast-decaying and represent the short-range, fast decaying, part of the coupling, while the second one represent an (eventual) power-law (coupling with $\sigma > 0$) which dominates for $r \gg 1$. We have:

$$\omega(q) = \int_{r>a} d^2\mathbf{r} J^S(r)\Big(1 - \cos(\mathbf{q}\cdot\mathbf{r})\Big) + J\int_{r>a} \frac{d^2\mathbf{r}}{r^{2+\sigma}}\Big(1 - \cos(\mathbf{q}\cdot\mathbf{r})\Big). \tag{A.4}$$

Since, by hypothesis, $\int_{r>a} d^2\mathbf{r}\, r^2 J^S(r)$ is finite, we can Taylor expand the cosine in the first integral on the r.h.s getting a term proportional to q^2 for small values of q. The same is true for the second terms as well, provided that $\sigma > 2$, so that we can conclude that

$$\omega(q) \sim q^2 \qquad \forall\, \sigma > 2 \tag{A.5}$$

with some non-universal proportionality constant.

Let us consider now the regime $\sigma \in (0, 2)$. In this case, the second term of the r.h.s. of Eq. (A.4) has no ultraviolet divergence, so that we can integrate over the whole space, up to $O(q^2)$ corrections that can be reabsorbed in the contribution coming from the short-range part of the coupling. We get than

$$\omega(q) = \int \frac{d^2\mathbf{r}}{r^{2+\sigma}}\Big(1 - \cos(\mathbf{q}\cdot\mathbf{r})\Big) + O(q^2), \tag{A.6}$$

which becomes, in polar coordinates

$$\omega(q) = 2\int_0^\infty \frac{dr}{r^{1+\sigma}} \int_0^{2\pi} d\theta \sin^2 \frac{qr\cos\theta}{2} + O(q^2). \tag{A.7}$$

In turn posing in term of $\rho = qr\cos\theta$

$$\omega(q) = q^\sigma 2^{1-\sigma} J \int_0^\infty \frac{d\rho}{\rho^{1+\sigma}} \sin^2\rho \int_0^{2\pi} d\theta |\cos\theta|^\sigma + O(q^2) \tag{A.8}$$

Then, we find

$$\omega(q) = J c_\sigma q^\sigma + O(q^2) \qquad \forall\, \sigma \in (0,2) \tag{A.9}$$

with

$$c_\sigma = 2^{1-\sigma} \int_0^\infty \frac{d\rho}{\rho^{1+\sigma}} \sin^2\rho \int_0^{2\pi} d\theta |\cos\theta|^\sigma = \frac{2^{1-\sigma}\pi |\Gamma(-\frac{\sigma}{2})|}{\sigma\Gamma(\frac{\sigma}{2})}. \tag{A.10}$$

Let us now consider the integral of Eq (A.2), which defines $G(r)$. We switch to polar coordinates and exploit the identity

$$\int_0^{2\pi} \cos(qr\cos\theta) = 2\pi \mathcal{J}_0(qr), \tag{A.11}$$

$\mathcal{J}_0(x)$ is the zeroth-order Bessel function of the first kind, obtaining

$$G(r) = a^2 \int_0^\Lambda \frac{dq}{2\pi} \frac{q(1-\mathcal{J}_0(qr))}{\omega(q)}, \tag{A.12}$$

For $\sigma > 2$, we have $\omega(q) \sim q^2$, so that

$$G(r) \sim \int_0^\Lambda dq \frac{1-\mathcal{J}_0(qr)}{q} = \int_0^{\Lambda r} dx \frac{1-\mathcal{J}_0(x)}{x}. \tag{A.13}$$

For large r, the dominant term in the integral above is $\ln(\Lambda r)$. We then conclude that:

$$G(r) \sim \eta \ln\frac{r}{a} + B, \tag{A.14}$$

η and B being two non-universal, cutoff dependent, constants. In particular, if we assume $J^S(r) = 0$, $J(r) = Jr^{-2-\sigma}$, we have $\eta, B \propto J^{-1}$, so that we can write

$$G(r) \sim \eta(J) \ln\frac{r}{a} + AJ^{-1} \tag{A.15}$$

with $\eta(J) = p/J$ for some p.

Let us now consider instead the case $J(r) \sim Jr^{-2-\sigma}$, with $\sigma \in (0, 2)$. The expression for $G(r)$ becomes

$$G(r) \sim \frac{1}{J} \int_0^\Lambda dq\, q^{1-\sigma}\, (1 - \mathcal{J}_0(qr)) \tag{A.16}$$

which asymptotically goes as

$$G(r) = AJ^{-1} + O(r^{\sigma-2}), \tag{A.17}$$

for some (non universal) A.

B | Fractional Laplacian

We want now to provide the definition of the fractional Laplacian, that we used, and derive the form (2.35) of $S_{\rm LR}$.

For any $\sigma \in (0, 2)$, and a function $f(\mathbf{x}) : \mathbb{R}^d \to \mathbb{R}$ one can define $\nabla^\sigma f(\mathbf{x})$ as:

$$\nabla^\sigma f(\mathbf{x}) \equiv \gamma_{d,\sigma} \int d^d r \frac{f(\mathbf{x}+\mathbf{r}) - f(\mathbf{x})}{r^{d+\sigma}}, \tag{B.1}$$

with

$$\gamma_{d,\sigma} = \frac{2^\sigma \Gamma(\frac{d+\sigma}{2})}{\pi^{d/2} |\Gamma(-\frac{\sigma}{2})|} \tag{B.2}$$

One can derive an alternative expression for this quantity in the momentum space. In terms of Fourier transform of $f(\mathbf{x})$, $f(\mathbf{q})$, one finds

$$\nabla^\sigma f(\mathbf{x}) = -\gamma_{d,\sigma} \int d^d q \, f(\mathbf{q}) \, e^{i\mathbf{q}\cdot\mathbf{x}} \int d^d r \frac{1 - e^{i\mathbf{q}\cdot\mathbf{r}}}{r^{d+\sigma}}. \tag{B.3}$$

and, exploiting the fact that,

$$\int d^d r \frac{1 - e^{i\mathbf{q}\cdot\mathbf{r}}}{r^{d+\sigma}} = \gamma_{d,\sigma}^{-1} \, q^\sigma, \tag{B.4}$$

one have

$$\nabla^\sigma f(\mathbf{x}) = -\int d^d q \, q^\sigma f(\mathbf{q}) e^{i\mathbf{q}\cdot\mathbf{x}}. \tag{B.5}$$

(from which, in the limit $\sigma \to 2$ one recovers the usual behavior of the standard Laplacian).

Let us now notice how the quantity present in Eq (2.34), namely

$$\int d^2 x \int_{r>a} \frac{d^2 r}{r^{2+\sigma}} [1 - \cos(\theta(\mathbf{x}) - \theta(\mathbf{x}+\mathbf{r}))]. \tag{B.6}$$

naturally fits into the definition of a two-dimensional fractional Laplacian. Indeed, provided that $\sigma < 2$, one can actually extend the integral on r on the whole space,

and absorb the contribution coming from the $r < a$ region into the definition of the SR term. Then, we can write the additional LR term as the real part of

$$\begin{aligned} &\int d^2x \int \frac{d^2r}{r^{2+\sigma}} [1 - e^{i\theta(\mathbf{x}+\mathbf{r})-i\theta(\mathbf{x})}] = \\ &e^{-i\theta(\mathbf{x})} \int d^2x \int \frac{d^2r}{r^{2+\sigma}} [e^{i\theta(\mathbf{x})} - e^{i\theta(\mathbf{x}+\mathbf{r})}]. \end{aligned} \tag{B.7}$$

In turn, this can be rewritten by exploiting the definition (B.1) of the fractional Laplacian,

$$-\gamma_{2,\sigma}^{-1} \int d^2x \, e^{-i\theta} \nabla^\sigma e^{i\theta}. \tag{B.8}$$

The expression above is already real, so that we recover the form of the long-range term given in Chapter 2.

C | Evolution of the magnetization in the fully-connected kicked Ising model

Here we revise the derivation of the dynamic map of Eq. (5.10) of the main text, i.e. the evolution equation of the magnetization

$$m_a(t) = \frac{1}{N}\sum_j \left\langle \hat{\sigma}_a^j \right\rangle \tag{C.1}$$

at stroboscopic times $t_n = nT$, in the thermodynamic limit, $N \to \infty$. First we notice how, due to the impulsive nature of the magnetic field $h(t)$, the Floquet propagator can be written as the product of two different operators:

$$U_F = e^{-2i\psi \hat{S}_z} e^{iT\hat{S}_x^2/N} \ , \tag{C.2}$$

where we introduced the global spin operators

$$\hat{S}_a = \frac{1}{2}\sum_j \hat{\sigma}_a^j \ , \tag{C.3}$$

with $a = x, y, z$. Being $\hat{S}_x$ the generator of $O(3)$ rotations around the x axis, the kick term $e^{-2i\psi\hat{S}_z}$ in Eq.(C.2) acts on the observable $\mathbf{m}$ simply as a rotation around the z-axis. On the other hand, the other term describes the evolution over one period T of $\mathbf{m}$ induced by the second term on the r.h.s of Eq. (C.2). The Heisenberg equations of motion corresponding to such evolution for the operators $\hat{S}_a$ are:

$$\begin{aligned}
&\frac{d}{dt}\hat{S}_x = 0 \ , \\
&\frac{d}{dt}\hat{S}_y = \frac{J}{N}\left(\hat{S}_x\hat{S}_z + \hat{S}_z\hat{S}_x\right) \ , \\
&\frac{d}{dt}\hat{S}_z = -\frac{J}{N}\left(\hat{S}_x\hat{S}_y + \hat{S}_y\hat{S}_x\right) \ .
\end{aligned} \tag{C.4}$$

According to the general theory developed in Ref. [66], for $N \to \infty$ the spin-spin correlation become negligible, that is $\langle \hat{S}_a \hat{S}_b \rangle \simeq \langle \hat{S}_a \rangle \langle \hat{S}_b \rangle$, so that Eqs. (C.4) become a closed set of equations for $m_a = 2 \langle S_a \rangle / N$, namely:

$$\begin{aligned} \dot{m}_x &= 0 \ , \\ \dot{m}_y &= J m_x m_z \ , \\ \dot{m}_z &= -J m_x m_y \ . \end{aligned} \tag{C.5}$$

In turn this results after a time T in a (clockwise) rotation around the x-axis, of angle $JT m_x(t)$.
Posing $J = 1$, the overall effect of the Eq. (C.2) on our observable $\mathbf{m}$ is the one of Eq.(4) of the main text.